Special Issue — Automotive Products

NSK

Cover photos:
   Automotive products

NSK Technical Journal

Motion & Control
No.17
May 2005

NSK

Contents

Special Articles

Automotive Products and Technologies

Hisashi Machida
Director, Executive Vice President NSK Ltd.

Since the Ford Motor Company introduced the Model T in 1908 and the following implementation of mass-production manufacturing, the number of vehicles worldwide has reached an approximate total of 800 million. Over the last 100 years, the automotive industry has grown and served as a growth engine for many other industries. During this period of development in the automotive industry, NSK has followed a similar path when our tapered roller bearings were used in vehicles for the first time in 1917. In 1950, we started mass-production of carburized bearings for automobiles. From the 1960s, we carried out research and development of specific bearings and other automotive products for various automotive applications during the rapid growth of motorization in Japan.

As we trace the history of our product development, starting with chassis-related parts, we developed a hub unit, which has since evolved into second- and third-generation hub units. We then introduced a sensor hub unit that dramatically enhances intelligent electronic control systems of vehicles. For steering systems, we developed ball-screw type steering in 1959 and rack and pinion steering in 1971. We also developed collapsible steering columns and power tilt-and-telescopic steering columns. Magnetic clutch bearings for automotive air conditioners, alternator bearings, water pump bearings, etc., were developed for electrical accessories coinciding with new automotive developments. In 1966, we commercialized one-way clutches for the drivetrain in addition to friction plates in 1973. We also introduced needle roller bearings for highly efficient and highly functional automatic transmissions, sealed-clean bearings with remarkably longer life, and low torque tapered roller bearings that promote enhanced fuel economy.

Future vehicles will demand even more comfort, enhanced intelligent electronic control system performance, and will have to lessen their impact on the environment in addition to meeting the basic requirements of greater fuel efficiency and vehicle stability. Ahead of the demands for energy conservation and actions that protect the environment, NSK released an electric power steering (EPS) system for minivehicles in 1988. In 1999, the world's first commercially available half-toroidal continuously variable transmission (CVT) fulfilled the hopes of a visionary transmission for mass-produced vehicles.

NSK has developed leading-edge technologies for our products by taking advantage of our primary technologies in materials, lubrication, numerical simulation, and mechatronics. We will continue to further develop our past achievements for next-generation products that will meet the needs of the future. We are also focusing greater resources to further our research and development that address such issues as lowering friction, reducing size, extending life, and improving performance in preparation for future demands. In this special edition, some of our recent technology achievements and new products for automotive applications are introduced. We hope you find this issue of Motion & Control to be informative as we strive to contribute with further developments in automotive technology by enhancing research and development of new products.

Hisashi Machida

Trends and New Technologies of Hub Unit Bearings

Junshi Sakamoto
Bearing Technology Center

ABSTRACT

The development of hub unit bearings for motor vehicles has made rapid progress in the area of unitization by integrating several axle components in order to meet the demand for automotive parts that realize weight and size reductions, and improved performance. In this article, we will discuss the latest trends and technologies that apply to hub unit bearings for the purpose of improving performance, making weight reductions, lowering torque, and enhancing capabilities by incorporating low flange run-out and integrated ABS sensors. We will also show how the hub unit bearings can further promote the environmentally friendly goals of the automotive industry.

1. Introduction

With the rapid spread of front-wheel-drive vehicles during the 1980s, unitization of bearings and several axle components such as steering knuckles and hubs has greatly expanded to meet the demand for weight and size reduction and easier mounting. In recent years, activities among automakers and related industries have placed greater emphasis on safety and lessening the environmental impact of their products. In order to meet various needs of wheel hub bearing, improved functionality and sophisticated functions have been added to wheel hub bearings. has progressed and newly sophisticated functions are added to wheel bearings. In this article, we will discuss the latest technologies of wheel hub unit bearings, their structures, and related trends.

2. Evolution

NSK's hub unit bearing has evolved over three significant design changes that have integrated the bearing with surrounding components (Fig. 1). Mass production of all three generations of hub units (HUB I, HUB II, and HUB III) continues to meet the needs of automakers for a product that is compact, lightweight, and highly reliable.

Lightweight aluminum steering knuckles are widely adopted over heavier steel knuckles to reduce wheel hub weight for improving fuel economy and driving stability. In addition, HUB II and HUB III are increasingly being used vehicle production lines due to their ease of mounting.
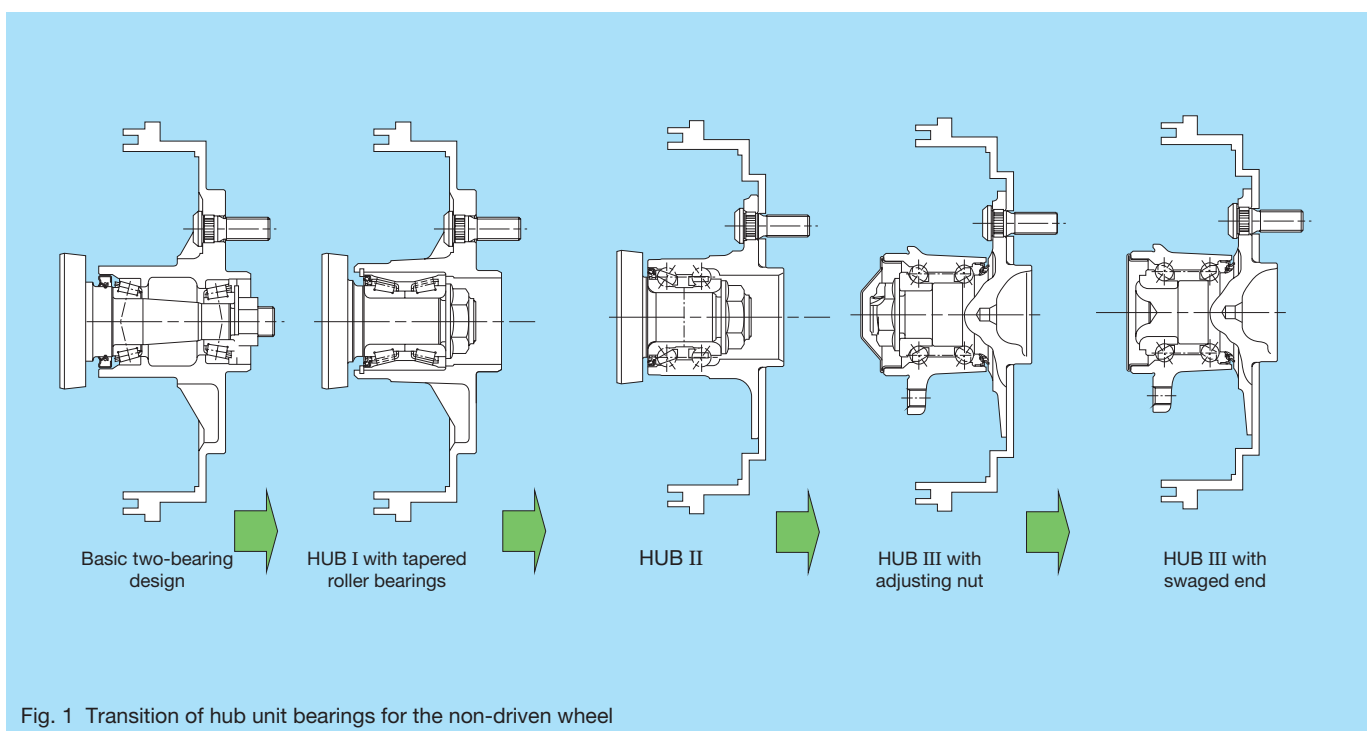

| Basic two-bearing design | → | HUB I with tapered roller bearings | → | HUB II | → | HUB III with adjusting nut | → | HUB III with swaged end |

Fig. 1 Transition of hub unit bearings for the non-driven wheel
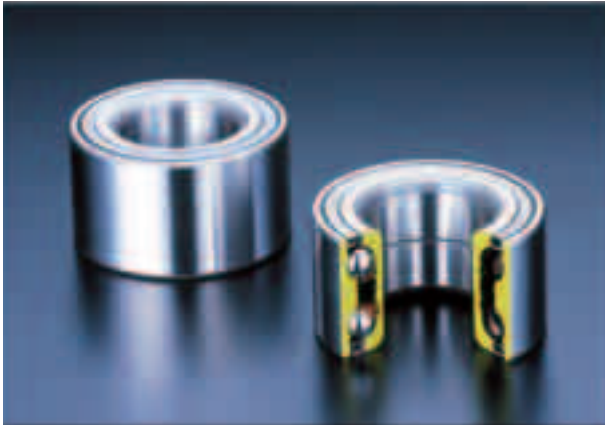
Photo 1 HUB I

Photo 2 HUB II

Photo 3 HUB III

2.1 HUB I (Photo 1)

HUB I consists of either double-row angular contact ball bearings (Photo 1) or double-row tapered roller bearings with a single outer ring in a back-to-back duplex arrangement. Initial axial clearance is preset for preload to fall within a specified range after mounting, which eliminates the need for preload adjustments with spacers, for instance, on an assembly line. Furthermore, integrating the seals with the hub unit bearings eliminates external mounting of the seals by assembly line workers.

2.2 HUB II (Photo 2)

HUB II (Photo 2) with flanged outer rings feature fewer assembly parts, reduced weight, and easier mounting in comparison to HUB I. HUB II is designed with an outer ring flange that bolts to the suspension (inner ring rotation), or a flange designed for mounting the brake and wheel (outer ring rotation).

2.3 HUB III (Photo 3)

HUB III consists of a flanged outer ring that bolts to the suspension and an inner ring flange for mounting of the brake and wheel. Unlike HUB II, HUB III is designed with an integrated ABS sensor.

3. Types and Characteristics

Table 1 lists the types and characteristics of NSK's various hub units.

4. Hub Unit Technologies

4.1 High performance seal

Hub unit bearings are exposed to a wide range of road driving conditions and harsh environments due to their close proximity to the ground and to high-temperature components such as brake rotors. The bearing seals must be impervious to heat, mud, and turbid water. Table 2 lists various the various types of seals that offer various capabilities.

4.2 Swaging

A self-retained inner ring held by rocking die forging (swaging) is standard in HUB III. Swaging harnesses axial forces that deform the flanged inner ring to capture the smaller inner ring. There are several advantages of a swaged end hub unit in comparison to conventional retaining nut assemblies. For example, HUB III for non-driven wheels (Fig. 2) helps to reduce size and weight, and are cost-effective. For driven wheels (Fig. 3), HUB III is preloaded prior to mounting, thus eliminating the need to seat internal components. HUB III is also fully interchangeable with either driven or non-driven wheels.

5. Latest Technologies

Growing awareness of environmental issues throughout the globe have placed greater pressures on automakers to reduce the environmental impact of their products by improving fuel economy among others. NSK hub unit bearings help the automotive industry meet such demands by reducing hub assembly weight, size, and torque.

Table 1 Types and characteristics

Characteristics	Items	HUB I		HUB II				HUB III
		Ball bearings	Tapered roller bearings	Ball bearings		Tapered roller bearings		
				Outer ring rotation	Inner ring rotation	Outer ring rotation	Inner ring rotation	
Functionality	Load capacity	Good	Excellent	Good	Good	Excellent	Excellent	Good
	Rigidity	Fair	Excellent	Fair	Fair	Excellent	Excellent	Good
	Rotation torque	Good	Fair	Excellent	Good	Fair	Fair	Excellent
	Seizure-resistance	Excellent	Fair	Excellent	Excellent	Fair	Fair	Excellent
Compactness	Axle weight	Fair	Fair	Good	Good	Good	Good	Excellent
	Cross-section space	Fair	Good	Fair	Fair	Excellent	Excellent	Excellent
	Width space	Good	Fair	Excellent	Excellent	Good	Good	Excellent
Reliability	Seals	Fair (Without seal) / Excellent (With seal)	Fair (Without seal) / Excellent (With seal)	Excellent	Excellent	Excellent	Excellent	Excellent
	Preload range under motion	Fair	Fair	Good	Good	Good	Good	Excellent
	Reliability in service	Fair	Fair	Good	Good	Good	Good	Excellent
Maintenance	Preload control	Fair	Fair	Excellent	Good	Excellent	Good	Excellent
	Mounting and serviceability	Fair	Fair	Good	Good	Good	Good	Excellent

5.1 Lightweight

5.1.1 Unitization

Hub unit bearings contribute to further reducing axle weight through enhanced unitization (Fig. 4). The HUB II achieved a 180 g weight reduction over its predecessor, while the HUB III achieved an additional reduction of 120 g.

5.1.2 FEM analysis

HUB II and HUB III are able to achieve further weight reductions while maintaining sufficient flange rigidity by incorporating finite element method (FEM) analysis into the design process. Fig. 5 shows examples of FEM analysis conducted for reducing thickness while maintaining rigidity for an optimum flange design of a HUBK (Photo 4).

5.2 Low torque

The low torque design of an NSK hub unit further enhances fuel economy of an automobile.

5.2.1 Low torque of bearing interior

Bearing torque is most influenced by the type of bearing and preload. Fig. 6 illustrates the gradual reduction of frictional torque for each generation of hub unit bearing.

5.2.2 Low-torque seals

Seal torque greatly influences overall torque in a bearing. Improving seal design enhances hub unit performance by reducing torque. Although reducing seal torque would normally result in sacrificing seal resistance against mud and turbid water, NSK has achieved the development of a low-torque seal by an optimal configuration of lip design and material.
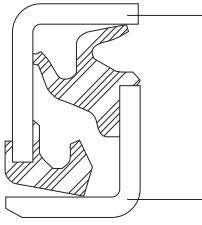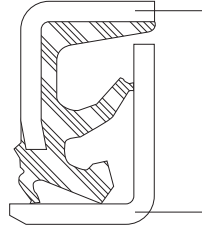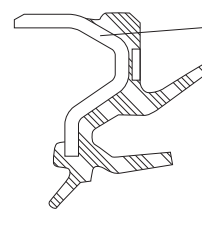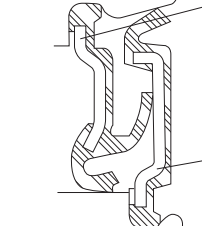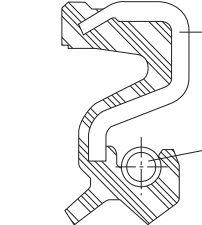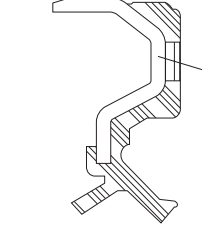
5.3 Reduction of brake judder

There are several causes of brake-disk vibrations or "brake judder," including lateral run-out of the brake rotor. In order to minimize the possibility of any lateral runout of the rotor, it is paramount that the hub unit flanges also be free of lateral runout to the greatest degree possible. To this end, NSK has established a processing technology to minimize flange runout to a satisfactory level.

5.4 ABS technology

An antilock braking system (ABS) is one of several automotive electronic safety systems. The ABS monitors rotation speed with sensors positioned at each wheel. An ABS electric control unit (ECU) uses the sensor information to automatically modulate brake pressure via the hydraulic control unit (HCU).

Hub units developed for the ABS include types with a sensor attached to the hub for detecting rotating speed of the wheel or types with an integrated sensor unit.

Table 2 Hub unit bearing seals

Type	Structure	Mud and Turbid Water Resistance
High-integral seal	Stainless steel plate / Stainless steel plate	AA
Low torque high-integral seal	Low-carbon steel plate / Stainless steel plate	A
Triple lip seal	Low-carbon steel plate	A
Double seal	Low-carbon steel plate / Low-carbon steel plate	BB
Garter spring seal	Low-carbon steel plate / Stainless steel spring	B
Shaft seal	Low-carbon steel plate	C

Low-cost

Compact

Lightweight

Fig. 2 Structure of the inner ring retaining mechanism for non-driven wheels

No need to adjust preload settings

Lightweight bearing assembly for

driven and non-driven wheels

Fig. 3 Structure of the inner ring retaining mechanism for driven wheels

HUB I   180 g   HUB II   120 g   HUB III

Fig. 4 Weight reductions achieved by integration of bearings and peripheral components

Thinner bore flange

Stress concentration / Optimum design for weight reduction / Relieved stress concentration

Redundant thickness eliminated on outboard flange

Optimum design for weight reduction / Limited stress within satisfactory range

Flange thickness reduced

Optimum design for weight reduction

Fig. 5 Samples of FEM analysis

Photo 4 HUBK for minivehicles

Fig. 6 Comparison of frictional torque for each type of hub unit bearing (straight travel at 500 rpm)

5.4.1 Hub units with sensor rotors

Fig. 7 shows examples of structures of conventional hub units. In conventional hub units, a sensor rotor is used to with a sensor element to monitor wheel-rotating speed.

The sensor rotor is mounted to the spindle and is made of sintered metal or machined into a gear-shaped ring. The sensor rotors are press-fitted onto the outer ring of the constant velocity (CV) joint of a driven wheel, or press-

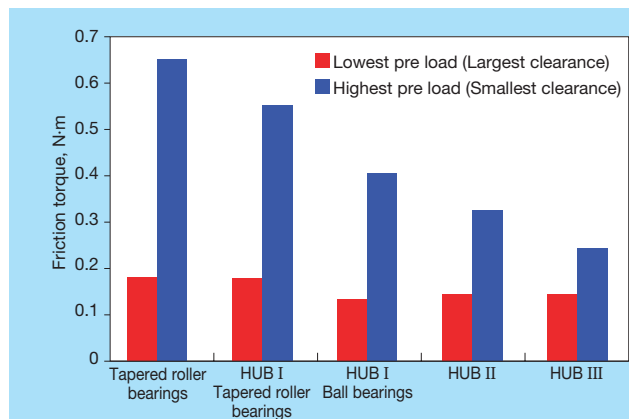fitted onto the bearing outer ring of a non-driven wheel. In both configurations (driven and non driven wheels), the wheel speed sensor element is mounted to the knuckle.

Passive sensor units (magnetic flux sensor) are the most common type of sensor unit. Magnetic flux in a passive sensor unit generates a sine-wave current in the sensor element as the sensor rotor rotates. As rotor speed increases, frequency and voltage also increase. Whereas frequency and voltage are in direct proportion to rotor speed, it becomes difficult to measure wheel speed as frequency decreases at lower speeds.

Multipole magnetic encoder seals (multipole magnetic rubber vulcanized to a metal ring) are more common than gear-shaped sensor rotors. A multipole magnetic encoder seal is much lighter than a conventional sensor rotor because of its integrated seal design. The elimination of component parts helps to reduce sensor unit size and weight. Adoption of multipole magnetic encoder seals has lead to the growing use of active sensor elements with semiconductor devices such as magnetic resistance element (MRE) rotation sensors and hall-effect sensors. MRE rotation sensors are not dependent on rotating speed, thus enabling them to detect wheel speed down to almost zero. Unlike conventional inductive magnetic sensors, MREs are integrated with multipole magnetic encoder seal, resulting in a more compact hub unit. Fig. 8 shows examples of HUB I and HUB II with multipole magnetic encoder seals.

5.4.2 Hub unit bearings with integrated ABS sensor units

One of the growing trends among wheel bearing technologies is the integration of both the sensor rotor and ABS sensor element with the bearing hub unit. In recent years, hub unit bearings with integrated ABS sensors have become prevalent. These hub unit bearings can be classified into three types: integrated annular sensors, integrated sensor elements between bearing rows, and integrated sensor cap elements.

<Integrated annular passive sensor>

The hub unit bearing with an annular sensor unit (Fig. 9) for a non-driven wheel is compact, lightweight, and more effectively uses available space in the hub/bearing assembly. Output signal of the sensor rotor in this configuration is strong enough for the passive sensor element to detect low wheel speeds.

<Integrated sensor unit between rows>

The hub unit bearing with a sensor unit located between the two rows of rolling elements (Fig. 10) is applicable to both driven and non-driven wheel applications, but is especially beneficial to driven wheel applications where space is limited. Both the sensor element and sensor rotor are integrated into the hub/bearing assembly for enhanced durability and improved resistance against possible bearing deformation or air gap fluctuation that would normally occur under harsh road conditions or sudden shock loads to the vehicle suspension. Either type of sensor element, passive or active, can be integrated into this hub/bearing assembly.

<Integrated sensor cap>

A hub unit bearing with a sensor cap (Fig. 11) is available in two configurations: separated and integrated.
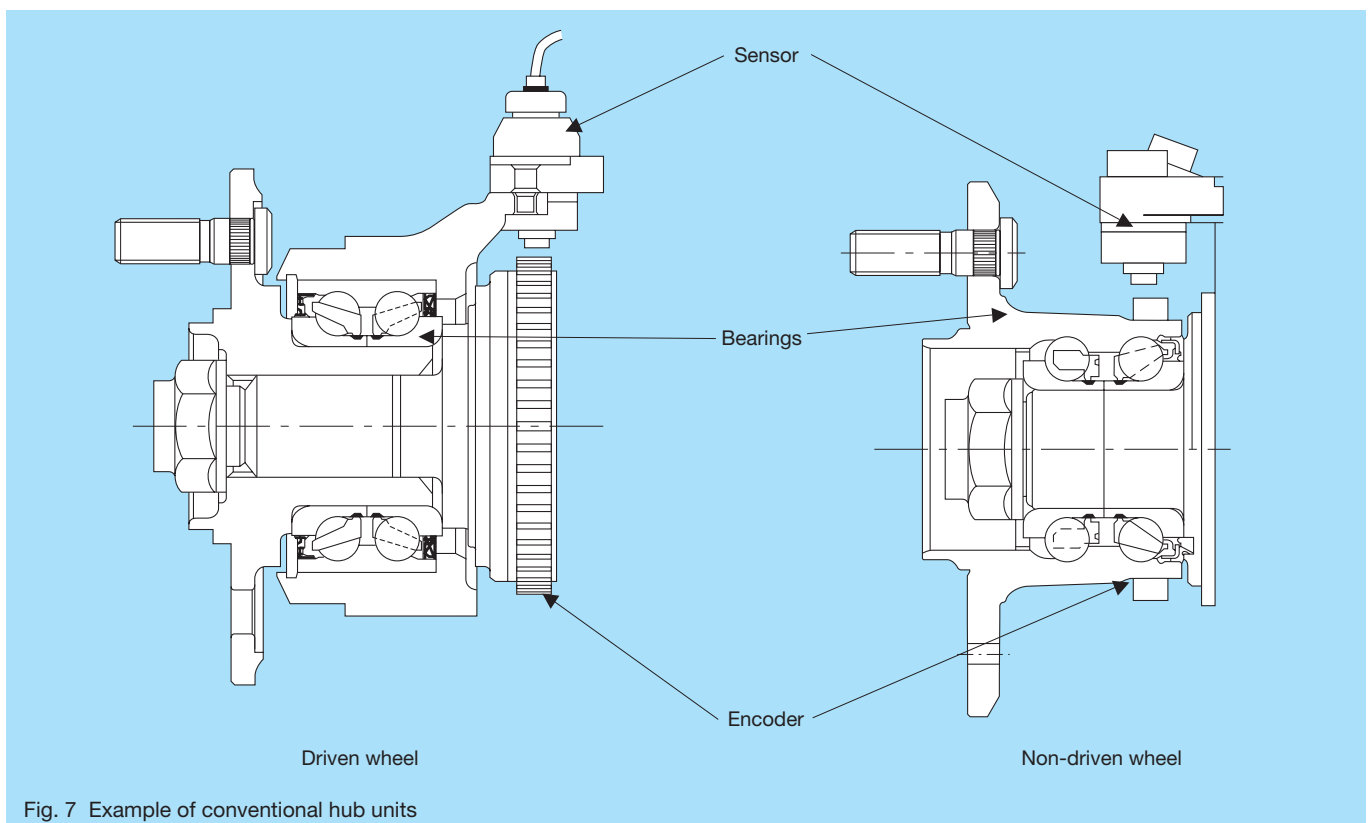

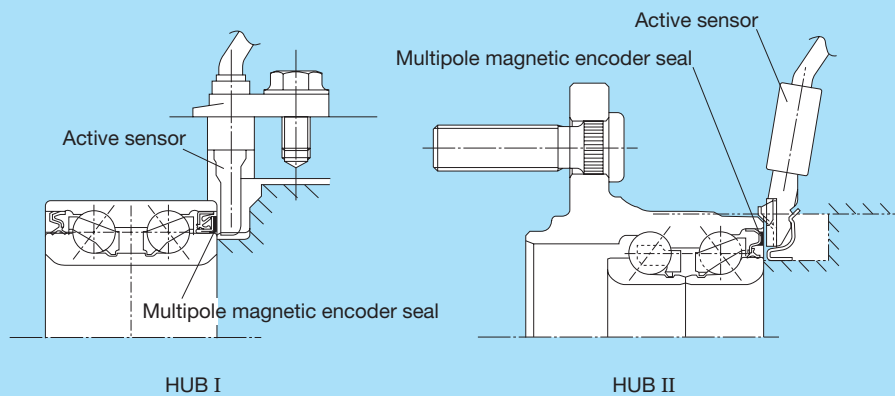Fig. 7 Example of conventional hub units

Fig. 8 Examples of HUB I and HUB II with multipole magnetic encoders
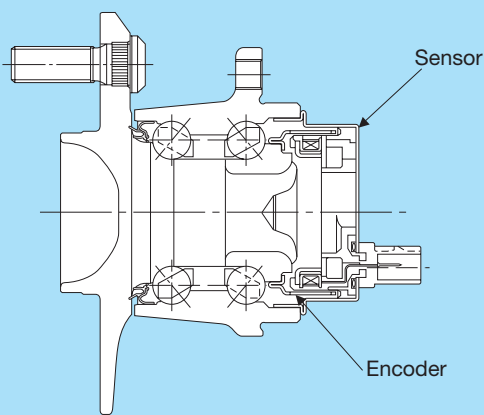
HUB I

HUB II

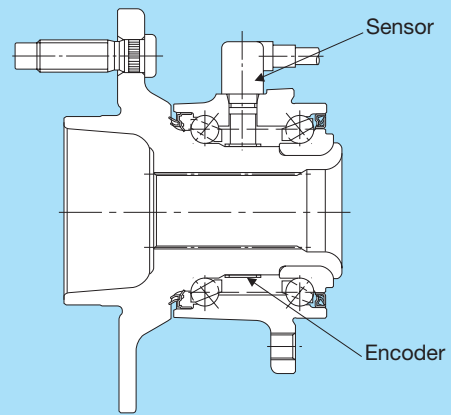Fig. 9 Hub unit bearing with annular sensor unit

Fig. 10 Hub unit bearing with sensor unit between rows

One advantage of the separated type, sensor cap is easy replacement with mass-produced standardized sensor elements. The integrated type sensor cap is compact, lightweight, and further promotes overall reduction of the hub/bearing assembly.

This assembly is best for non-driven wheels and integrated annular passive sensor units with either passive or active sensor elements. Both types of sensor units ensure reliable performance in hub/bearing assemblies due to integration of sensor element and sensor rotor within the hub/bearing assembly.
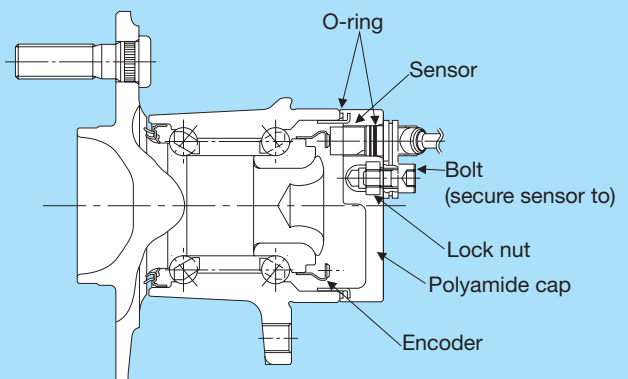
Fig. 11 Hub unit bearing with end-cap sensor (separated type)

6. Conclusion

The automotive industry is under increasing pressure to meet demand for greater vehicle handling and control the introduction of information technology into vehicle systems. Demand will further increase for system integration and enhanced modular production systems. NSK will continue its efforts to anticipate what the market needs in order to improve hub/unit assemblies with greater integration for sophisticated performance systems.

Junshi Sakamoto

Simulation Technology for Developing EPS Brushless Motors

Yuushi Momo, Chunhao Jiang and Sachio Nakayama
NSK STEERING SYSTEMS Co., Ltd.

ABSTRACT

In recent years, market share for electric power steering (EPS) systems has expanded from compact and subcompact vehicles to include midsize vehicles. In this article, we will discuss the development process of NSK's EPS brushless motor. Some important highlights to be discussed are as follows:

• Evolution of a brush motor (power-assist steering motor) to a brushless motor that provides higher power output.
• Development of a control system that meets diverse steering performance requirements.
• Improvements made for increased fuel economy and reduced exhaust emissions.

In order to meet the demands of our customers, we have had to shorten our development time to correspond with the release of new vehicle models and have had to reduce prototype-manufacturing costs. The necessity to make some design trade-offs in order to meet these requirements, while ensuring an optimum quality design, has played an important role in our development process. Consequently, we succeeded in applying these requirements towards the design of our EPS brushless motor by applying the V-model for simulation modeling.

1. Introduction

In recent years, market share for electric power steering (EPS) systems has expanded from compact and subcompact vehicles to include midsize vehicles, in order to improve integral performance, such as lane-keeping assist systems, emergency driver-assist controls, etc., and fuel economy to ensure environmental compatibility in comparison to hydraulic systems. Technological requirements needed to support this trend toward larger vehicle applications include the following:

• Migrate from brush motors to brushless motors for increasing output capability to provide drivers with power assist steering.
• Control system to meet a wide variety of steering performance requirements.

Some of the challenges we face in EPS development include shorter lead-time due to increasingly frequent vehicle model changes, the need to reduce prototyping costs, and the need to compromise in order to achieve an optimum quality design. In order to respond effectively to these challenges, NSK has successfully applied the requirements given above towards the design of an EPS brushless motor by applying a V-model for simulation modeling. In this article, we will report on the development process of NSK EPS brushless motors.

2. Development Process of EPS Brushless Motors

2.1 Challenges faced in development of the EPS brushless motor

EPS products are currently faced with market-driven demands including shorter development periods, requirements to reduce prototyping costs, and requirements to improve design quality. However, the development process of EPS is becoming system-oriented, more complex, and requires a high-level development process. In the development process of an EPS brushless motor, making compromises must be considered in product design. In order to develop a prototype, more than three months is also required.

As a result, the Plan-Do-Check-Act (PDCA) cycle of development was somewhat limited by the short development period available for the conventional development processes. Therefore, the most important task was to immediately improve a development process of the EPS brushless motor. In this paper, we will discuss the process of brushless motor development in detail. Performance requirements of EPS brushless motors include:

• Lower cogging torque
• Lower torque ripple
• Lower torque loss
• Noise reduction

There are numerous compromises. Fig. 1 illustrates characteristics related to the required performances of brushless motors. Typical examples include a trade-off between a high power motor and the performance requirements of torque loss, noise, and steering feel.

Torque loss is increased as a result of higher motor output, which leads to increased magnetic flux density and iron loss. This increased torque loss is one of the main factors that substantially impact steering feel, including decreased sensitivity of the reactive force from the steering wheel around its neutral position. Luxury vehicles with larger engine displacement also require higher motor output while higher levels of noise reduction and steering feel are in demand in this segment.

In an EPS system, the motor shaft is mechanically connected to the steering wheel, which conveys vibrations directly to the driver's hands. Therefore, pulsating torque,

which consists of torque ripple and cogging torque generated in the motor, is one of the main factors that has a negative impact on steering feel. These kinds of torque are required to be on the order of one-thousandth that of the rated torque for high output motors because torque ripple, cogging torque, and torque loss are transmitted to the driver after being multiplied by the inverse of the reduction gear ratio between the worm and the worm wheel.

One of the requirements to ensure driver and passenger comfort is to reduce the amount of noise generated by the EPS system since the driver interacts directly with it. The principal source of noise generated in an EPS system comes from the motor. Therefore, motor noise is the primary target for enhancing noise reductions.

Specifically, magnetic noise, including noise from the controller, and mechanical noise are generated from the bearings. Since these noises are transmitted as a radiated noise generated from the motor, the noise source itself needs to be reduced.

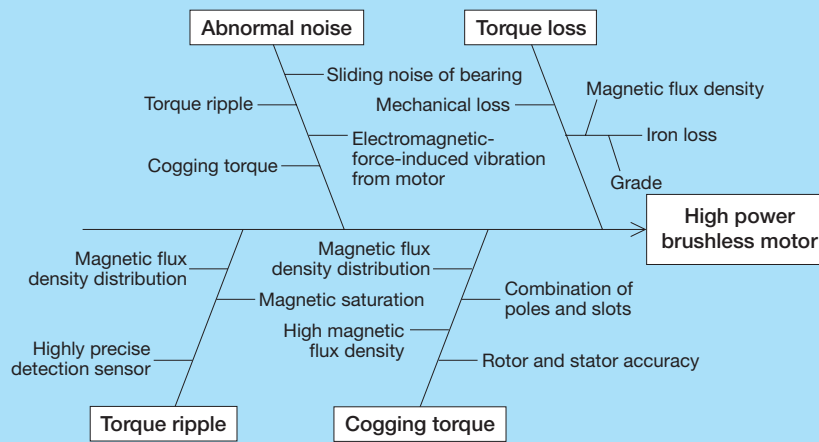Since there are compromises that must be considered in

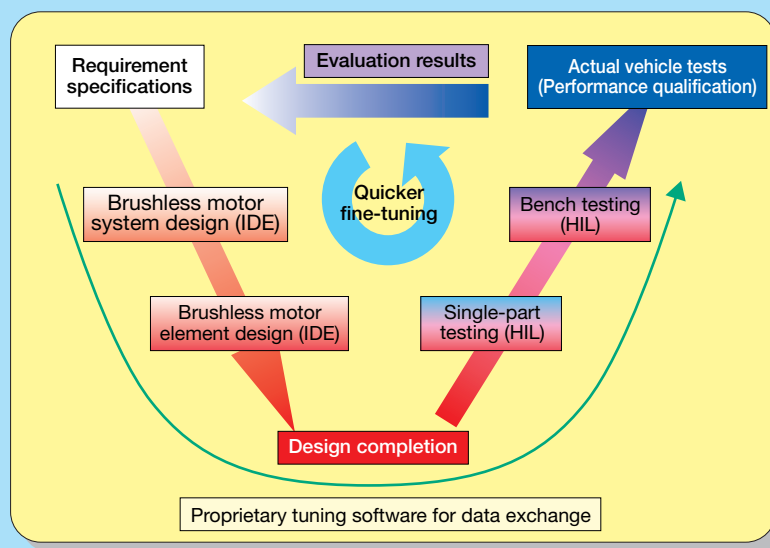Fig. 1 The required performance for brushless motor

Fig. 2 Outline of V character model

the design of brushless motors under development, improving the development process utilizing simulation technology is expected to provide effective solutions. Depending on the design specifications, some capabilities can be evaluated during the development stage of each element, but others should be evaluated on an actual vehicle. We established a new development process based on a V-model to reflect evaluation results corresponding to development phases.

2.2 Advantages of brushless motor development based on a V-model

This section provides an overview of the V-model. The V-model is a graphical representation that consists of two tails. The left tail represents the specification phase, and the right tail represents the testing phase. Design specifications are defined and flow down on the left side. The bottom of the V where the two tails meet represents the design phase. The design specifications, which flow up on the right side, are evaluated to see if performance conforms to design specifications.

The V-model clarifies the relationships between the entire design process and the evaluation process. This approach is widely accepted as a process methodology leading to product quality improvement. Making use of the V-model for brushless motor development in NSK, we divided the specification phase into required specifications, system design, and element designs, with each step corresponding to actual test driving, bench tests, and single-part tests in testing phase.

Making use of MATLAB®/Simulink®∗ and NSK's proprietary tuning software during all processes of the

V-model, the integrity of data exchanged between processes and sharing of database information are made possible. Fig. 2 illustrates the V-model development process.

2.2.1 First Stage: Required specifications and actual vehicle testing

At the first stage (first horizontal pair), actual vehicle tests are performed to see if the required specifications are satisfied or not. Evaluation at the last step determines merchantability of a given product. If the required specifications are not satisfied at this stage, the design is reviewed from the 1st step. Through each stage, evaluation results should be carefully reviewed and contained (stage containment) before proceeding to the next process (stage) to ensure that no defects will be detected in the last step.

2.2.2 Second stage: System design and bench testing of the brushless motor

At the second stage of system design of the brushless motor, a fundamental control system and basic specifications of the brushless motor are built, and bench tests are conducted for validation and stage containment. Simulation techniques are employed to develop basic specifications for brushless motors, and design reviews including control systems are performed. At this stage, we built our integrated development environment (IDE) focusing on an optimal brushless motor system design by developing interfaces between MATLAB/Simulink and JMAG. In this process, bench tests are performed to see whether test results satisfy the system design specifications or not.
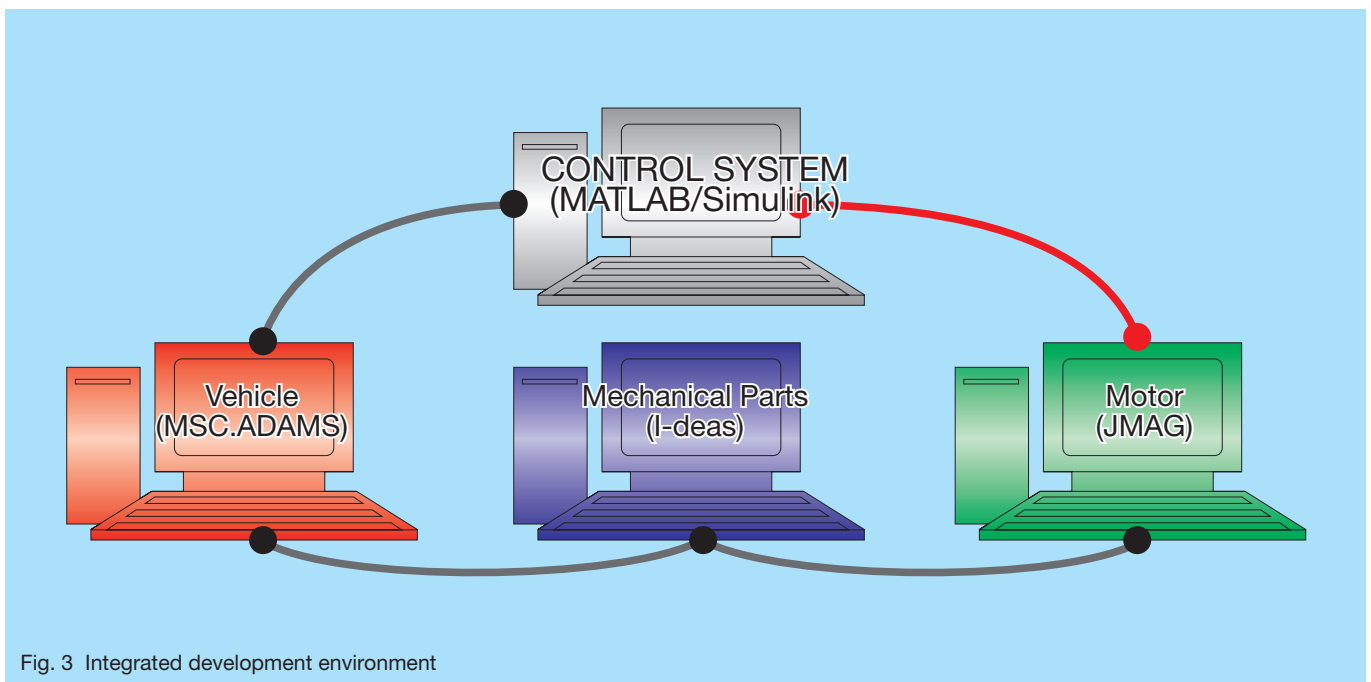

Fig. 3 Integrated development environment

2.2.3 Third stage: Brushless motor element design and single-part testing

The third stage comprises the processes of receiving the best suitable specifications factor obtained in the second stage, executing each single product test for specifications designed in detail for each element, and inspecting adjustability to the specifications. At this stage, the following three approaches are used for validation.

(1) EPS control system specifications

Making use of MATLAB/Simulink, validity of specifications is evaluated, control specifications are examined, algorithms are constructed, and identification with control specifications are executed and evaluated in the EPS control system.

(2) ECU detailed specifications

The ECU detail design is evaluated making use of TargetLink. The improvement of development efficiency and the shorter development period can be obtained by automatically generating programs written in the C programming language from a model created with MATLAB/Simulink using TargetLink.

(3) Detailed motor hardware specifications

Detailed motor hardware design is validated making use of dSPACE. MATLAB and Simulink are integrated with dSPACE for evaluating robustness, designing functions and parameters, evaluating dispersion sensitivity, and verification of optimal motor hardware design.

3. Simulation Development Environment in the Brushless Motor System Design Phase

3.1 Simulation development in the requirements phase

In this phase, fundamental control technologies are developed and the motor's basic specifications are examined. The EPS control system was constructed using the MATLAB/Simulink, a technical computing environment; the vehicle characteristics were constructed using MSC. ADAMS*, a mechanism analyzing software; the motor characteristics were constructed using JMAG, an electric magnetic field analyzing software; and the mechanical elements were constructed using I-deas**. Further, by integrating each element, an IDE was built for the following purpose:

• Optimization of system design
• Initial review of the EPS specifications
• Evaluation of fail-safe capabilities

Fig. 3 shows an overview of the IDE. In this article, we focus on the coupling analysis method that serves as an IDE between the control system (MATLAB/Simulink) and the motor (JMAG.)

A detailed description of this methodology is described here.

3.2 Brushless motor system design method utilizing an IDE

*MSC is a registered trademark of MSC.Software Corporation.
**I-deas is a registered trademark of UGS Corporation.

In system design, the coupling analysis approach for MATLAB/Simulink and JMAG is used to develop optimum system requirements.

MATLAB is a technical computing environment integrating numerical computation for scientific technical computation, data analysis, data visualization, and programming capabilities. Simulink is a packaged software most commonly used for model-based design of dynamic systems that enables us to develop reliable control systems in a shorter period.

In the MATLAB/Simulink model, however, the motor characteristics are expressed as a simple model with only two input items of resistance and inductance. Therefore, cogging torque, armature reaction, inductance variation, and torque loss, which are important characteristics for evaluating a motor, are not considered, and consequently the compromises cannot be sufficiently examined.

JMAG is a proven and top-rated magnetic field analysis program that supports the development and design of electromagnetic devices such as motors. JMAG provides accurate analysis for motor units, but cannot examine optimization for the entire system since it does not cover characteristics of drive circuits and current control methods.

A simulation development environment integrating the analysis approaches for the JMAG motor model and the MATLAB/Simulink drive control system was needed to address this issue. We reviewed the coupling analysis approach for JMAG and MATLAB/Simulink to develop interfaces between JMAG and MATLAB/Simulink in collaboration with The Japan Research Institute, Ltd.[1], and established the IDE shown in Fig. 4.

Fig. 5 illustrates a current control system and a drive system created with MATLAB/Simulink, and a coupled analysis of a motor model created with JMAG.

Fig. 6 illustrates simulation results for phase current and torque during commutation time when a motor model (created with JMAG) is incorporated into a drive control system model (including inverter circuits and current detection) that is built with MATLAB/Simulink, where the parameters of the current control system are appropriately chosen. One of the effective results obtained by integrated
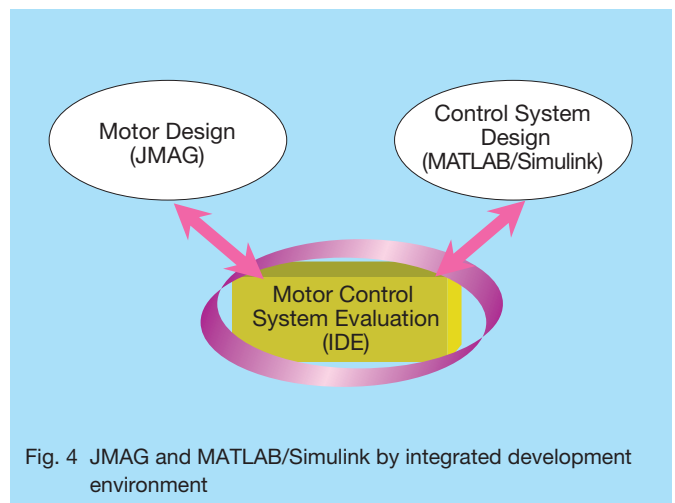
Fig. 4 JMAG and MATLAB/Simulink by integrated development environment

analysis was that current fluctuation and torque fluctuation at commutation time obtained by the integrated analysis were lower than the results obtained by separate analysis. The results obtained by integrated analysis show that torque wave form is influenced by armature reaction among others in comparison to a simulation result created with MATLAB/Simulink.

Furthermore, the results obtained by integrated analysis show that torque waves have less ripple or fluctuation in comparison to the simulation results created with JMAG. Therefore, the results agree with the vehicle characteristics obtained from experiments.

4. Simulation Development Environment for Brushless Motor Element Design Technology

In the element design process, IDE software assets developed during the system design phase are combined together and incorporated with MATLAB/Simulink as a single platform. Common data from this platform is shared with dSPACE and TargetLink, thus improving the development efficiency. Each process in each element development is described in the following paragraphs.

4.1 Simulation technology for control system design

In this process, an evaluation making use of a simulation in the process of a detailed examination of the control design is executed.

In order for the model built in an IDE, the control specifications with MATLAB/Simulink are examined, the algorithms built, identification of control specifications is

evaluated, and finally the validity of the specifications is evaluated.

Validity of control specifications are evaluated as follows:
- Optimization of motor commutation and voltage saturation
- Optimization of motor counter EMF estimation

Fig. 7 provides an example showing simulation results of motor commutation current control.

The right side of Fig. 7 shows the relationship between current waveform and torque under conventional current control. This figure proves that the current pulse causes torque fluctuation. Since this torque pulse is the main cause of noise, it should be prevented.

The results obtained by taking measures against the current waveform ripples are shown on the left. Eliminating waveform turbulence from commutation substantially reduced torque pulse.

4.2 Simulation technology in ECU design

In this process, the ECU detail designs are evaluated using TargetLink. The C programming language automatically generated from MATLAB/Simulink via TargetLink enables improved development efficiency and reduced development time.

4.3 Simulation technology in motor hardware design

In this process, detailed designs of motor hardware are evaluated through control system simulation using dSPACE and the actual motor hardware.

Features of dSPACE simulator include:
- A wide variety of installed interface functions
- Implementation of Simulink-based models
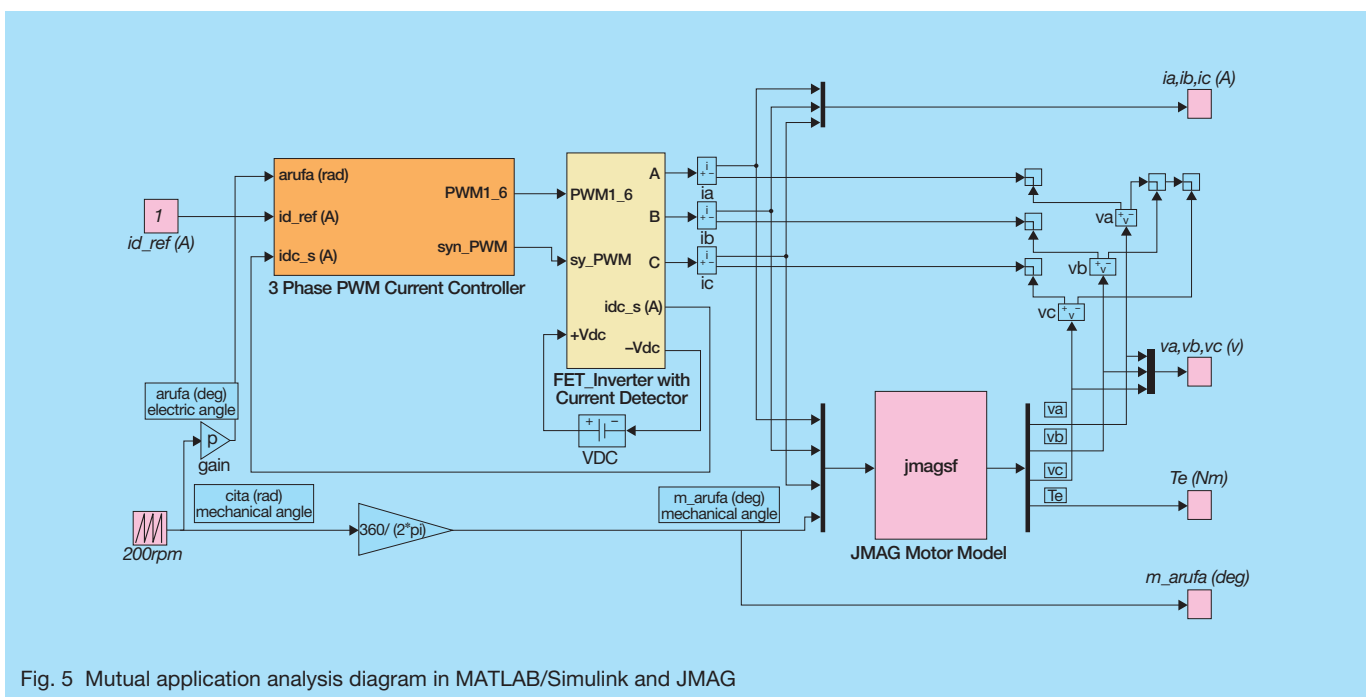
Fig. 5 Mutual application analysis diagram in MATLAB/Simulink and JMAG
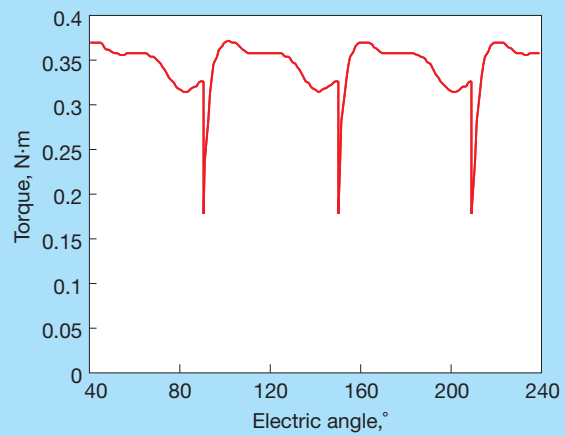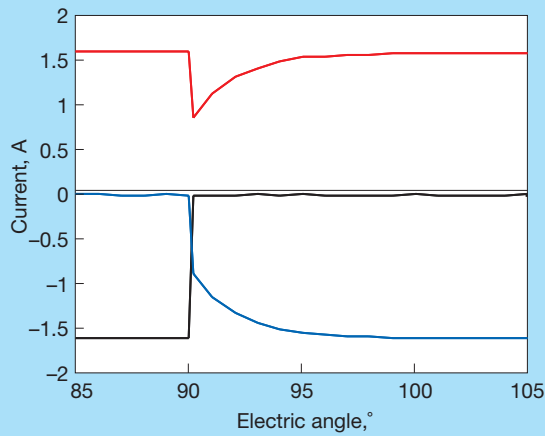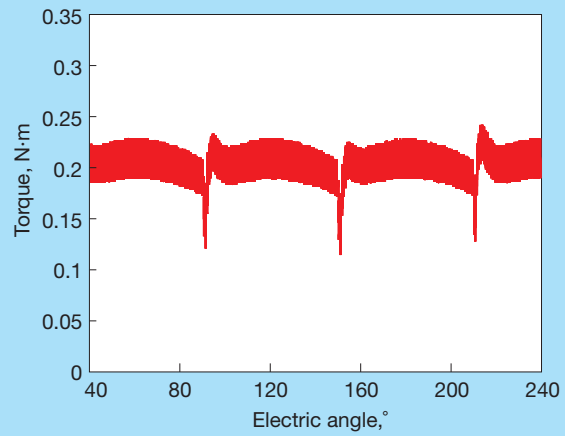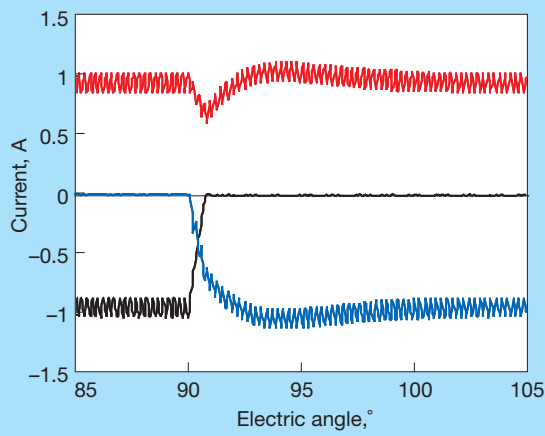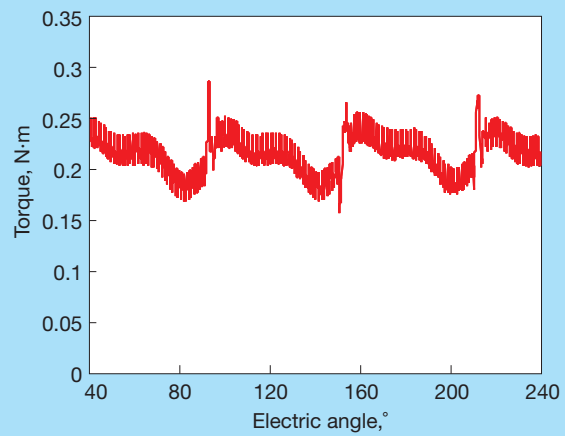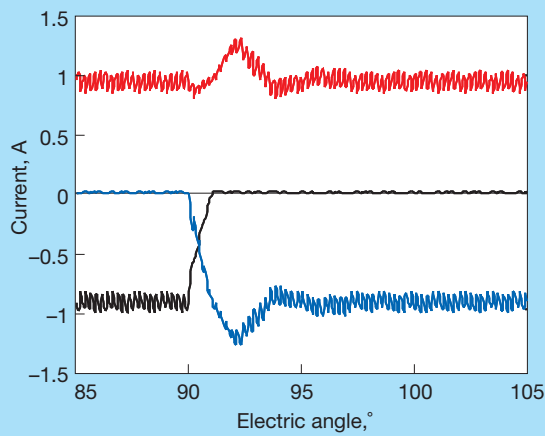
Fig. 6 Simulation result by JMAG MATLAB/Simulink and mutual application analysis

• Quick coding to implementation
• Interactive operations allowed for monitoring and data measurement
• Online parameter tuning

• Continuous display of variables
• Display of two or more running instrument panels
Making use of dSPACE, we can efficiently evaluate robustness, incorporate design functions, incorporate
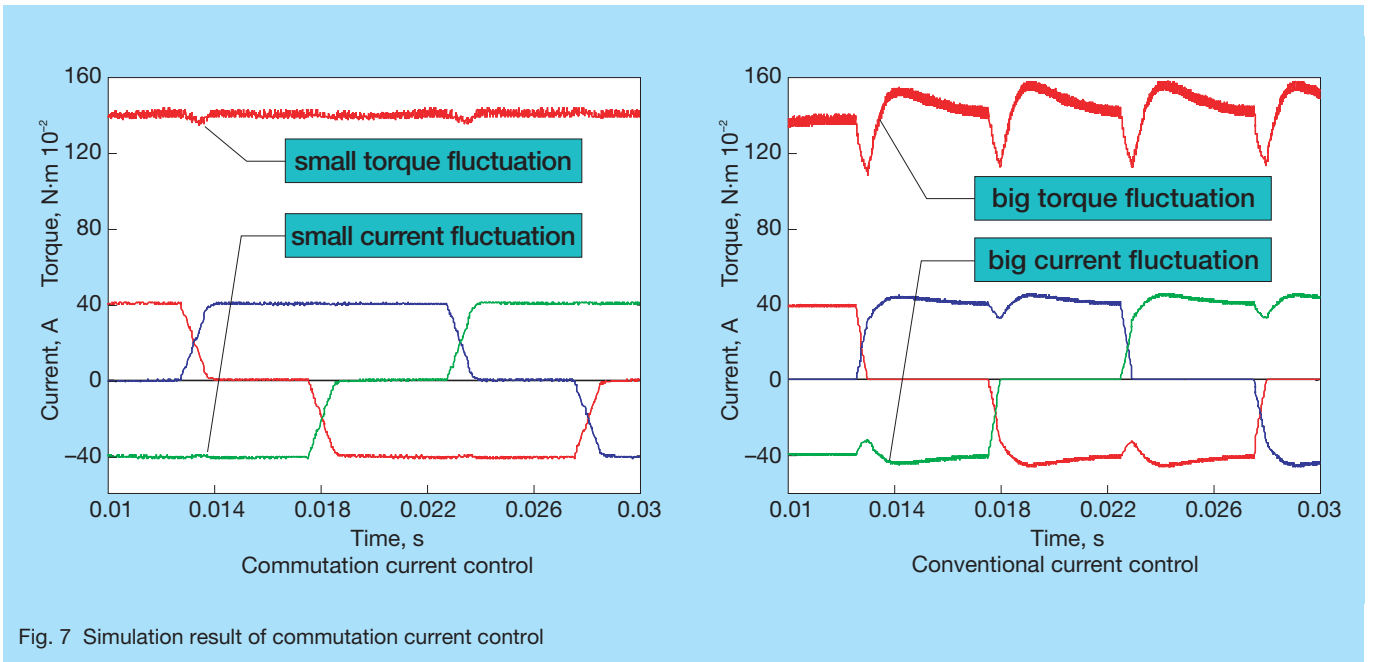
Fig. 7 Simulation result of commutation current control
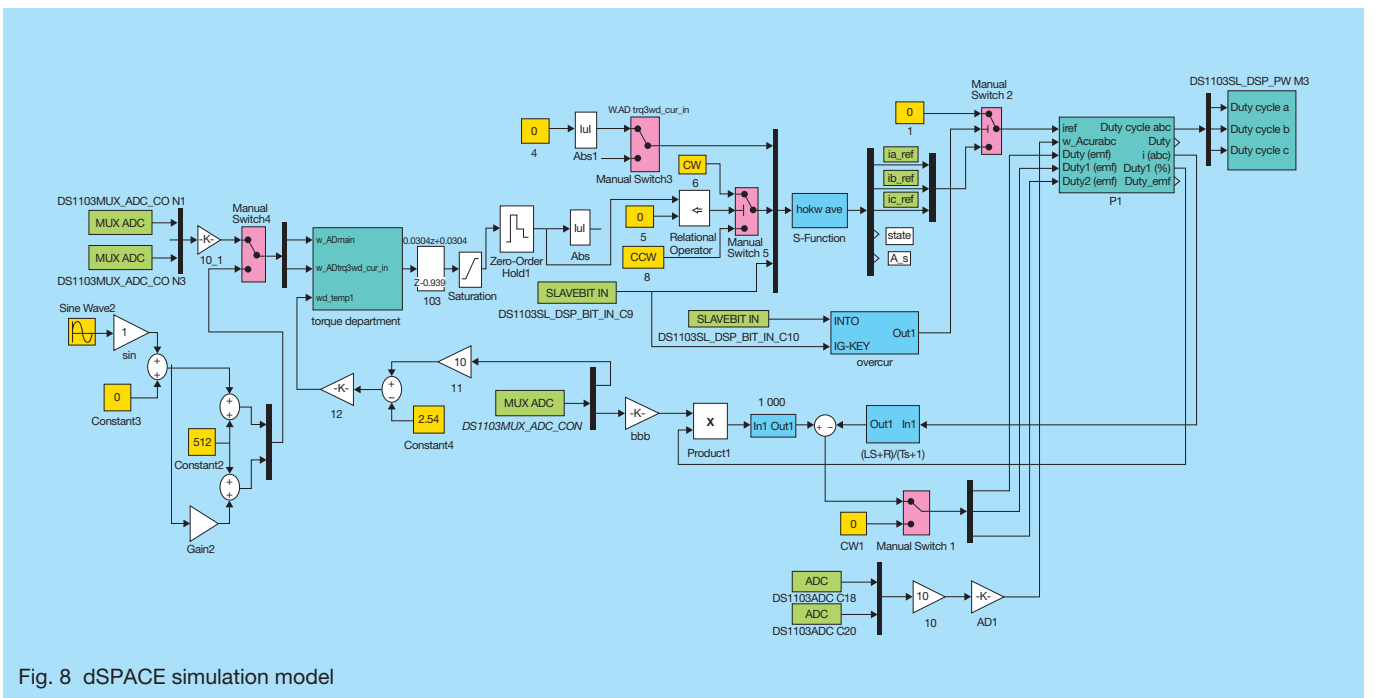
Fig. 8 dSPACE simulation model

parameter designs, and evaluate motor hardware dispersion sensitivity.

Fig. 8 shows the dSPACE simulation model for brushless motors.

5. Integration of Test Drives and Simulation Technologies

Fig. 9 shows an overview of the driving simulator environment for modeling actual test-drives and simulating actual test-drives. This section describes the device for simulating steering reactive force. The actuator control is executed on the basis of the rack shaft force calculated by inputting a steering angle signal and a steering angle velocity signal of a steering wheel into a vehicle model built into a computer.

Fig. 10 shows the evaluation results from actual test drives and the driving simulator. The left figure shows steering torque measured under cornering conditions while driving in a circle with an actual vehicle and

Fig. 9 Driving simulator

Steering torque measured under steady cornering

Relationship between steering angles and steering torque under stationary steering
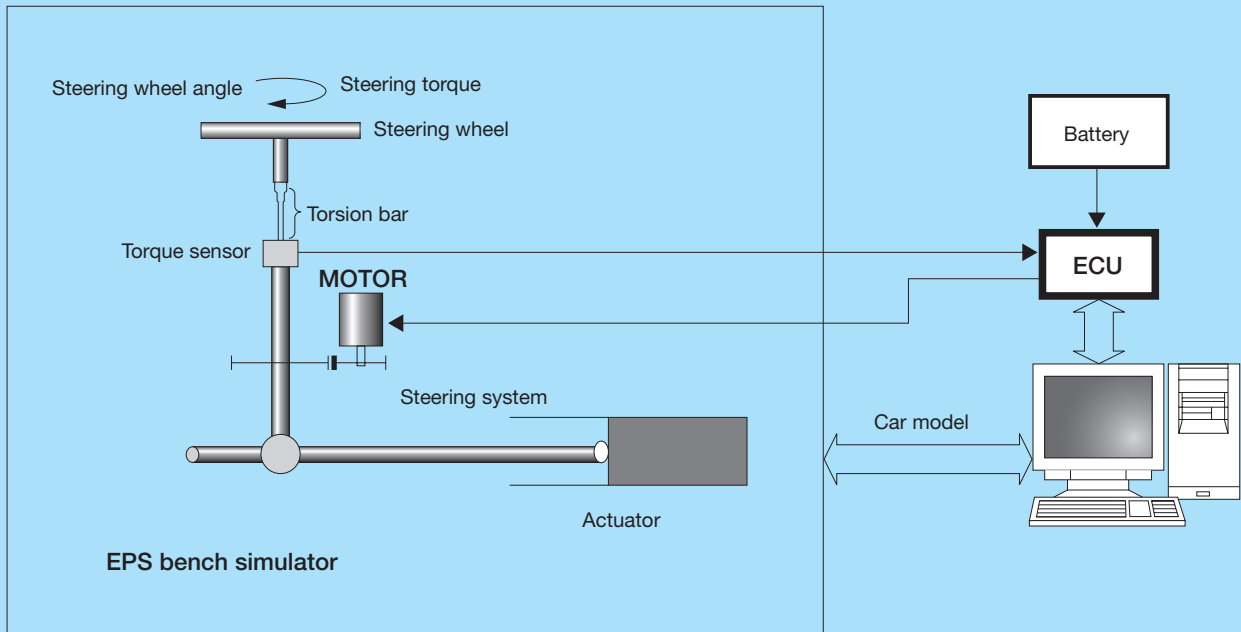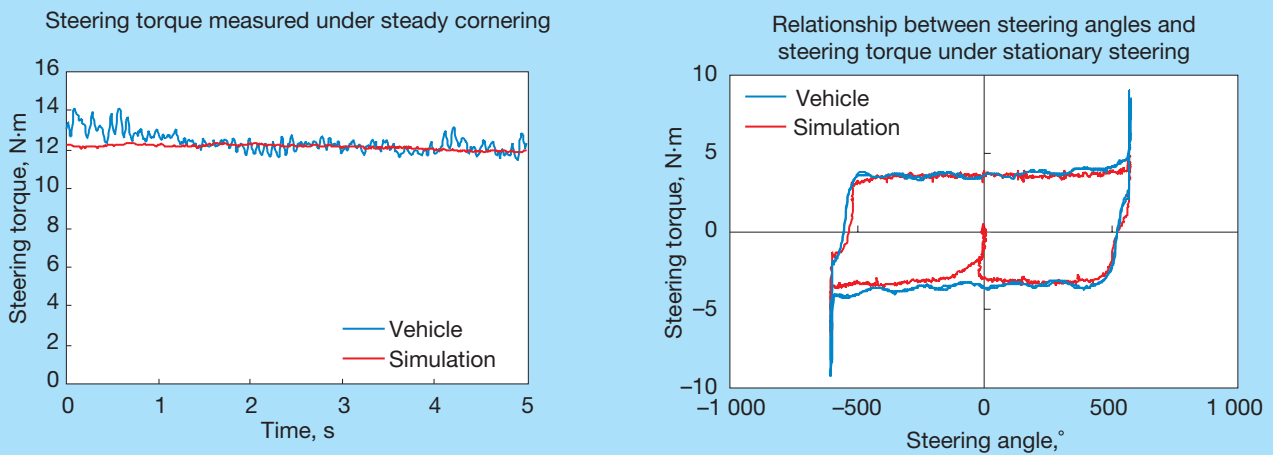
Fig. 10 Evaluation result of driving simulator and vehicle

simulation. The torque calculated by simulation is almost identical to measured results obtained from actual driving. This confirms that our simulation model was successful.

The right figure compares results from a test drive and a simulation with a focus on the relationship between steering angles and steering torque under stationary steering. As is the case for the left figure, the test drive and the simulation show almost the same results, and that the simulation results correlate well with the measured

data. This means that replicating experiments for fail-safe measures of brushless motors, which are difficult to carry out on actual vehicles, can be performed in advance.

6. Conclusion

Methods for improving specific features related to brushless motors have been established NSK's unique development process that takes advantage of simulation

technology based on a V-model in regards to performance evaluations of brushless motor development processes. By applying the aforementioned methods into EPS system development, we will develop a system that enables shorter lead-time in developing new products and allows commercialization ahead of our competitors.

References:

1) H. Chen, "Integrated Development Environment (IDE) for Motor Drive Control System Using JMAG & MATLAB/ Simulink", JMAG User Conference 2000 (2000)

Yuushi Momo

Chunhao Jiang

Sachio Nakayama

Latest Trends and Technologies of Automotive Electrical Component Bearings

Masamichi Iketani, Bearing Technology Center

ABSTRACT

This article discusses the latest trends and technologies of the electrical accessory bearings for alternators, air conditioner compressors, idle pulleys, water pumps, and electrical accessory motors.

1. Introduction

A wide variety of serious challenges facing the automobile market are driving ever-increasing demands for improved fuel economy, higher efficiency, safety, and comfort. Accordingly, more sophisticated and unitized bearings are in demand for the electric equipment of automobile engine components. This article discusses the latest trends and technologies involved in bearings for use in automotive electrical components.

2. Alternator Bearings

2.1 Operating environment

High-performance engines, electronic controls, and electric equipment that have been increasingly used require more power, resulting in demand for compact yet high-output alternators. Luxury passenger automobiles require further reduced noise levels; quiet operation at high speeds under high-temperature conditions is a requirement that bearings must satisfy. In light of environmental concerns, automatic idle-stop systems have been incorporated and a new type of alternator that also serves as a starter has been brought to the market. Therefore, the operating conditions for bearings are also changing.

2.2 Features

Since the mid 1980s, ribbed belts have been used to drive alternators (Fig. 1). We have been concerned about flaking resulting from white microstructural changes detected on the front bearing outer ring of the alternator at early stages. In 1992, NSK developed MA7 grease, which is a urea-ether based grease to address the flaking problem, and to help satisfy the demands for prolonging bearing life at high temperatures and speeds. Even with MA7 grease, however, white microstructural flaking similar to that previously mentioned only occasionally occurs under the most severe of operating conditions. (See Photo 1.)

We then refocused on determining how this flaking occurs, specifically on how static electricity facilitates the infiltration of hydrogen into steel. To permit electrical discharge, NSK added carbon-black to a grease to develop HAB grease for improved conductivity. Table 1 shows the main characteristics of HAB grease and conventional grease products. Fig. 2 illustrates our alternator simulation test results using very rigorous conditions.

3. Air-Conditioner Pulley Bearings

3.1 Operating environment

A pulley that is rotated by an engine accessory belt drives an air-conditioner compressor. Since the pulley uses an electromagnetic coupling (electromagnetic clutch) for engaging or disengaging power transmission, the compressor can be rotated only when the air conditioning is actually needed. In the center of the pulley, a double row angular contact ball bearing is mounted and used for rolling the outer ring. Today's higher-speed and more space-saving compressors increase the demand for more reliable miniature bearings that can function under high temperatures at high speeds.

3.2 Features
3.2.1 Highly reliable grease

Air-conditioner pulleys operate under severe operating conditions at a maximum speed range of 7 000 to 13 000 min^{-1} under a 1 500 N maximum radial load with a maximum 25 mm off-set at a maximum of 160 °C. Therefore, more reliable grease is vital to prolonging bearing life under high-temperature and high-speed conditions.

NSK developed MA6 grease by improving seizure and flaking resistance of traditional ENS grease. We then developed MA8 grease by further improving the flaking resistance of MA6. MA8 grease is widely used for its enhanced reliability, and is packed in most compressor pulleys. Typical properties of NSK grease products are shown in Table 2.

3.2.2 Optimum cage pocket profile

In addition to reliable greases, NSK developed a new molded-plastic cage with a spherical pocket profile (for lubricant reservoir) and cylindrical shaped profile in the axial direction where the ball contacts the cage (Fig. 3). As shown in the Fig., opposing sides of pocket profile that were initially spherical, have been cut in a cylindrical shape in the axial direction to enable a constant supply of lubricant for rolling elements during rotation in the spherical profile of the pocket.
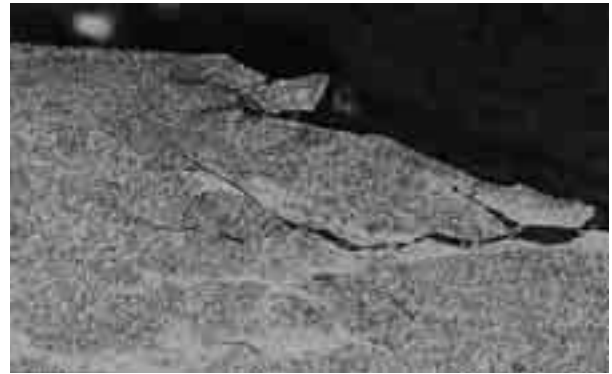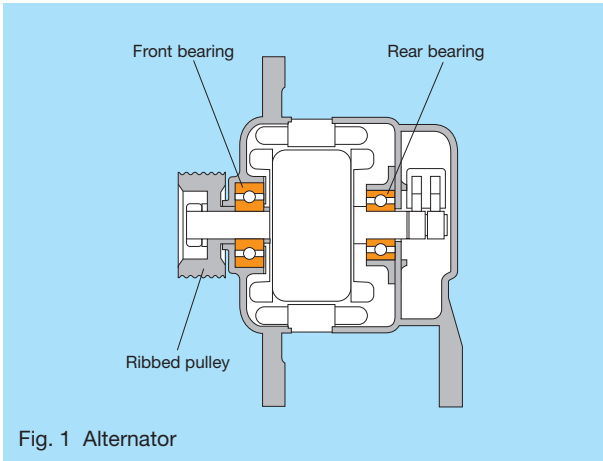
Fig. 1 Alternator

Photo 1 White structure flaking

Table1 Grease characteristics

Grease		HAB	HA1	MA7
Color		Black	Light brown	Light brown
Thickener		Diurea	Diurea	Diurea
Base oil viscosity	40℃	100	100	100
mm^2/s	100℃	13	13	13
Worked penetration 25℃		290	280	290
Torque (low temperature) –30℃	Starting	300	330	300
mN·m	Rotation	100	120	200

Test conditions
Test bearing : 6303 or 6303 equivalent
P/C : 0.10
Speed : 10 500rpm
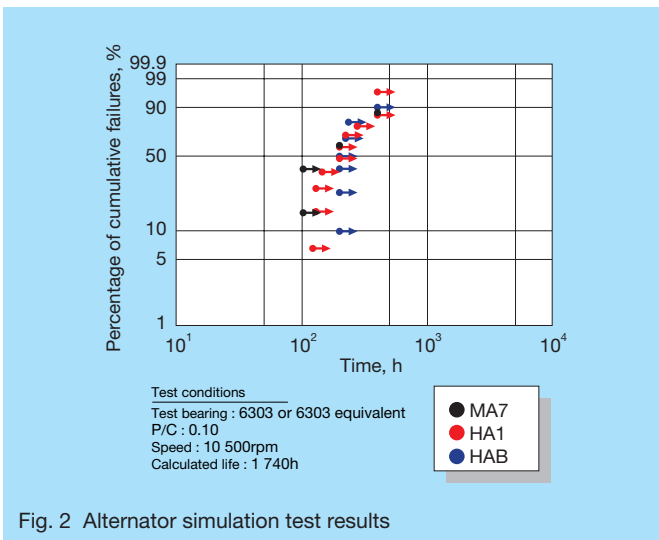Calculated life : 1 740h

● MA7
● HA1
● HAB

Fig. 2 Alternator simulation test results

3.2.3 High-performance seals

Air-conditioner compressor pulley bearings are operated under conditions of high loads, extreme temperatures, and varying speeds as described above. In addition to compressor pulley bearings, other engine accessory pulley bearings must be resistant against water and dirt that can accumulate from operating a vehicle in all manner of road conditions and wet weather. To satisfy these requirements, NSK uses high-performance contact seals

for the rolling outer ring. Table 3 shows the typical types of seals and their degree of sealing performance.

3.2.4 Space requirements

Today's compact air-conditioner compressors are accelerating demand for even smaller bearings. At NSK, we offer bearing products in a wide range of sizes to meet downsizing needs of manufacturers. Table 4 shows our main bearing products.

4. Belt Tensioner/Idler Pulley Bearing Units

4.1 Operating environment

A serpentine drive belt that transmits power from the engine's crankshaft drives engine accessories, including the alternator and air-conditioner compressor. Belt tensioner pulleys (idler pulleys) are used to guide and maintain tension on the belt. In recent years, a single serpentine drive belt is typically used to drive all the various engine accessories (See Fig. 4) thus saving space in the engine compartment (bay) since there is no need to stack or stagger all the pulleys and accessories. The number of V-shaped ridges has also started increasing to as much as eight on some belts in new vehicles for improving power transmission capability.

An automatic tensioner pulley is typically placed on the slack (or nonload-carrying) side of the belt in the drive
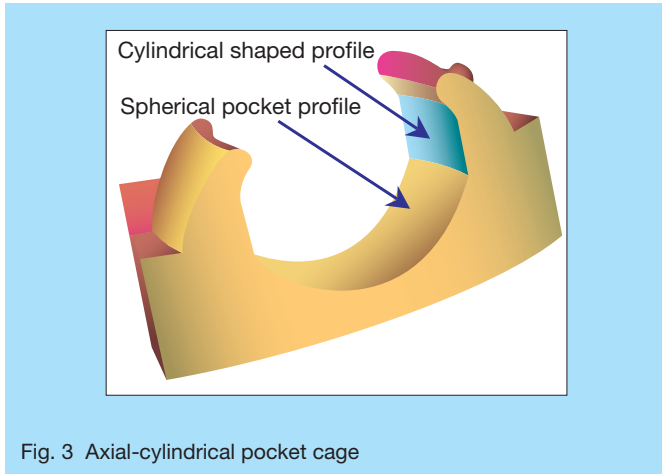
Fig. 3 Axial-cylindrical pocket cage

direction. Axial load on the pulley bearing is determined by the amount of tension that the pulley applies to the belt. The idler pulley is placed on the tight (load-carrying) side and has a larger area of contact with the belt, thus receiving considerable load including variable loads from accessories such as the air-conditioner compressor. Requirements for pulley bearing units include high-load capacity, high-temperature and high-speed durability, and high-performance seals. Given that these units are operated under substantially harsh conditions, we have set the worst possible test conditions at 18 000 min⁻¹ under a 3 000 N load.

4.2 Types

Pulleys come in two basic types: grooved (V-ribbed) pulley and flat or crowned pulleys. The ribbed side of a serpentine belt mates with the grooved pulley, and the smooth backside of the belt wraps around the flat pulley. Pulleys are manufactured using machining process, press forming, or injection molding of a resin material for weight and cost reductions (Fig. 5). Resin pulleys make use of special molding technologies to improve manufacturing quality and use materials that are resistant to chemicals used for deicing winter roads.

Typical bearing products include 6301 and 6203. NSK has developed and uses comparable specifications with those for air-conditioner pulley bearings to attain the required performance of these bearing units:
a. Axial cylindrical pocket cage: Improves lubrication for quiet operations in low-temperatures and greater seizure resistance.
b. DUM customized seal: Improves water resistance, prevents grease leakage, and provides low-torque and high-sealing performance
c. MA or HA grease: Prevents subsurface originating flaking (white microstructure cracking) and greater seizure resistance
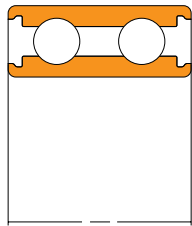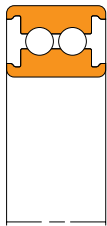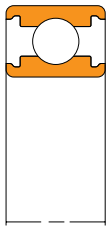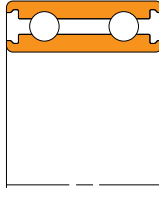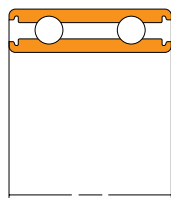
Table2 Grease characteristics

Grease		ENS	MA6	MA8
Color		Creamy white	Light yellow	Light yellow
Thickener		Diurea	Diurea	Diurea
Base oil viscosity	40℃	32	79	76
mm²/s	100℃	5.8	11	11
Worked penetration 25℃		276	265	276
Torque (low temperature) −30℃	Starting	107	190	176
mN·m	Rotation	27	40	39

Table 3 Types of seals and sealing performance

Seal type	DU	DUK	DUM	New DUM
Seal structure				
Under high-speed operating conditions	○	○	◎	◎
Water and dust resistant properties	○	◎	◎	◎
Grease leakage rates	○	○	○	◎

Table 4 Bearing specifications

Bearing number	35BD5222	35BD5212	BY35	35BD4820	35BD4520
Bearing structure					
Outside diameter (mm)	52	52	52	48	45
Bore diameter (mm)	35	35	35	35	35
Width (mm)	22	12	12	20	20

5. Water Pump Bearings

5.1 Operating environment

Fig. 6 shows the cross-section view of a water pump bearing. Water pumps are required to provide optimum reliability while reducing weight in line with the increasing demand for long-lasting high-performance fuel-efficient automobiles. Todayís high-performance engines generate massive amounts of heat from the combustion process, creating greater challenges for water pumps. To address these challenges, NSK has improved the water pump bearing seals for optimum reliability in addition to offering various types of bearings to meet weight reduction requirements.

5.2 Features

We conducted an investigation of used bearings in the marketplace and learned that most failures were caused by coolant entering through the mechanical seal into the bearing interior and adversely affecting lubrication. We

Fig. 4 Engine belt layout

improved sealing performance to minimize the amount of coolant or moisture reaching the main lip, by providing a third lip and flinger to the conventional seal, thus reducing the effect of water on the main lip and stopping it from further entering the bearing. Fig. 7 illustrates the types of seals and Fig. 8 shows the results of our comparison tests.

6. Motor Bearings

6.1 Operating environment

The growing reliance on enhanced electronic controls as well stricter requirements regarding fuel efficiency, higher performance, and safety, have resulted in a substantial increase of motors used in passenger vehicles. Automobiles use electric throttles, idle speed control valves (ISCV), and exhaust gas recirculation (EGR) systems to reduce toxic emissions; electric power steering (EPS) systems, electric water pumps, and electric fans to improve efficiency; and antilock braking systems (ABS) for safety. Most of these are driven and controlled by motors. When fuel cell vehicles (FCV) come into practical use, the demand for motors will rapidly grow.

6.2 Features

The following sections describe the features of bearings used for common automotive motors.

6.2.1 Electric fan motor bearings

Electric fan motor bearings are required to have long life under high-temperature operating conditions while maintaining a close tolerance fit. However, fan motor manufacturers demand that bearing makers reduce the number of component parts, such as snap rings. NSK solved this dilemma with heat-resistant grease, heat treatment of the inner and outer rings, and non-contact metal shields with high-sealing capability. The following bearing specifications ensure that the bearings provide
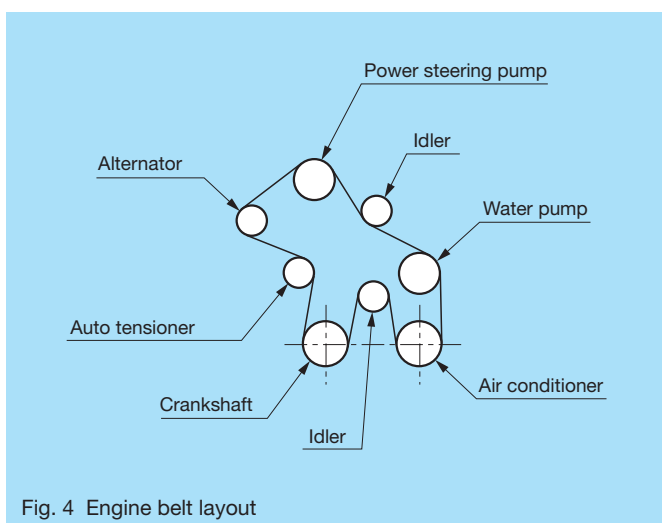
Fig. 5 Types of pulleys

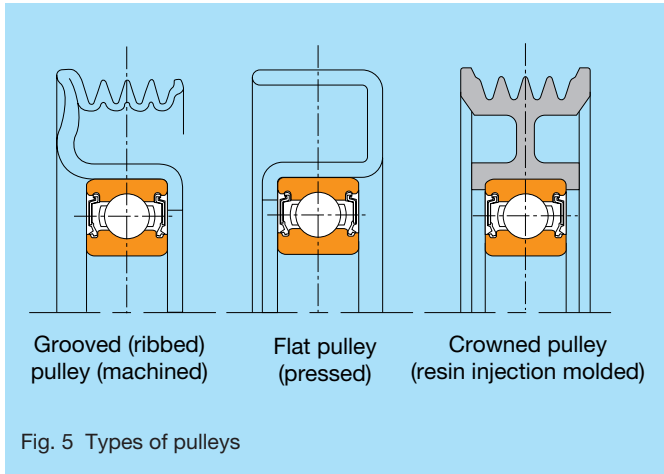Grooved (ribbed) pulley (machined)

Flat pulley (pressed)

Crowned pulley (resin injection molded)

excellent performance:

    a. Seal: high sealing-type shield (ZZ1)

    b. Cage: plastic cage

    c. Grease: EA3 grease (special-purpose grease)

    d. Heat dimensional stabilization treatment: special heat treatment (Note: special heat treatment for dimensional stabilization also improves indentation resistance.)

6.2.2 Blower motor bearings

    Advancements in development and performance of blower motor bearings, including the conversion from sliding bearings to roller bearings, have been made for improved reliability and reduced assembly costs. Whereas a blower motor is located on the passenger compartment (cabin) side of the engine bay firewall (behind the dash trim paneling), the blower motor bearings must operate quietly. Key specifications are as follows:

    a. Seal: light contact DDW seals

    b. Cage: plastic cage

    c. Acoustic rating: extremely low level (ERU6)

    d. Grease: NS7 grease with excellent acoustic qualities

    e. Indentation resistance in case of poor handling: special heat treatment (Note: Heat dimensional stabilization was also achieved. See Fig. 9 for indentation resistance.)

6.2.3 ABS pump/motor assembly bearings

    Antilock braking systems (ABS) have a pump/motor assembly that uses either a single or dual piston-reciprocating pump. Mounted to the output shaft is a ball or needle bearing assembly consisting of an eccentric inner ring and outer ring that functions as an eccentric cam. Piston plungers are held in contact with the outside surface of the bearing's outer ring and reciprocate when the eccentric drive is running. With each stroke of the piston plunger, output of the pump (pressurized brake fluid) is delivered to the accumulator (Fig. 10). Traditionally needle bearings or standard ball bearings
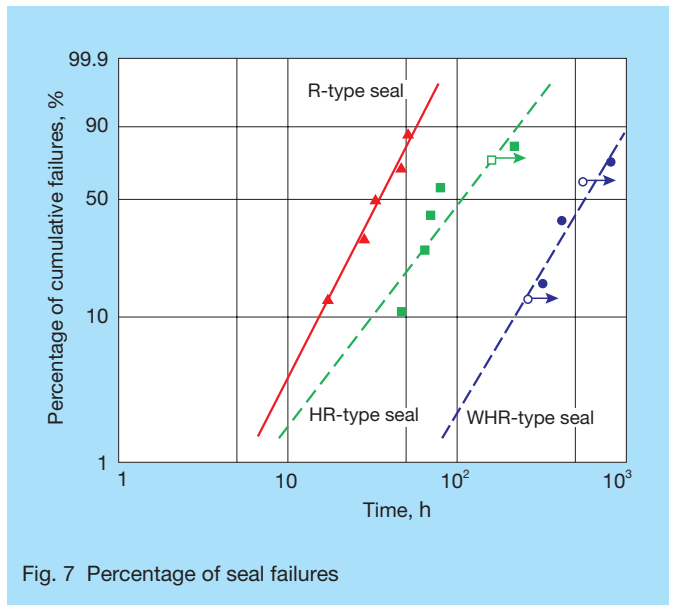
Fig. 7 Percentage of seal failures

Fig. 6 Cross-section view of water pump bearing
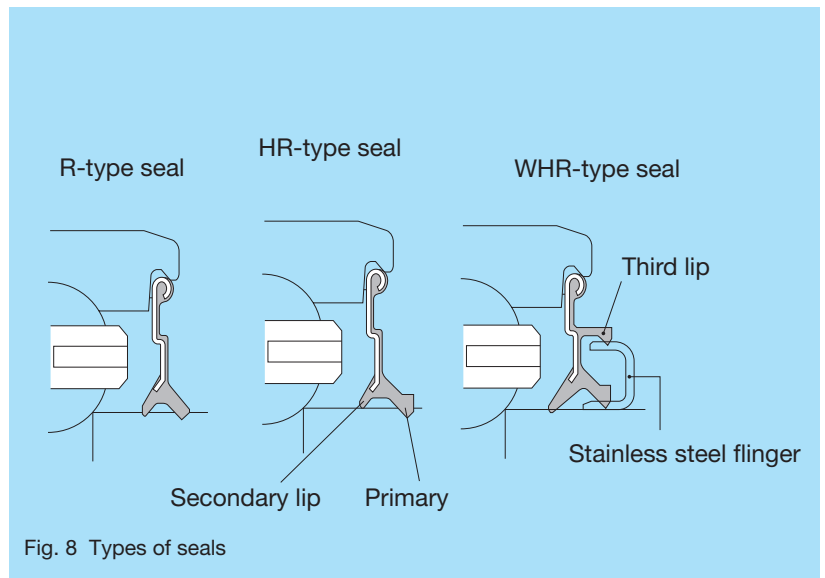
Fig. 8 Types of seals

are used for the eccentric cam, but the use of a bearing with an eccentric inner ring has come under review to reduce the machining cost of the eccentric cam.

6.2.4 Throttle valve support bearings

Throttle bodies, including electronic throttle control systems, control the amount of air intake. Traditionally, shaft seals have been used to maintain an airtight throttle body shaft, but they are increasingly being replaced with bearing seals to reduce costs. For this reason, support-bearing seals must be airtight regardless of negative or positive pressure generated in the chamber. NSK conducted a variety of analysis and evaluation tests to develop technologies that satisfy requirements for optimum airtight seal specifications.

7. Conclusion

This article discusses the latest trends and technologies related to bearings used for engine accessories. Since a wider variety of requirements will be imposed on electrical components in the future, we will make every effort to develop high-performance bearings to meet a wide range of application needs.

Fig. 9   Acceleration between special heat treatment and standard heat treatment
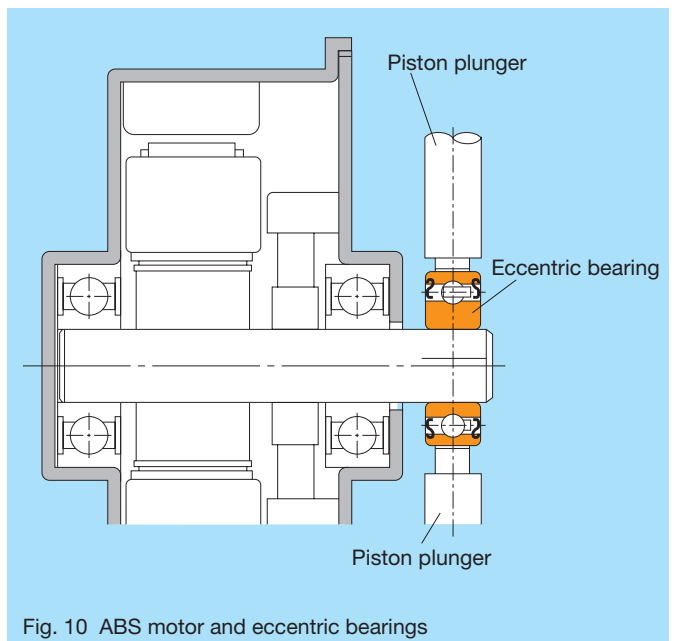
Fig. 10   ABS motor and eccentric bearings

Masamichi Iketani

Low Frictional Torque Technology of Rolling Bearings

Hirotoshi Aramaki
Corporate Research and Development Center

ABSTRACT

In recent years, low frictional torque technology of rolling bearings have had to meet increasingly stricter requirements in response to growing concerns over environmental issues, such as the reduction of green house gases and conservation of natural resources. In this article, we will briefly discuss the basics of rolling friction and sliding friction of bearings. Then, we will cover details on how bearing design, contact angle, seals, and surface roughness can influence the lowering of torque in bearings. Lubricating methods and feeding rates are also critical factors that we will expand on. Finally, examples will be given of the optimum selection of bearings for lowered frictional torque for ball bearings and tapered roller bearings.

1. Introduction

Whereas rolling bearings are a mechanical component that enables a shaft to rotate smoothly while supporting a load, it must exhibit low friction, low torque, and provide sufficient durability to transmit force with minimal loss over an extended period of time. The need for low torque technologies has become even more stringent in recent years out of concern for environmental issues, particularly the reduction of greenhouse gas emissions and conservation of natural resources.

Demand is high for low-torque bearings of machine tool main spindles that offer higher machining efficiency by controlling temperature rise under high-speed operations to prevent seizure and ultimate bearing failure. In order to develop higher speed with low torque, high-speed bearings with smaller balls and an optimal groove radius employing design and material technologies, such as wear- and seizure-resistant materials, are being developed. Standard jet lubrication and under-race jet lubrication systems that cool bearings using large quantities of oil are also used. Lubrication methods that emphasize lowered costs, energy conservation, and use minimal quantities of lubrication are being developed. Examples include oil-air lubrication[1], super lean lubrication[2], and grease lubrication[3] systems.

Size reductions made in automotive bearings have been brought about through technologies that offer longer life in terms of material and design while reducing torque. More demands are, however, being placed on reducing energy consumption by developing low-torque technologies due to environmental issues. This paper provides a brief description of the factors by which shafts produce torque and discusses the possibility of reducing torque with numerical calculation technology.

2. Friction Analysis Technology

Fig. 1 shows the friction areas of a ball bearing. Under ordinary circumstances, rolling friction is primarily produced by hysteresis loss of material due to repeated stress. Hysteresis loss of material is, however, slight for rolling bearings, so friction is primarily produced by viscous resistance of the lubrication[4].

Fig. 2 shows friction areas of a tapered roller bearing. Tapered roller bearings are designed to allow sliding between the rollers and rib contact surface, thus producing sliding friction. This sliding friction is the primary cause of friction at low speeds; friction decreases as speed increases. Conversely, there is significant friction between the rolling elements and raceway contact surface, and is predominant at medium and high speeds.

High contact surface pressure of 1 to 3 GPa is produced between the rolling elements and the contact surface of the raceway, which forms an elastohydrodynamic lubrication (EHL) oil film. When the EHL oil film is formed, friction moment is produced by asymmetric EHL fluid pressure distribution in the rolling direction and shearing resistance of the fluid near the contact entrance. This is the primary cause of frictional loss for rolling bearings.

The thicker the oil film on the contact surface (under conditions of high viscosity and high speed), or the higher the fluid pressure (under conditions of a large load), the more rolling friction increases, and the thinner the oil film becomes, the more rolling friction decreases. If the surface roughness is approximately the same as or smaller than the oil film, metal contact occurs at the rough projections that consequently support some of the load. The oil film thus partially loses load supporting capability and rolling friction decreases[5].

Sliding friction between the rolling elements and the rotating ring (usually the inner ring) is the driving force by which the rolling elements rotate. Rolling motion is caused by sliding friction produced to counterbalance rolling friction (resistance). If rolling friction exceeds sliding friction, geometric rolling cannot occur and a type of sliding referred to as "skidding" occurs. This phenomenon tends to occur under low loads and high-speed rotation. If contact occurs at high speeds, there is danger of wear and surface damage called "skidding

Fig. 1 Friction areas of a ball bearing

Friction between the inner and outer ring, and rolling elements (predominant under oil lubrication)

Sliding friction between cage and rolling elements

Lubricant churning resistance

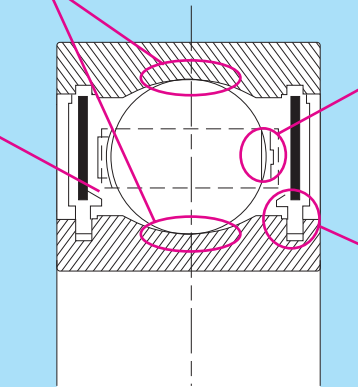Sliding friction between seal and inner ring

Fig. 2 Friction areas of a tapered roller bearing

Friction between the inner and outer ring, and rolling elements (predominant at medium and high speeds)

Sliding friction between cage and rolling elements

Lubricant churning resistance
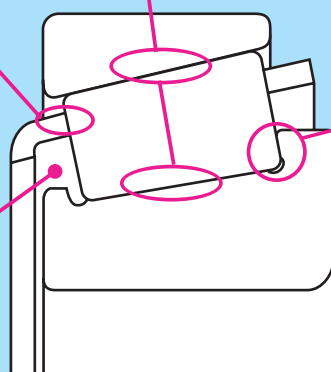
Sliding friction at rib (predominant at start and low speeds)

Sliding between inner ring rib and roller end face

F_a =9 800N
F_r =4 900N
F_r =980N
experiment
calculation

Torque loss, N·m

Rotational speed, rpm
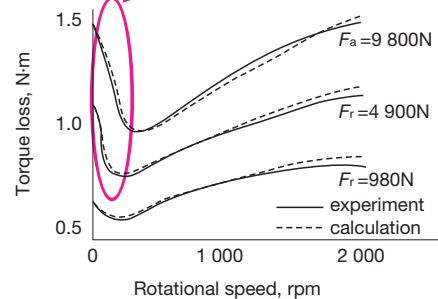
damage." With ball bearings and spherical roller bearings, positive and negative sliding friction always occurs where contact is made because of their geometric shape.

Fig. 3 shows the sliding velocity and contact pressure distribution in the contact ellipse area of a ball bearing. The figure shows that sliding velocity is distributed in the contact surface area. The parabola-shaped distribution represents sliding produced because the raceways and balls or rollers have a curvature, which is called "differential slip." Sliding that has different slip speed on the left and right edges is called "spin slip." This type of sliding occurs in angular ball bearings and spherical roller bearings. In the case of tapered roller bearings, the contact angle of the inner and outer rings is designed to intersect with the center of the shaft, so spin slippage does not

occur. Sliding distribution is determined by the size and position of the contact ellipse, so it is important to conduct a study of design specifications that take load conditions into account.

3. Factors That Affect Bearing Friction

3.1 Effect of bearing design

Fig. 4 shows the results of calculating the effect of design specifications on torque of tapered roller bearings. With "1" as the existing design value of HR30306C (72 mm outside diameter, 30 mm bore diameter, and 20.7 mm width), other design values were fixed and a parameter study was conducted. The bearing was run at 6 000 min^{-1} under a 10 kN axial load. In the parameter study of roller diameter, the

Fig. 3 Contact pressure and slip velocity distribution in the contact ellipse area of a ball bearing

pitch circle diameter (PCD) was changed to maintain a certain contact angle (cup angle), and the PCD was also altered to maintain roller diameter related to contact angle.

The red lines in the figures indicate calculated torque ratio, the green lines indicate maximum surface pressure ratio, and the blue lines indicate life ratio. Here, with the exception of the effect of roller diameter, life and torque show similar trends. In other words, as torque decreases,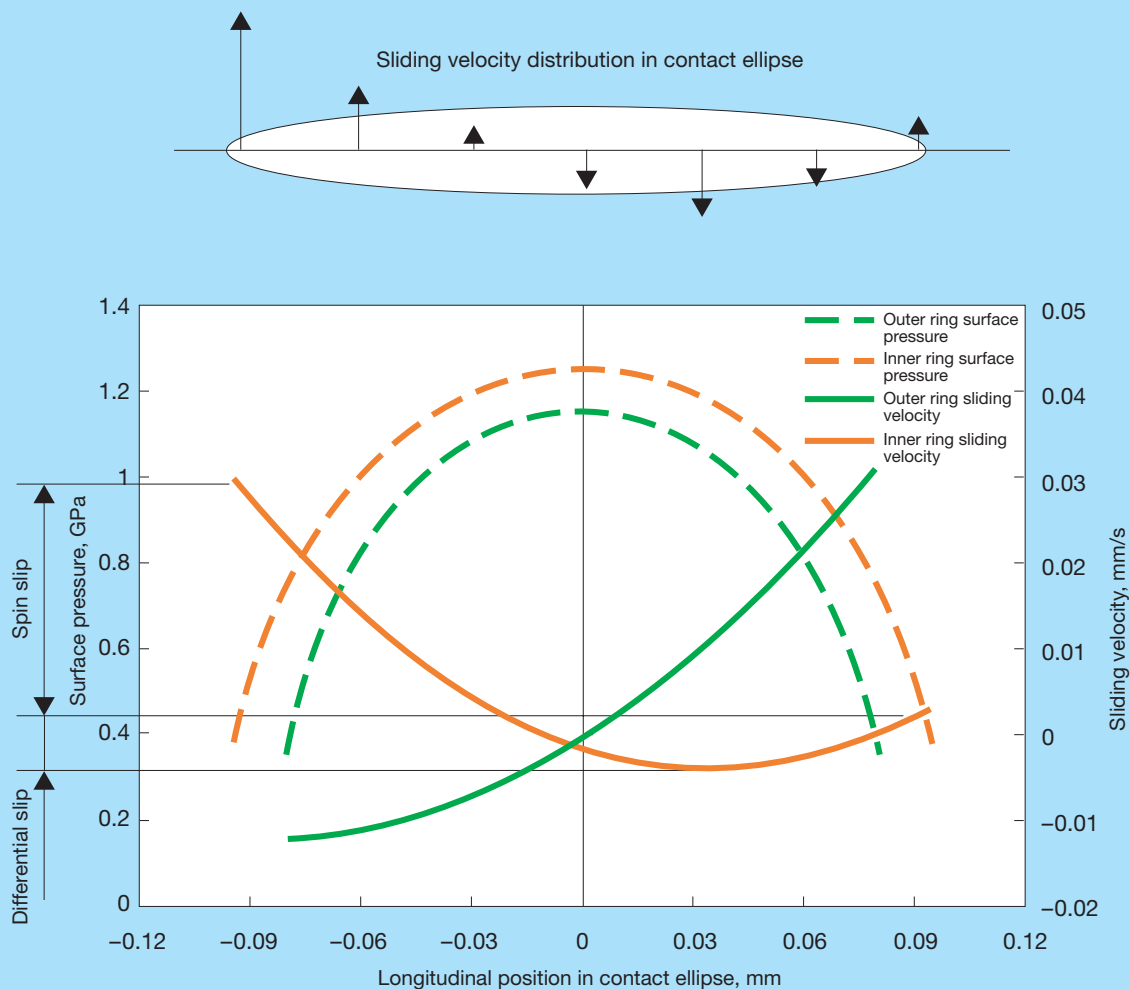 so does life. Concerning roller diameter, torque and life show opposing trends. As diameter increases, rolling friction decreases, and because PCD becomes smaller, torque decreases. Furthermore, when contact angle increases, rolling element load decreases, but because PCD also increases, so does torque. We therefore know that the effect on torque of PCD is comparatively large. In other words, taking measures for longer life and reducing PCD are effective means for lowering torque.

3.2 Effect of contact angle

Selecting the proper contact angle is an effective way to lower torque for angular ball bearings. Fig. 5 shows the change in calculated frictional loss for a bearing operated at 8 000 min^{-1} under a 500 N radial load and a varied axial load. The studied bearing was an angular ball bearing with a 75 mm outer diameter, a 33 mm inner diameter, and a 20 mm width, whereby the contact angle was varied to 0°, 15°, 30°, 45°, and 60°. The figure shows that as axial load increases, frictional loss decreases for the larger contact angles. When F_a/F_r = 2 to 4, bearing frictional loss is particularly high at a 60° contact angle, and a phenomenon where frictional loss decreases when axial load increases is observed.

To explain this phenomenon, Fig. 6 shows gyroscopic slip of balls. When balls turn with a contact angle, gyroscopic moment acts on the balls, resulting in gyroscopic slip. When the load is large, this sliding is controlled by friction where contact is made; but, if load is insufficient, gyroscopic moment surpasses friction where contact is made, resulting in gyroscopic slip. Consequently, a sharp rise in frictional loss is observed. Sufficient study is therefore required when using bearings with a large contact angle under conditions where rotation speed is high and load is slight.
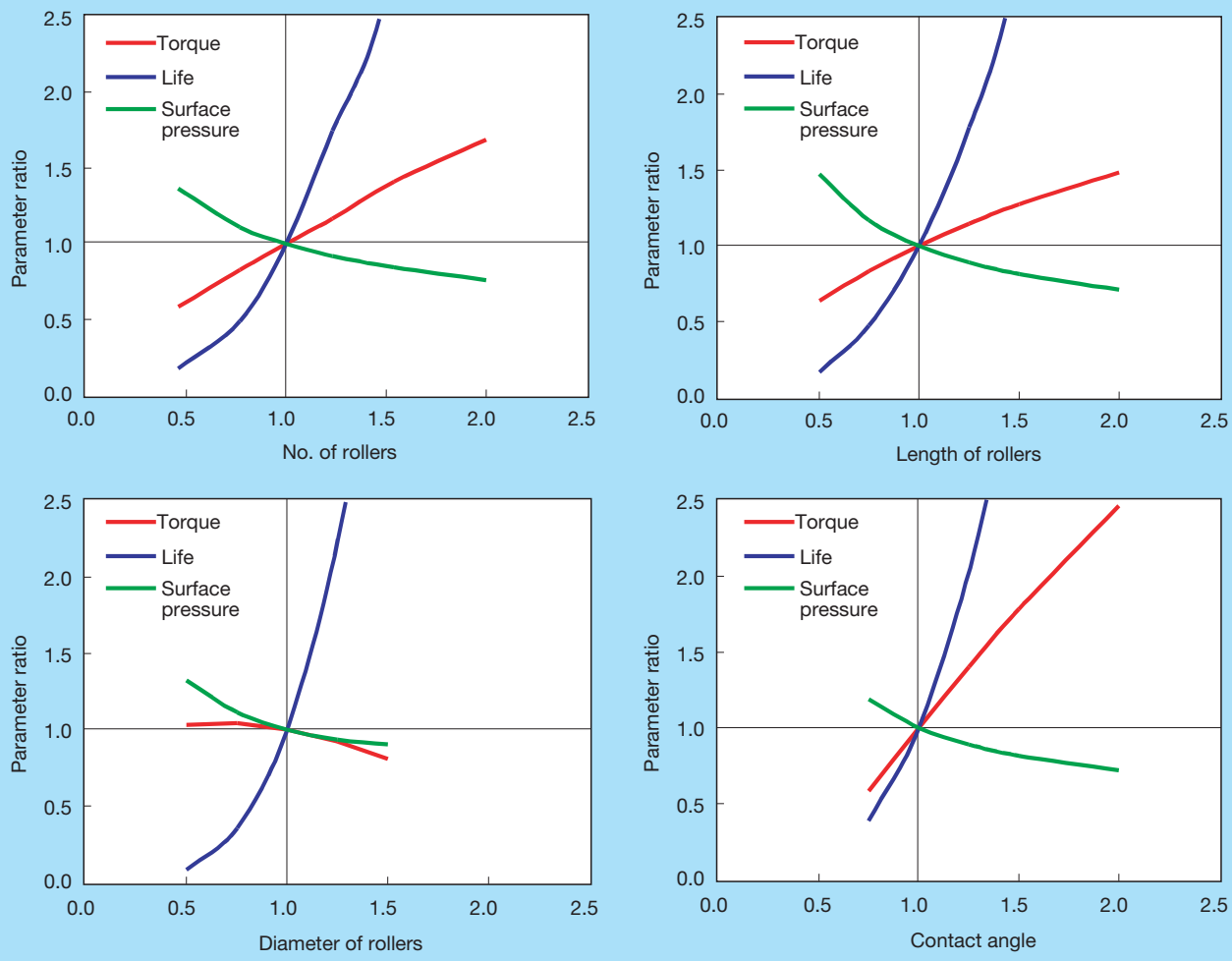
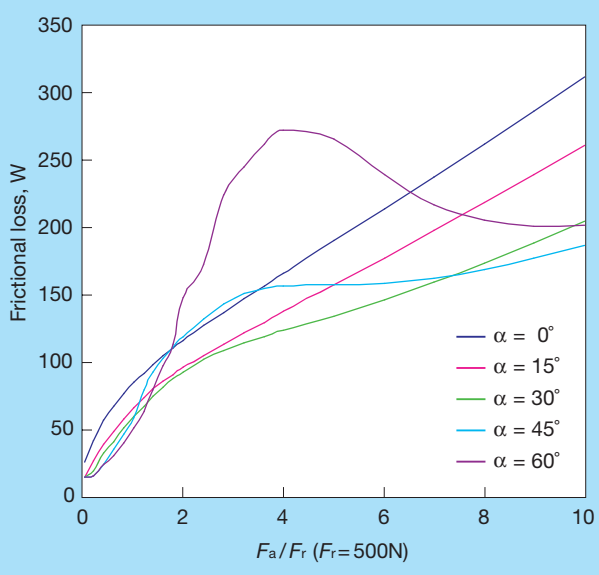Fig. 4 Frictional torque comparison for various parameters of a tapered roller bearing

Fig. 5 Frictional loss of a ball bearing for varying contact angles
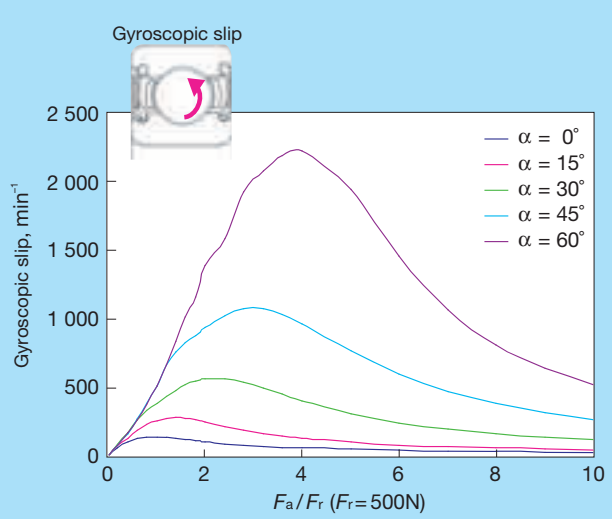

Fig. 6 Gyroscopic slip of a ball

3.3 Effect of seals

Sealed bearings, where grease is sealed inside the bearing, and sealed clean bearings, used for automotive transmissions, contain seals. Fig. 7 shows a comparison of torque measurements for sealed clean bearings for automotive transmissions and for bearings with the seals removed. The measured bearings are ball bearings with a 25 mm bore diameter, a 62 mm outside diameter, and a 17.5 mm width. The test was conducted by varying speed using forced circulation oil feed with oil equivalent to VG32 for lubrication and axial loads of 300 N, 500 N, and 700 N. The figure shows seal torque accounts for 20 % to 50 % of the bearing torque. Lower torque of the seal therefore affects torque of bearings having seals. Research and development of seals with a low friction coefficient that minimizes tension while maintaining seal performance is now being conducted.

3.4 Effect of surface roughness

Aihara et al studied the correlation of roughness and rolling friction, and have indicated that rolling friction decreases as roughness increases[5]. When oil film thickness becomes approximately equal to the roughness, asperity contact occurs in the contact area, with part of the load being supported by the surface roughness (asperities). The load supported by the lubrication therefore decreases and rolling friction decreases. Bearing friction may therefore decrease when raceway surface roughness of rolling bearings increases. Fig. 8 shows calculation results when raceway surface roughness of a ball bearing becomes large. Ball bearing specifications consisted of a 68 mm outside diameter, a 25 mm bore diameter, and a 19 mm width. Calculations were based on a 1 000 N radial load and a 1 000 N axial load at 2 000 min^{-1}.

The oil film parameter Λ, which is the ratio of roughness to oil film thickness, was set at 0.25 and at 2.0 by changing roughness. The figure shows rolling friction

steadily decreasing but sliding friction increasing. In the case of ball bearings, sliding in accordance with the curvature of the raceway and balls (differential slip and spin slip) exists with negative and positive signs in the contact surface. Loss due to sliding friction therefore increases because friction at the parts where metal contact is made is large due to contact of roughness asperities even when roughness is large and rolling friction is reduced. By increasing roughness, therefore, torque decrease is limited because the decrease in rolling friction and the increase in sliding friction cancel each other out.

The results, however, are different for tapered roller bearings. Fig. 9 shows the results of calculations when raceway surface roughness of an HR30306C tapered roller bearing (72 mm outside diameter, 30 mm bore diameter, and 20.7 mm width) is increased. Here calculations have been made at 2 000 min^{-1} under a 3 000 N radial load and a 3 000 N axial load. In the case of a bearing with near true rolling over the entire contact surface of the raceway, such as occurs with a tapered roller bearing, there is no wasted sliding such as spin sliding or differential slip of ball bearings, and only sliding that exactly balances with rolling friction is produced. Sliding friction therefore decreases in response to the drop in rolling friction. The drop in rolling friction is therefore connected to a decrease in torque. Here the disadvantage of increasing roughness is the decrease in bearing life. Increasing roughness produces contact at the roughness asperities and makes surface originated flaking and peeling likely to occur. Development of a method of strengthening the surface is the key to solving this problem.

3.5 Effect of oil feed rate

Decreasing the oil feed rate can control torque. Using a method to eliminate any unnecessary oil to the greatest degree possible, sufficient lubrication can be provided with a minimal amount of oil. Machine tool main spindles are
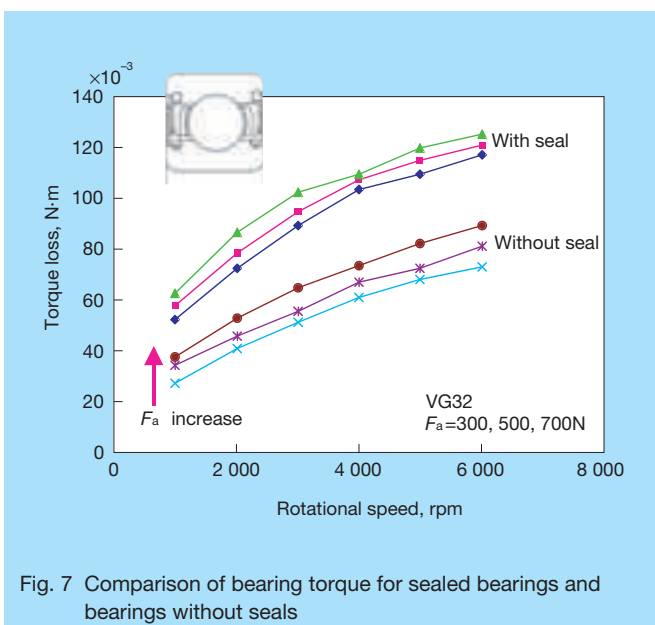

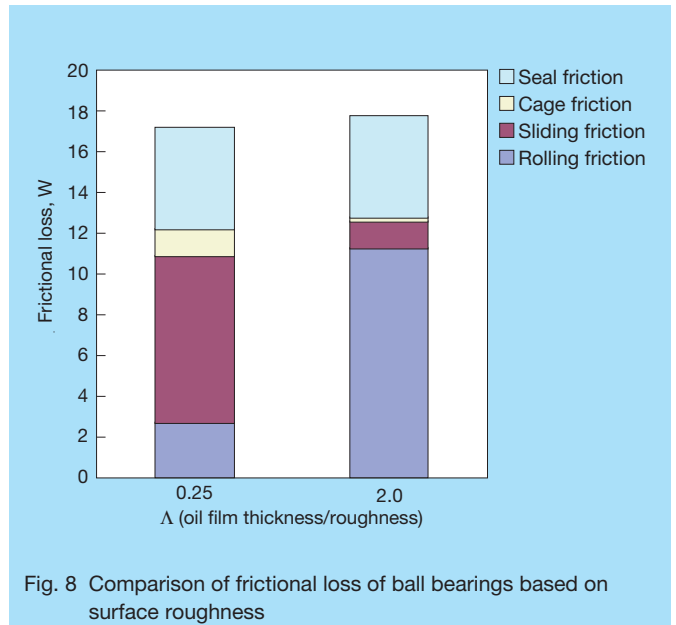Fig. 7 Comparison of bearing torque for sealed bearings and bearings without seals

Fig. 8 Comparison of frictional loss of ball bearings based on surface roughness

one example of an application that uses oil-air lubrication[1] and super lean lubrication[2]. Fig. 10 shows the calculated results for oil feed rate, frictional torque, and outer ring temperature rise. The calculations for a 6208 bearing were made at 10 000 min^{-1} under 1 960 N and 3 920 N axial loads with an oil equivalent of VG32. Oil was supplied by oil-air lubrication for areas where there was a minute quantity of lubrication, and forced circulation oil feed was supplied to other areas.

Fig. 10 shows that torque decreases as the amount of oil decreases. With the rise in temperature, conversely, the maximum value appears with an oil feed rate of about 100 ml/min. Torque increases with oil feed rate, but heat removed by the oil simultaneously increases, and as a result, the maximum value for temperature increase is reached. Reducing the oil feed rate results in a decrease in the amount of heat removed by the oil; if heat transfer conditions are poor, there is danger of seizure. Sensitivity to thermal disturbance requires due caution.

4. Lower Frictional Torque by Selecting Optimal Bearing

Selecting the optimal type of bearing is an important factor for running torque. Fig. 11 shows a comparison of frictional loss for a ball bearing and a tapered roller bearing. The bearings used for the comparison were an HR30306C and a 6306. Both bearings have the same internal and external dimensions (72 mm outside diameter and 32 mm bore diameter), but the HR30306C is slightly wider. Here calculations were made under 500 N and 3 000 N radial loads, and different axial loads. Because radial load alone cannot be applied to a single row tapered roller bearing, a minimal axial load comparable to the radial load was applied. Fig. 11 shows that when load is slight (F_r = 500 N), the calculations in all areas were lower for the ball bearing than the tapered roller bearing.

When load is large (F_r = 3 000 N), frictional loss is lower for the tapered roller bearing than the ball bearing.

Frictional loss for the ball bearing is sensitive to load because of point contact. However, frictional loss of the tapered roller bearing is not as sensitive to load because of line contact. Therefore, when load increases, torque is lower for the tapered roller bearing. Friction is not always lower for the ball bearing than the tapered roller bearing, and there is a need to do a thorough study of load. Because load dependency and speed dependency of friction differ according to the type of bearing, bearings should not be compared by maximum load alone; more studies under varying operating conditions need to be carried out.
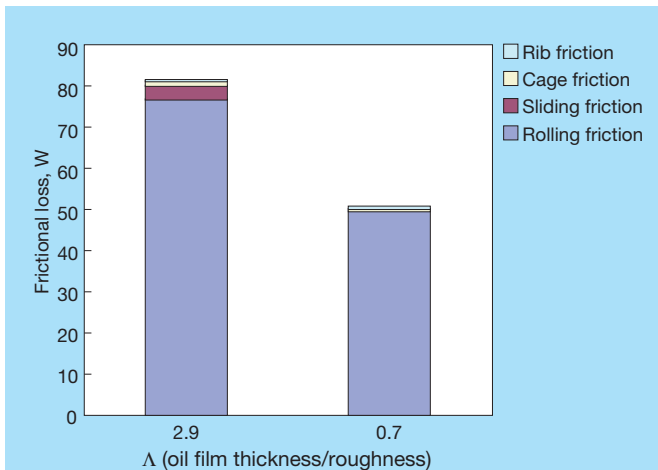
Fig. 9 Comparison of frictional loss of tapered roller bearings based on surface roughness
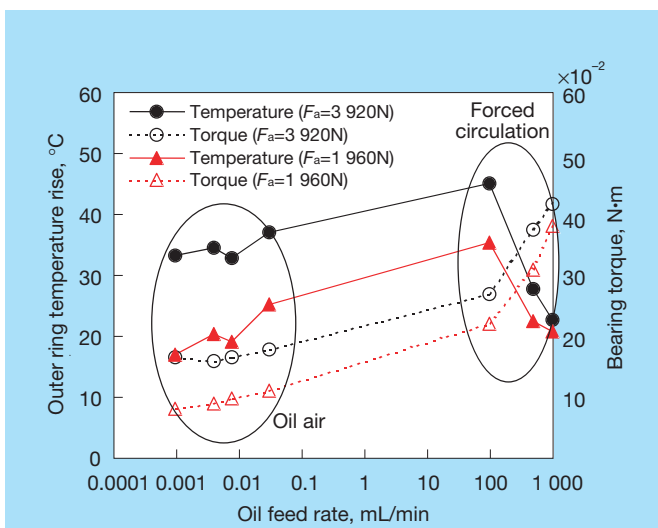
Fig. 10 Oil feed rate, frictional torque, and temperature rise of a ball bearing
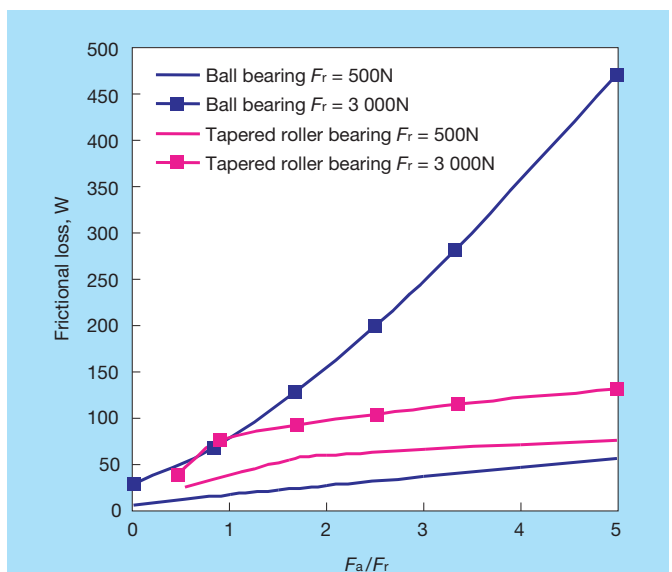
Fig. 11 Comparison of frictional loss for a ball bearing and a tapered roller bearing

5. Conclusion

This paper has described technology for achieving lower frictional torque for rolling bearings. Bearing torque and life have a contradictory relationship. Using long-life technology, it is possible to extend operating life under low torque conditions, or sacrifice long-life for greater durability under high torque conditions. Whereas bearing torque differs largely according to bearing operating conditions, the lubrication method, the bearing type, and the bearing mounting arrangement are extremely important for developing an optimal design. As environmental issues play an increasing role in bearing design, requirements for durability and lower torque, which are basic functions of rolling bearings, will probably become increasingly severe, so research and development will continue to be conducted to provide products that meet the needs of the age.

References:

1) Yoshiaki Onose, "Bearings for higher speed used for main shaft of machine tools and lubrication methods for such bearings," NSK Technical Journal, 646 (1986), 32-46
2) Tomio Sugita, "Super high-speed spindle," NSK Technical Journal, 676 (2003), 11-15
3) Mitsuho Aoki, Koji Morita, "Development of grease-lubricated, built-in motor spindle,"
4) S. Aihara, "A New Running Formula for Tapered Roller Bearings Under Axial Load" Trans., ASME, JOT, 109 (1987), 471-478
5) Satoru Aihara, Tsuyoshi Sawamoto, "Influence of surface roughness on rolling viscosity resistance in EHL contact area," Lubrication, 3-11 (1986), 805-811

Hirotoshi Aramaki

Latest Technologies Applied to AT Maji-Band™

Tamotsu Fujii, Xiaoming Gu and Hideaki Takabayashi
NSK-Warner K.K.

ABSTRACT

Various products with paper-based wet-friction material have been developed for smoother shifting of automatic transmissions (AT). Band brakes have been featured as friction engagement elements for planetary gears, which provide higher holding-torque capacity than same-size multiple friction-disk brakes caused by a self-energizing mechanism. The advantages that should be focused on are better shift quality for the release element during upshifting because of the different torque capacity in the drum rotating direction. In 1988, BorgWarner developed the Maji-Band for band brakes (coiled-steel straps joined into bands), which is lightweight and compact, and provides approximately 3.5 times higher torque capacity than single wrapped band brakes and lower drag torque than multiple friction-disk brakes . However, it is difficult to control shift quality as the engaging element for upshifting is caused by instability in attaining the required torque to dynamically follow the servo-applied force. This article describes a more robust Maji-Band that is controlled mainly by servo-applied force in comparison with multiple friction-disk brakes .

1. Introduction

Various friction-related products using paper-based wet friction materials for sliding parts have been developed for smoother shifting of automatic transmissions (ATs). Among these AT components, band brakes are widely used as reactive elements for planetary gears.

Band brakes have a higher holding torque capacity than multiple friction-disk brakes of the same size because of the flexible metal band (brake band) that tightens the clutch pack drum in place on the transmission shaft. Band brakes also have the advantage of being able to provide good shifting characteristics for the release element when upshifting due to a difference in torque capacity according to braking direction of the drum. In 1988, BorgWarner developed band brakes called the Maji-Band, which is coiled-steel strap joined into a band . This type of band brake further enhances torque capacity by 3.5 times that of a single-wrapped band brake. The Maji-Band produces lower drag torque and contributes to a lighter, more compact AT. It has, however, been pointed out that it is difficult to control shifting performance as a friction element when upshifting(compliance of torque with applied load). The factors behind this effect have been studied and include the creation of a model and the behavior analysis of the mechanism by which band torque is generated.[1-3]

This paper provides a clear description of the mechanism by which torque is produced relative to applied load of the band and introduces a more robust Maji-Band with a structure capable of controlling these factors and providing controllability as good as or better than multiple friction-disk brakes.

2. Maji-Band™ Configuration and Features

2.1 Configuration

Band brakes consist of a band, a drum, and a servo piston that applies hydraulic pressure. Fig. 1 shows a picture of a Maji-Band assembly and a drawing of the band itself. One end of the Maji-Band is anchored against the transmission case with a guide pin while the other end is connected to a servo piston. The servo piston applies mechanical force to tighten the band around the drum. The Maji-Band is linked to the anchor guide pin by a connecting rod and the drum is held in place by contact angle ß.

2.2 Features

The Maji-Band is a double-wrapped stamped band brake developed by BorgWarner in 1988. Table 1 lists the features of multiple friction-disk brakes and a Maji-Band. Band brakes are generally advantageous in that they provide good shifting characteristics as a releasing element during upshifting due to difference in torque capacity according to braking direction of the drum. Band brakes also enable transmission brakes to be lighter and more compact than multiple friction-disk brakes of the same size because of high holding torque capacity produced in the contact angle of the band on the drum.

It is difficult, however, for band brakes to control shifting performance as a friction element when upshifting. Fig. 2 shows a comparison of drag torque when rotating without a load. The fastening position of a Maji-Band when disengaged is more stable than the plates of a multiple friction-disk brakes, and less friction area is required to produce the same torque capacity, so drag torque can be reduced for the entire speed ranges.

Although the energy capacity of band brakes is relatively small for a given torque capacity, the Maji-Band offers a high level of design flexibility in the radial

direction so sufficient drum heat capacity can be secured. Automatic transmission fluid (ATF), which is dispersed from the shaft core through oil holes in the drum, can also be maintained on the sliding surfaces. For these reasons, in cases where the same torque is generated as shown in Fig. 3, temperature of the sliding surfaces on the Maji-Band can be maintained at a lower level than that of multiple friction-disk brakes .

3. Torque-Generating Mechanism and Control Characteristics

3.1 Calculating band torque (self-energizing)

The static relational formula for produced torque and applied load on the band is as follows: [4]

T : Torque
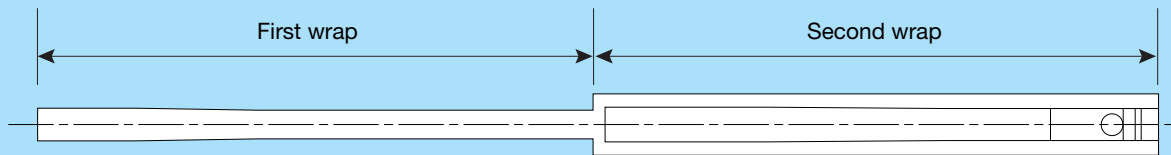
Fig. 1 Construction of a Maji-Band™and drum assembly

First wrap   Second wrap

Table 1 Comparison of a multiple friction-plate disk assembly and a Maji-Band

Band   Multiple friction-disk brake
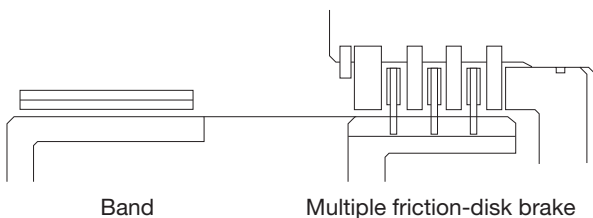
	Multiple friction-disk brake	Conventional Maji-Band
Size	Good	Better
Weight	Good	Better
Drag torque	Good	Better
Heat resistance	Good	Better
Self-energizing shifting characteristics	Good	Fair
De-energizing shifting characteristics	Good	Good
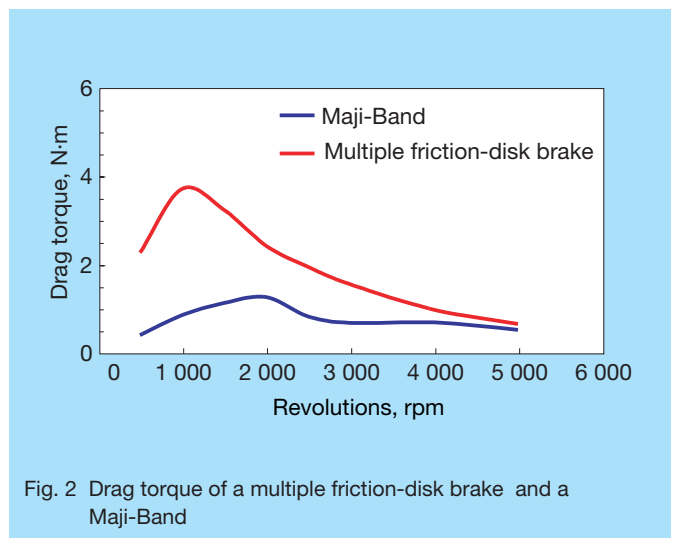
Fig. 2 Drag torque of a multiple friction-disk brake and a Maji-Band

μ : Friction coefficient

b : Contact angle

F : Applied load

R : Actuation radius

Because contact pressure between band and drum increases from the place where it is applied to the anchor (amplification of braking force by the band pressing against the drum), we know the friction coefficient (μ) expressed in the formula is the conceptual value of friction force (μ is the index for friction coefficient; because contact pressure is distributed on the band, friction coefficient differs according to position). In previous studies, μ is considered to be a variable, including effect factors for torque produced, and the transient friction behavior has been discussed.[1)2)] If μ can be estimated as a constant or function of an effect factor as in multiple friction-disk brakes, it will be possible to make torque directly conform to applied force to control friction material products.

3.2 Controlling pressure and torque characteristics of conventional bands

Fig. 4 shows the relationship between pressure and torque characteristics for conventional Maji-Bands. Because friction force produced between the drive plates, such as friction plates, and driven plates, such as steel plates, turns directly into torque, torque is produced when a load is applied to the sliding surface (the torque produced passes through the origin in the figure in proportion to the applied load).

Conversely, friction force produced between the band and drum in a Maji-Band overcomes the reactive force of the band at initial engagement, before working as pressure against the drum. It has a mechanism that subsequently transmits torque while amplifying braking force (value of torque has a vertical intercept against applied force). The slight torque that is produced under load conditions is largely affected by permeability of the

friction materials, relative velocity, temperature that alters ATF viscosity (hydrodynamic torque) and friction force (boundary torque), and the effect of which has been discussed in previous studies.[1)2)]

If these factors cannot be predicted, ideal controllability, where torque conforms directly to the applied force, and follows its change precisely, cannot be obtained.[3)4)] Generally speaking, difficulty in controlling the band is due to the complicated effect of these factors, which are also the reasons why torque response to applied force cannot have reversibility (variation of torque and force).

4. Enhancing Shifting Characteristics

Although Maji-Bands have many advantages as a mechanical element that supports AT shifting, there are issues concerning application of enhanced controllability when upshifting. So far, we have conducted various research concerning engagement characteristics of the Maji-Band as a friction element. This research has been primarily concerned with torque compliance under load, behavior analysis of the affecting factors, model creation, and controllability.[1–3)]

A mechanism that subsequently transmits torque while amplifying self-energizing braking force is a mechanical characteristic of Maji-Bands with high torque capacity. There are no examples of analysis concerning the transitional characteristics of Maji-Band as it repeatedly comes into and out of contact with the brake drum. The following is an introduction to efforts by the authors to improve shiftablity of Maji-Band.

4.1 Effects of contact angle ß

Contact angle ß is ordinarily treated as a constant in the band torque calculation formula; it expresses holding torque capacity. In the transitional phase when the band is engaged, contact angle ß changes during the actuation of compression against the drum, so the value only
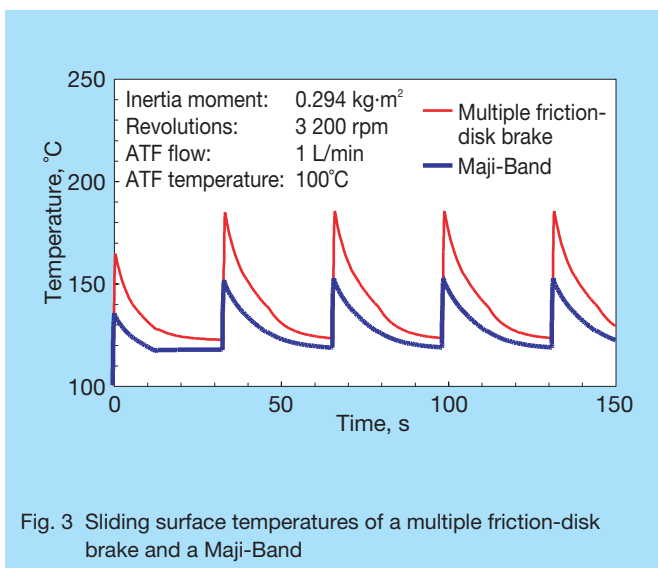

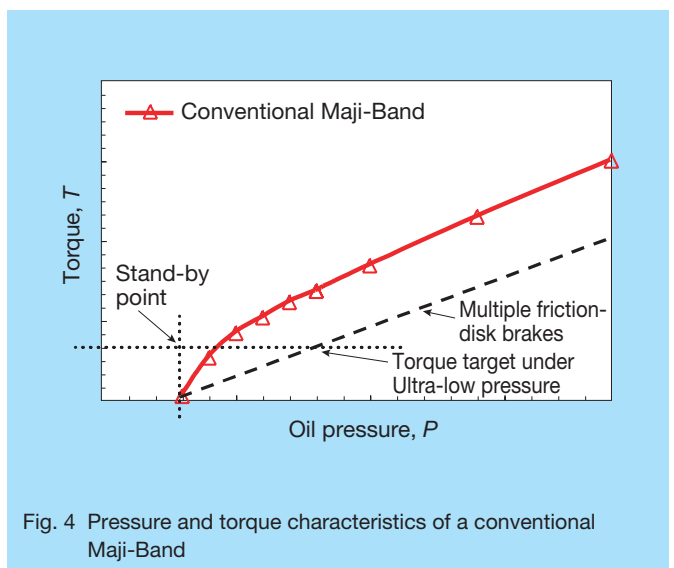Fig. 3   Sliding surface temperatures of a multiple friction-disk brake and a Maji-Band

Fig. 4   Pressure and torque characteristics of a conventional Maji-Band

expresses the shape characteristics of the Maji-Band (a circular piece of spring steel that is rectangular in cross section that loops through itself and wraps twice around a circular drum). Fig. 5 shows the relation between contact angle ß and torque produced under low loads.

During the transitional phase at initial engagement, there is a process where the Maji-Band overcomes reactive force and compresses tightly around the drum. If the sequence (time control: ß) by which the Maji-Band mechanically tightens around the drum can be changed at certain stages, the form of produced torque can be intentionally controlled. In other words, if a wrapping sequence and position can be provided with shape characteristics by utilizing rigidity when the band is mounted, it is possible that torque form can be adjusted.

Studies have shown that if the µ and ß in the torque calculation formula are assumed as constant value, these express the holding torque capacity when band engagement is complete. In order for the band to produce torque, the band must overcome the reactive force and compress tightly around the drum in the transitional phase of initial engagement. In this transitional phase, µ and ß also change according to the amount of the applied load. As for the developed Maji-Band , if band-applied force is light (Fig. 5), the Maji-Band doesn't have enough force to overcome its own rigidity under compression thus delaying initial torque locking.

In the heavy load area (Fig. 6), there is sufficient strength to overcome rigidity under compression even at the initial engagement. Therefore, the developed Maji-Band has the same torque characteristics as the conventional Maji-Band without any delay in torque locking.

Fig. 7 shows the pressure and torque characteristics of the developed Maji-Band. Torque level can be controlled in the low load area of the newly developed Maji-Band without losing high torque capacity under self-energizing torque, which is a feature of Maji-Band, by controlling contact angle ß. The developed Maji-Band is designed so that the produced torque passes through the origin in the figure in proportion to the applied load, thereby achieving ideal pressure and torque characteristics.

Fig. 8 shows the torque shape of the inertia absorption test using SAE#2 in the light loaded area. Holding capacity seen in the end torque for Maji-Band theoretically does not change as far as the shape expressed by contact angle ß is the same. As for the torque shape for the developed Maji-Band, therefore, the end torque rises from initial engagement toward ending state by suppression of holding torque. Torque change toward ending state results in the end shock, when shifting is complete.

4.2 Improving friction characteristics

As shown by the calculation formula for torque, the torque produced by Maji-Band is affected by contact angle ß and friction coefficient µ as well as applied load, which is a controlling factor. Friction characteristics of friction material products are affected by the type of friction material, and the lubrication conditions of the ATF, so it can be adjusted according to friction material specifications including groove design.

Fig. 9 shows the image of the drum surface against which the developed Maji-Band slides. A groove runs parallel to the direction in which the band slides on the drum surface. The crown of the groove is pressed in order to suppress wear of the friction material and obtain smooth engagement. As a result, holding torque generation is improved by discharging a film of ATF existing on the sliding surface at initial engagement. By maintaining a film of ATF when engagement is complete a sudden increase of end torque is prevented to provide smooth shifting.

4.3 Reducing deterioration and temperature dependence

It is necessary to assure compatibility to operating conditions and ideal torque shape and reducing
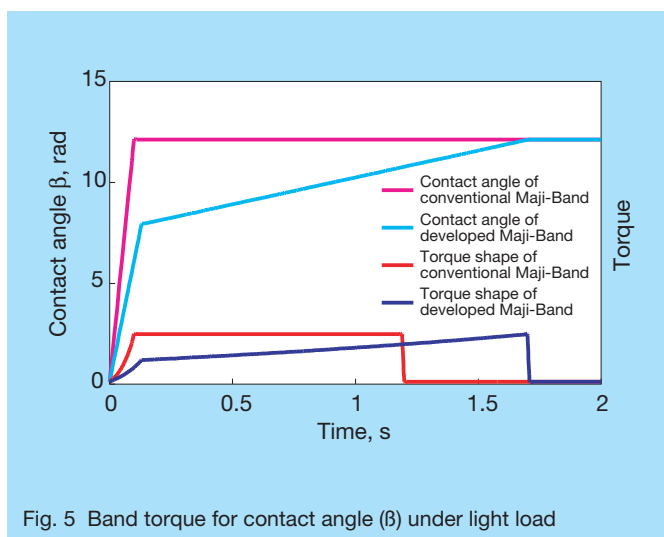
Fig. 5 Band torque for contact angle (ß) under light load
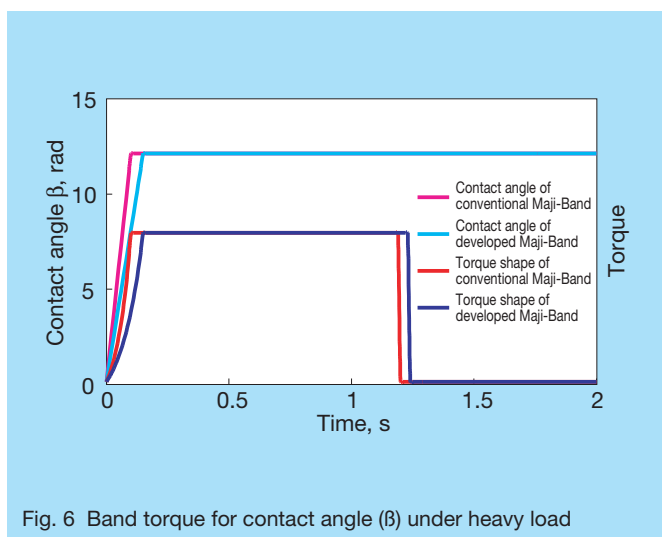
Fig. 6 Band torque for contact angle (ß) under heavy load
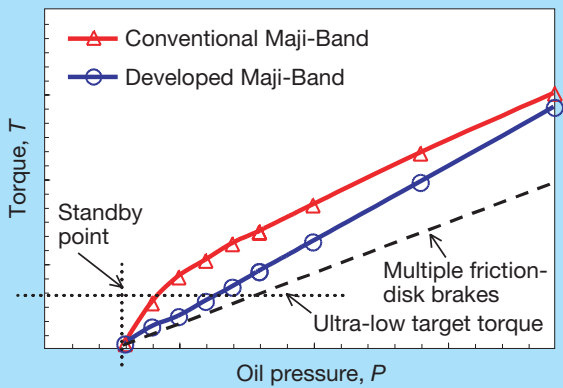
Fig. 7 Pressure and torque characteristics of the developed Maji-Band
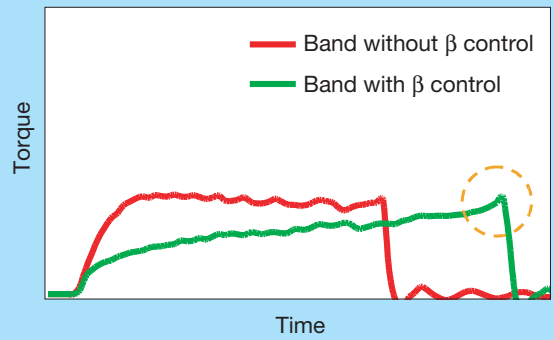
Fig. 8 Torque of the developed Maji-Band under contact angle control
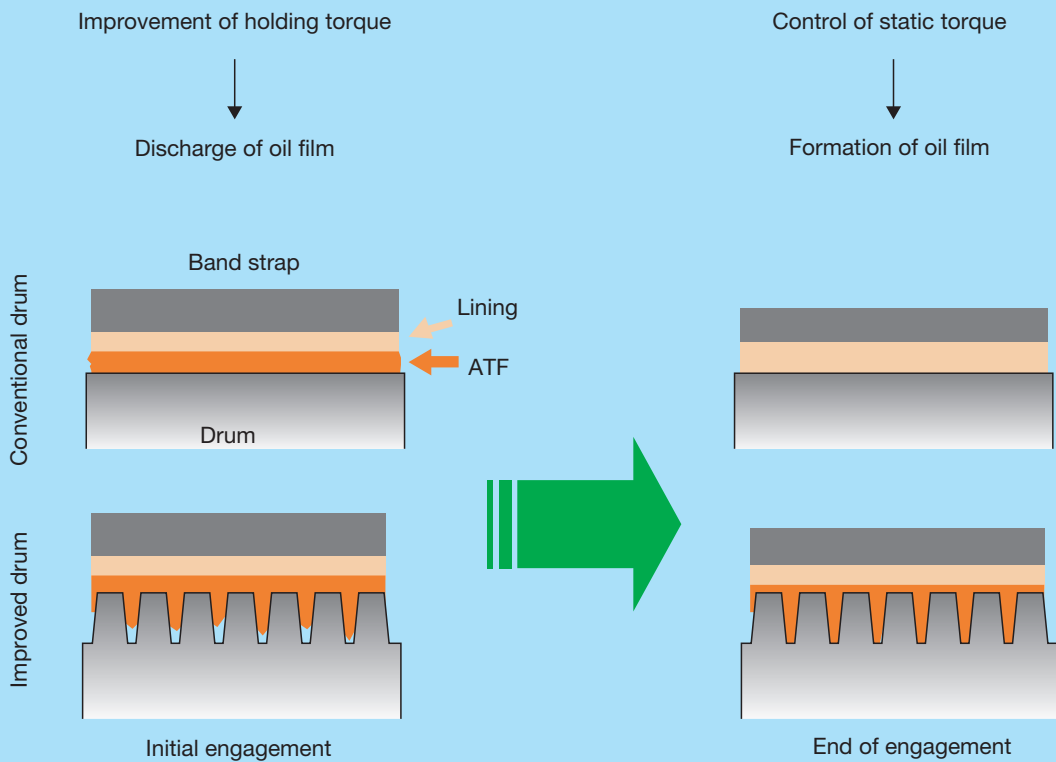
Fig. 9 Drum surface conditions

deterioration for adapting Maji-Band to the requirements of ATs. Robustness for variable operating conditions (performance change according to variable operating conditions) and break-in behavior (deterioration and operating repeatability) are particularly required to obtain better shifting characteristics.

The most important compatibility to operating conditions is temperature dependency (difference in performance according to operating temperature). Here, temperature dependency refers to the change in torque shape and level caused by the change in viscosity of ATF due to variation in temperature. Change in torque shape due to operating condition largely affects controllability of hydraulic pressure during shift. Groove design applied to

Fig. 10 Torque of the improved drum with surface treatment

Fig. 11 Improved temperature dependency for different groove types.

Fig. 12 Break-in behavior of developed Maji-Band

Fig. 13 Band torque for stroke using servo piston
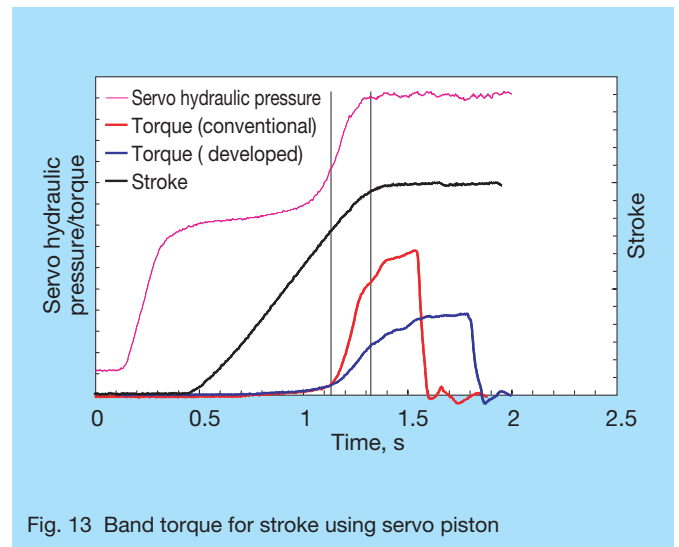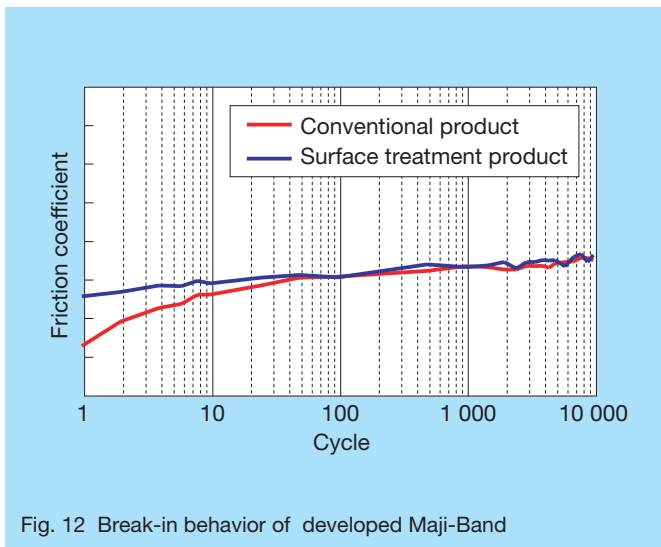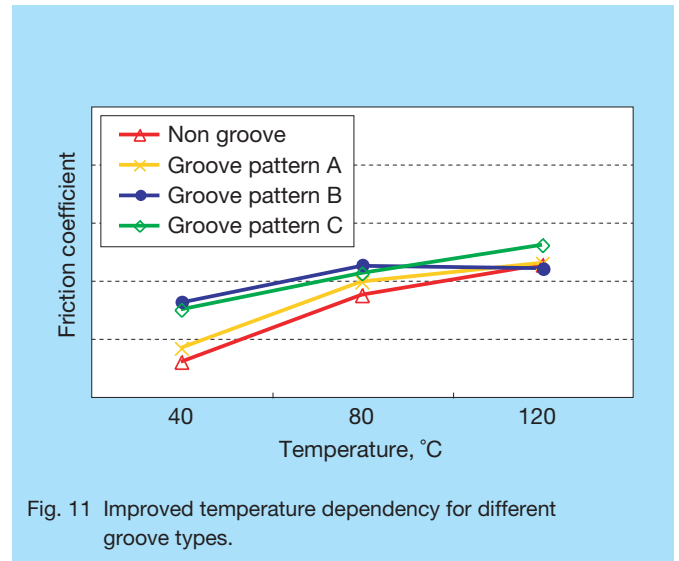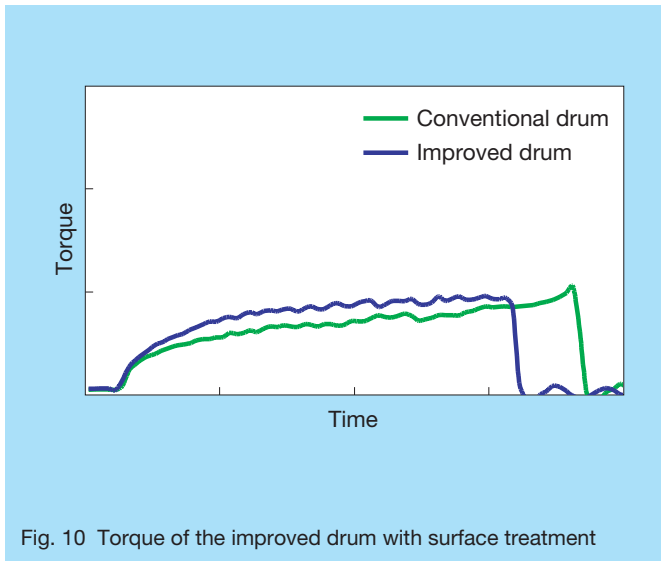
friction materials of the developed Maji-Band were optimized in order to improve the temperature dependency. Fig. 11 shows temperature dependency with the different specifications.

Here, the friction coefficient for the material with no groove is higher at 120°C than that at 40°C. Providing the optimum groove enables temperature dependency to be suppressed. Torque of friction materials can generally be derived from hydrodynamic torque and boundary torque.

The frictional coefficient rise according to temperature increase is caused by the decrease of oil film thickness in low ATF viscosity. The optimized groove pattern to control oil film enabled a reduction of temperature dependency according to hydrodynamic torque. Groove pattern B is used for the developed Maji-Band. Surface treatment of the lining could not be applied to Maji-Bands easily because of its structure, but break-in behavior and durability were improved with surface treatment to realize

the stability of shifting performance for the developed Maji-Band. Fig. 12 shows stability of friction coefficient level with surface treatment.

5. Maji-Bands™ for Shifting

It is important to control the initial torque and the end torque to achieve optimal shift control of ATs. One of the reasons why a conventional Maji-Band has been difficult to use as a shift component is the instability of initial torque. Fig. 13 shows the torque shape under ultra-low pressure for self-energizing engagement using a servo piston. The dynamic test of normal SAE#2 machine applies proper constant pressure using air piston for the sake of convenience and repeatability of the test to evaluate friction characteristics. Fig. 13 shows results of analyzing transitional characteristics of torque generation including piston stroke behavior.

In order to maintain stable initial torque, torque generation must be robust against hydraulic pressure control. The conventional Maji-Band is highly sensitive to hydraulic pressure, and pressure and torque characteristics have no linearity under light loads as illustrated in Fig. 4. Therefore, torque varies largely relative to variations in hydraulic pressure. This explains why it is hard to control initial torque. As a result, the targeted shifting characteristics cannot be obtained and repeatability is low resulting in some shift shock.

The developed Maji-Band offers linearity and pressure and torque characteristics that pass through the origin in the figure, and low sensitivity to hydraulic pressure control under light loads, and is able to provide stable initial torque to enable smooth shifting control with good repeatability.

6. Conclusion

Compared with multiple friction-disk brakes, the developed Maji-Band has improved self-energizing shifting characteristics while taking advantage of features such as being lightweight and compact (Table 2).

The developed Maji-Band can still be used as a transmission brake component. In addition, dramatic improvement of shifting characteristics makes it possible to provide shifting characteristics equivalent to that of multiple friction-disk brakes. Maji-Band has been reborn as a Maji-Band for shifting, and holds promise as a mechanical component to support weight and size reductions for ATs in the future.

Table 2 Comparison of a multiple friction-disk assembly, conventional Maji-Band, and the newly developed Maji-Band

	Multiple friction-disk brakes	Conventional Maji-Band	Developed Maji-Band
Size	Good	Better	Better
Weight	Good	Better	Better
Drag torque	Good	Better	Better
Heat resistance	Good	Better	Better
Self-energizing shifting characteristics	Good	Fair	Good
De-energizing shifting characteristics	Good	Good	Good

References

1) Fujii, Y., Tobler, W.E. and Snyder,T.D. "Prediction of wet band brake dynamic engagement behavior Part 1: mathematical model development", Proc Instn Mech Engrs, Part D, Journal of Automobile Engineering, 2001, 215 (D4)

2) Fujii, Y., Tobler, W.E. and Snyder,T.D. "Prediction of wet band brake dynamic engagement behavior Part 2: experimental model validation", Proc Instn Mech Engrs, Part D, Journal of Automobile Engineering, 2001, 215 (D4)

3) Snyder,T.D. and Denault C. C. "Quantification of Friction Component Engagement Controllability" 2001, 01-1156, Society of Automotive Engineers, New York

4) Fanella, R. Design of Band. In "Design Practices: Passenger Car Automatic Transmissions, 3rd edition" 1994, pp.419-426, Society of Automotive Engineers, New York

5) Fanella, R. Development and testing of bands. In "Design Practices: Passenger Car Automatic Transmissions, 3rd edition" 1994, pp.427-430, Society of Automotive Engineers, New York

Tamotsu Fujii

Xiaoming Gu

Hideaki Takabayashi

Trends and New Technologies of Automatic Transmission Bearings

Tatsuya Ootsubo and Satoshi Kadokawa
Bearing Technology Center

ABSTRACT

Greater efficiency is required of automatic transmissions, which have become the mainstream transmission of modern vehicles in Japanese and North American markets. This trend is in response to automakers placing more emphasis on developing vehicles with better fuel economy and lower exhaust emissions. The bearings used in automatic transmissions of these vehicles, including six-speed automatic transmissions, must meet stringent requirements for low frictional torque, high-speed performance, compact size, and long life. In this article, we will introduce the latest in NSK bearing technologies that respond to these very needs.

1. Introduction

Automotive transmission systems play an important role in transmitting optimum driving force under varying driving conditions. Manual transmissions require that the driver push a clutch pedal to engage and disengage the gears. Automatic transmissions (ATs) eliminate the need to manually operate the clutch and shift lever for each gear. Also, ATs create conditions where drivers can focus more on steering and braking. ATs have been criticized for their fuel consumption and "jerk" under acceleration. However, by improving overall performance, ATs have become more common in Japan and North America. We will cover features and the latest technologies of bearings that play a key role in the progress of AT technologies.

2. AT Technology Trends and Required Bearing Performance

The automobile industry has been called upon to develop fuel-efficient low-emission vehicles. In order to promote this development, improved engine designs, efficient power management, and related technologies for reducing friction among components and improving aerodynamics have been introduced into the market. Table 1 lists the required performance of AT bearings for improved fuel economy.

a) Reduction of frictional loss

Fig. 1 shows the location of specific bearings (Table 2) in a five-speed automatic transmission for a front-wheel drive vehicle, which requires numerous bearings. Fig. 2 illustrates AT bearing frictional loss rates. Based on the results of these calculations, we can see that fuel consumption is reduced by 1 % if bearing frictional torque is reduced by half.

b) Automatic transmission

Since 2002, vehicles with multi-overdrive automatic transmissions, most notably six-speed ATs, haven been commercialized and have been garnering considerable attention in recent years. Many of these ATs have adopted the recently developed Lepelletier gear set for a more compact and lightweight transmission. Whereas rotating speeds of planetary pinion become rather high in a Lepelletier gear set, which is the key design of a compact six-speed AT, the planetary pinion gear needle roller bearings must endure high rotating speeds.

c) Size reduction and high-torque capacity

The compact size of the AT restricts the amount of space available for the bearings resulting in smaller bearings that would normally suffer from reduced load capacity and shorter bearing life. These conditions are further complicated by the need to increase torque capacity of the transmission without increasing AT dimensions, which adds to bearing load and increases likelihood of bearing failure. Therefore, long-life bearing technology is critical for achieving weight and size reductions while ensuring high-load capacity and improved fuel economy of the vehicle.

Specifically, the bearings in such an automatic transmission must meet the following criteria:

Low frictional torque
Durability under high-rotating speeds
Compactness
Long life
(See Table 1)

Let's take a closer look at these four items.

Table 1. Bearing performance requirements

AT technology for improved fuel economy	Required performance of AT bearings
Lockup torque converter	
Reduction of frictional loss ·············►	Low frictional torque
Reduced churning resistance of automatic transmission fluid	
Computer technology	Durability under high-speed operations
Multi-overdrive gears	
Size reduction and high load capacity	Compact size and long life

Planetary shaft (Table 2-2)

Tapered roller bearing (Two single-row bearings used) (Table 2-6)

Planetary pinion needle roller bearing (Table 2-1)

Thrust needle roller bearing (Table 2-3)

Drawn-cup needle roller bearing (Table 2-4)

Drawn-cup needle roller bearing (Table 2-5)

Double-row tapered roller bearing (Table 2-7)

Cylindrical roller bearing (Table 2-5)

Tapered roller bearing (Table 2-8)

Tapered roller bearing (Table 2-9)

Fig. 1. Cross-section view of an AT[1)]

Table 2. Application of bearings in an AT

	Part		Bearing type	Page
1	Planetary gear		Planetary pinion needle roller bearing	41 & 42
2			Planetary shaft	42
3	Between planetary gears		Thrust needle roller bearing	42 to 43
4	Shift gear support	Intermediate shaft	Drawn-Cup needle roller bearing	44
5		Counter shaft		
6		Counter drive gear	Tapered roller bearing (two single-row bearings)	44 & 45
7		Counter driven gear	Double-row tapered roller bearing	64 & 65
8		Differential	Tapered roller bearing	44 & 45
9				
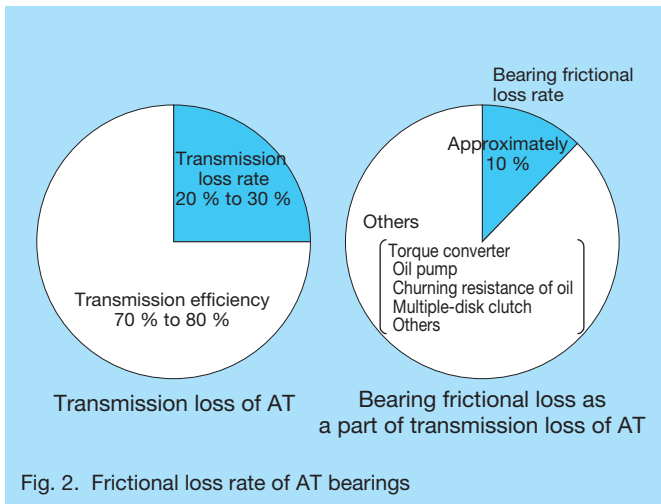
Fig. 2. Frictional loss rate of AT bearings

Fig. 3. Severity index of needle roller bearings in multi-overdrive transmissions

3. Features and Latest Technologies of AT Bearings

3.1 Planetary pinion gear needle roller bearings

3.1.1 Cage and roller for planetary pinion needle roller bearings

The increased rotating speed of the planetary pinion gear needle roller bearings is due to their application in multi-overdrive automatic transmissions and the wider range of gear ratios. Fig. 3 shows the severity index of planetary pinion needle roller bearings in an AT. The severity index is defined as the parameters of the centrifugal force affecting bearings and a speed of the bearing interior. Consequently, operating conditions of bearings in a six-speed AT are approximately seven times severer than a three-speed AT. In response to the high-speed operating conditions of the planetary pinion needle roller bearings and the need for low frictional torque, conventional full complement roller bearings (Fig. 4) have been replaced with cage and roller assemblies (Fig. 5).

a) Conventional full complement needle roller bearings

Full complement needle roller bearings lack a cage, which makes it difficult to mount the rollers smoothly. This makes assembly of the planetary pinion gears a time-consuming process. Although, a full complement needle roller bearing assembly has many rollers that provide large load capacity, frictional torque and bearing temperatures rise considerably due to the metal-to-metal contact between the rollers.

b) Most recent cage and roller design

Incorporating a cage prevents sliding friction between rollers, but load capacity is somewhat reduced due to the fewer number of rollers. Fig. 6 illustrates the difference in frictional torque for both a full complement needle roller bearing assembly and a cage and needle roller bearing assembly. Compared to the full complement needle roller assembly, frictional torque of the cage and roller bearings achieved a 40 % reduction in the range exceeding 1 000 rpm of pinion rotating speed. The optimal design of the
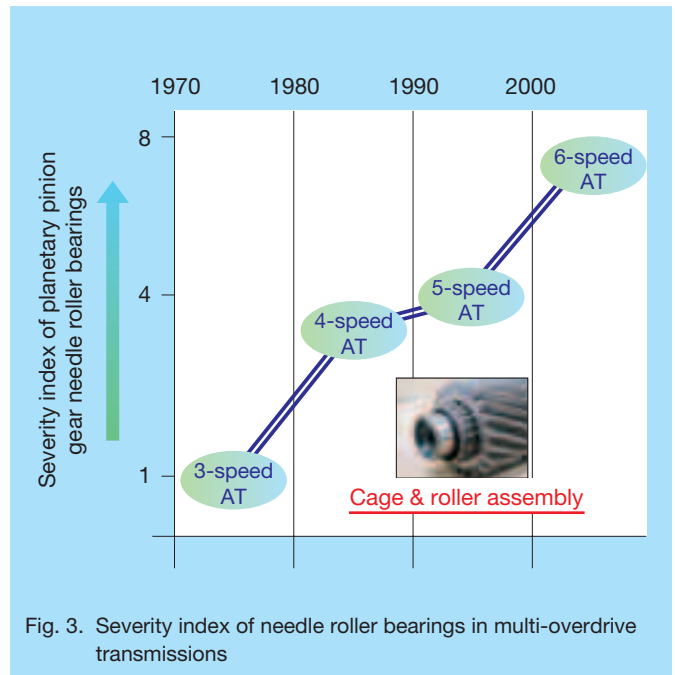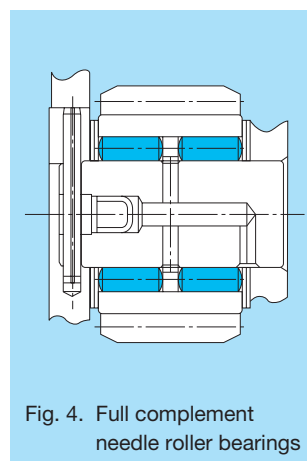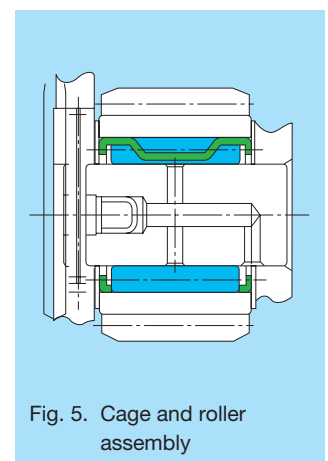

Fig. 4. Full complement needle roller bearings

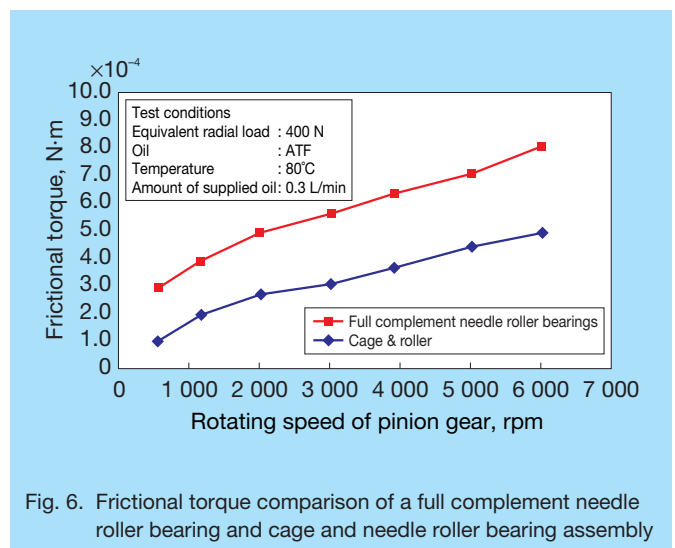Fig. 5. Cage and roller assembly

Fig. 6. Frictional torque comparison of a full complement needle roller bearing and cage and needle roller bearing assembly

cage and needle roller bearing assembly allows for higher rotating speeds, greater weight reductions, and promotes an easier mounting process.

3.1.2 Improvement of planetary shaft durability

By introducing a cage and needle roller bearing assembly for planetary pinion gears, the number of rollers is decreased and contact surface pressure between rollers and shafts is increased in comparison to conventional full complement needle roller bearings. Therefore, NSK subjected the steel pinion shafts to carbonitriding in order to improve durability. We were thus successful in adopting a cage and needle roller bearing assembly for those shafts. However, this technology is disadvantageous in a Ravigneaux gear set, where a combination of single pinions and double pinions are used. The double-pinion planetary gear unit is called a long pinion since it is axially long, in addition to having greater mass. Furthermore, the double-pinion planetary gear unit subjects the bearings to extreme centrifugal forces and loads, creating severe operating conditions. Operating temperatures of the planetary gear components are also higher in a compact AT as opposed to those of a conventional AT.

Under such high-load and high-temperature conditions, concentrations of retained austenite are deposited on the entire heat-treated shaft, which deforms and loses dimensional stability. Life of this type of shaft may be shorter than that of normal heat-treated shafts. In order to overcome this drawback, we have adopted a special induction heat treatment process that deposits retained austenite only on the required regions of the shaft. Fig. 7 illustrates application of this process while Fig. 8 compares test results and degree of shaft deformation. Until now, there was no method for fixing shafts into carriers, apart from using rivets. However, using special induction heat treatment, which allows for greater control of the application of heat treatment, we are now able to secure the pinion shaft using a caulking shaft-end method while maintaining the same level of hardness.

Fig. 8. Relationship between the amount of shaft deformation and heat treatment
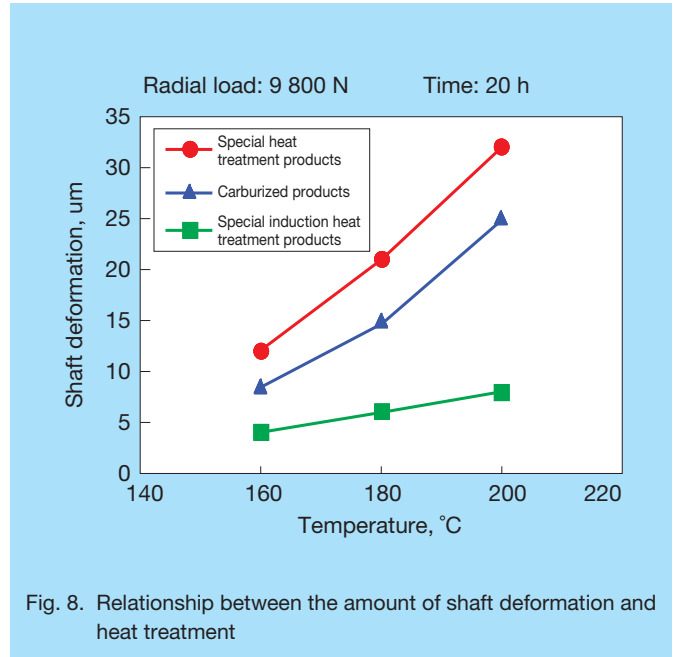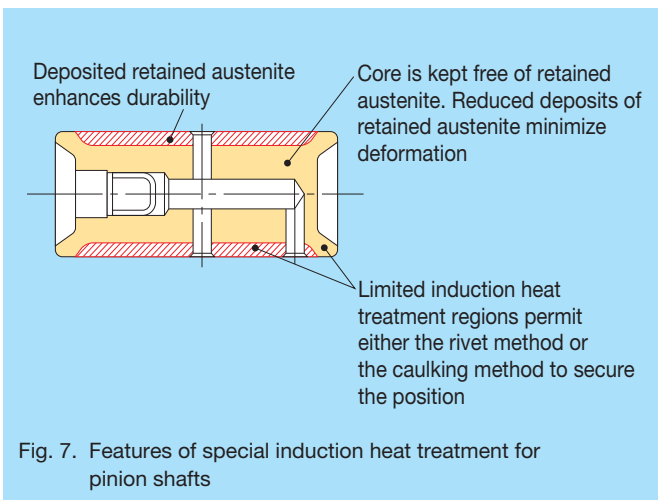
3.2 Thrust needle roller bearings

Thrust needle roller bearings are required to improve efficiency and to enhance rotating-speed applications, as well as planetary pinion gear needle roller bearings. Some methods for reducing frictional torque are:
a) Fewer but larger rollers

By decreasing the number of rollers, the contact area between rollers and the raceway is reduced thus reducing frictional torque. Increasing the diameter of the rollers reverses deterioration of load capacity. This is the fundamental design of thrust needle roller bearings for ATs (Fig. 9).

Fig. 7. Features of special induction heat treatment for pinion shafts

Fig. 9. Relation between frictional torque and roller specifications
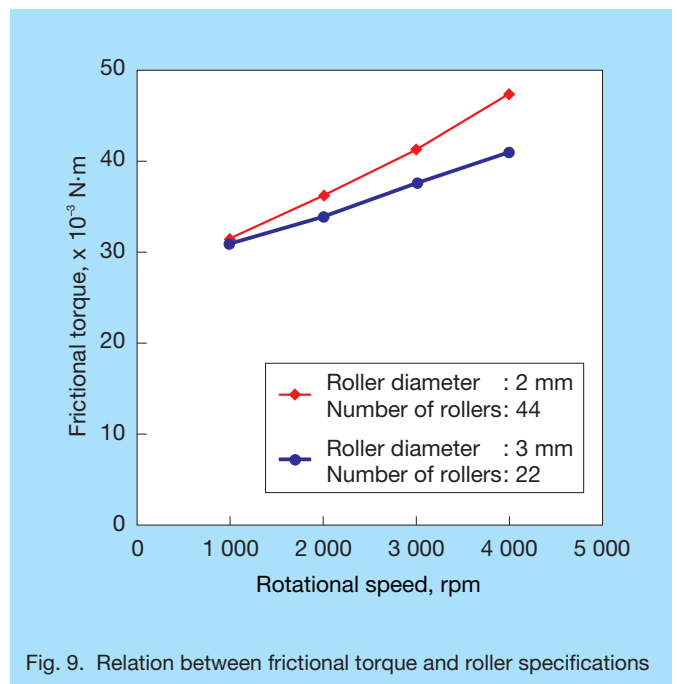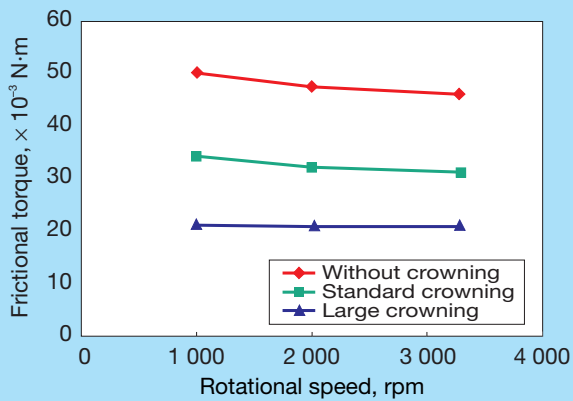
Fig. 10. Relation between frictional torque and roller crowning

Fig. 12. Thrust needle roller bearing with two rollers per pocket

b) Crowning of rolling contact surface

Roller end face crowning reduces the contact surface area between rollers and the raceway, which also reduces frictional torque. This is also a fundamental design of thrust needle roller bearings for ATs (Fig. 10).

c) Single-pocket cage and double rollers

The rollers of thrust needle roller bearings revolve around the rolling shaft as they simultaneously rotate as rolling elements of radial bearings. Circumferential speed on the outside diameter of the rollers of thrust needle roller bearings under rotating movement of rollers is axially uniform. The speed of the outside diameter of rollers under revolving motion is slower on the axial side of the inner circumference and is faster on the axial side of the outer circumference. Therefore, rollers are rotating with some sliding motion. The rate of sliding increases as the gap of circumferential speed between inner circumference and outer circumference increases, or in

other words, the amount of frictional torque is relative to the length of rollers. Consequently, integrating two short rollers into the pocket of the cage instead of one long roller reduces bearing frictional torque (Fig.s 11 and 12).

d) Improved roller end face profile and cage profile

Excessive wear of cage pockets may occur due to inadequate lubrication (starvation leading to boundary conditions) when roller ends make metal-to-metal contact against the cage pocket (along the outer circumference) due to centrifugal force under high-speed operations (Fig. 13 and Photo 1).

Crowning of the roller end faces helps to reduce excessive wear of roller end faces and the cage pocket as a measure against centrifugal force during rotation. With the roller end face contact point moved from the faster rotating outer periphery to the slower rotating center of the end face, we were able to reduce frictional torque and achieve longer life (Photo 2 and Fig. 14).

Fig. 11. Frictional torque comparison of cages of conventional thrust needle roller bearings, and of bearings with two rollers per pocket

Fig. 13. Contact point of conventional cage and the improved contact type cage

Photo 1. Wear of cage pockets (red circles)

Photo 2. Improved contact type cage

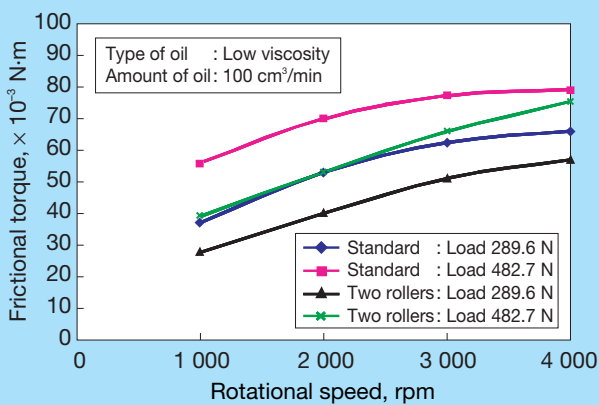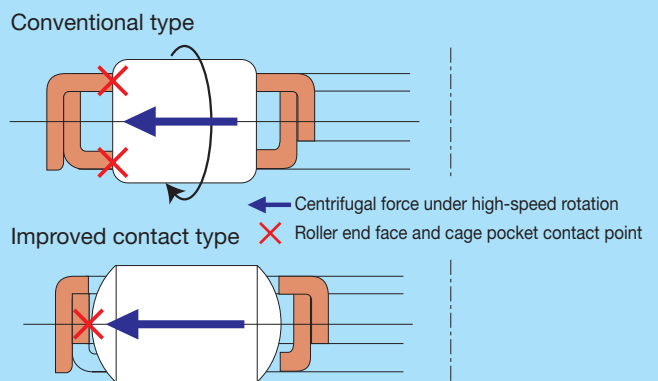Photo 3. Bushing and drawn-cup needle roller bearing

Test conditions
Relative rotating speed: 18 000 rpm
Load: 200 N

Conventional type

Improved contact type — No abnormalities
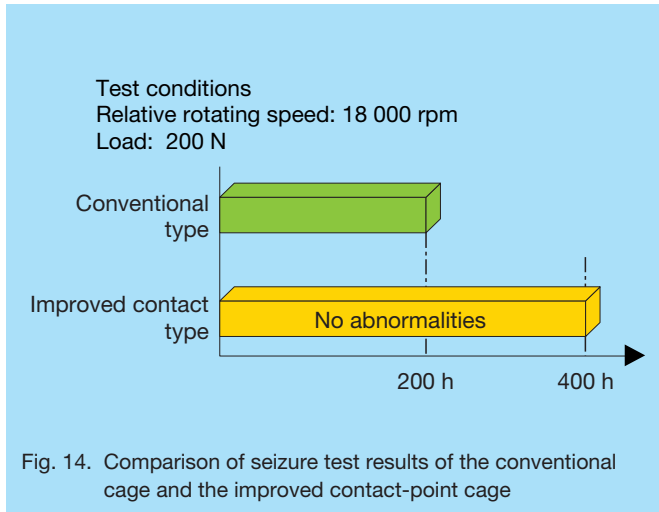
200 h   400 h

Fig. 14. Comparison of seizure test results of the conventional cage and the improved contact-point cage
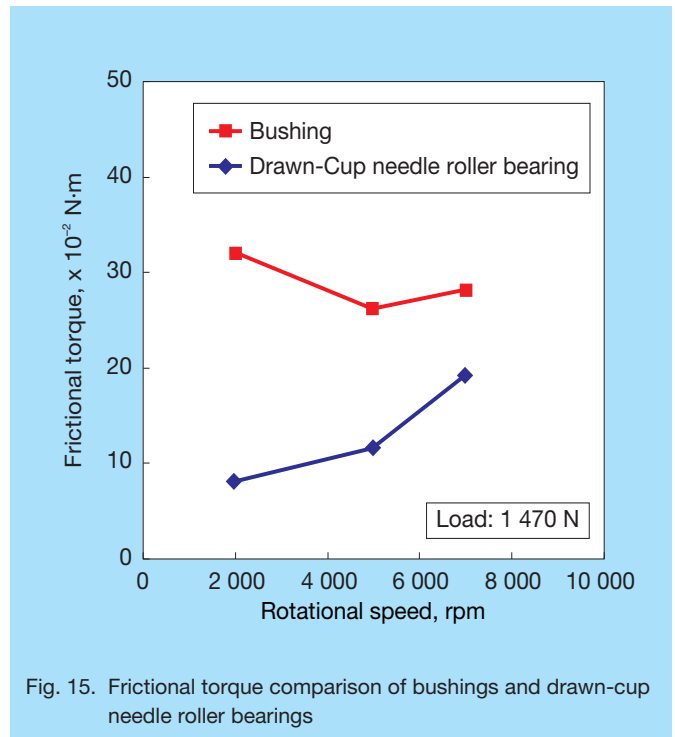
Fig. 15. Frictional torque comparison of bushings and drawn-cup needle roller bearings

3.3 Support bearing for shafts and gears

3.3.1 Drawn-cup needle roller bearings

NSK has expanded the use of drawn-cup needle roller bearings to replace sliding bearings that use copper alloy bushings in response to the requirement for higher speeds in AT applications. Due to the growing trend to avoid using products with lead (Pb), we expect that the adoption of drawn-cup needle roller bearings will increase in the future. Whereas drawn-cup needle roller bearings largely supplant copper alloy bushings, the bearings must maintain the same radial thickness and section height as copper alloy bushings. NSK has met this requirement by developing thin section drawn-cup needle roller bearings through the technology of 1 mm diameter rollers and a resin cage that is manufactured with highly accurate injection molding technology. Photo 3 shows a bushing and a thin section drawn-cup needle roller bearing. Fig. 15 shows the frictional torque of each product.

3.3.2 Low frictional torque tapered roller bearings

Tapered roller bearings are often adopted for AT applications due to their high-load capacity. However, frictional torque is also high, which poses a disadvantage. Frictional torque in tapered roller bearings can be expressed as follows:

$$T \fallingdotseq Tr + Ts$$

Tr: Rolling friction between the inner ring raceway and rolling contact surface of the rollers, and rolling

friction between the outer ring raceway and rolling contact surface of the rollers

Ts: Sliding friction between the roller end face and bearing inner ring rib

As shown in Fig. 16, sliding friction Ts is dominant under low-speed running operations, and rolling friction Tr is dominant and under high-speed running operations.

a) First-generation low frictional torque tapered roller bearings

Internal dimensions of this bearing (length, number of rollers, contact angle) remain the same as conventional tapered roller bearings. Low frictional torque was achieved by improving the profile and roughness of the contact areas. For example, we optimized the surface roughness of the roller end face geometry and bearing inner ring rib to reduce sliding friction Ts. We also improved the crowning profile to reduce rolling friction Tr. With these improvements, we achieved a 20 % reduction of torque in comparison to that of conventional tapered roller bearings (Fig. 17).

b) Second-generation low frictional torque tapered roller bearings

Fig. 16. Correlation between Tr and Ts

Fig. 17. Frictional torque comparison of low-friction tapered roller bearings and conventional tapered roller bearings
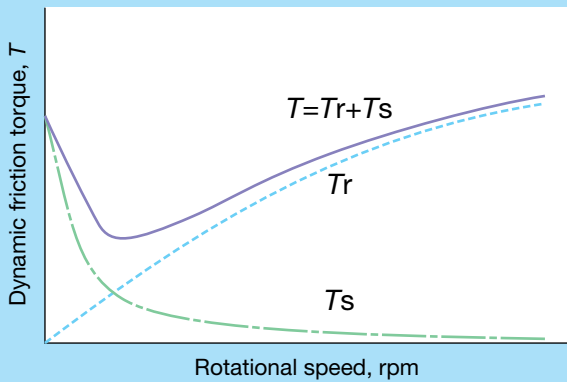
Bearing size: $\phi 40 \times 90 \times 35.25$
Load : Fa=5 000 N
Oil viscosity: 70 mm²/s

First-generation low-torque tapered roller bearings
Second-generation low-torque tapered roller bearings
Conventional tapered roller bearings

18-1. Conventional design   18-2. Low frictional torque design
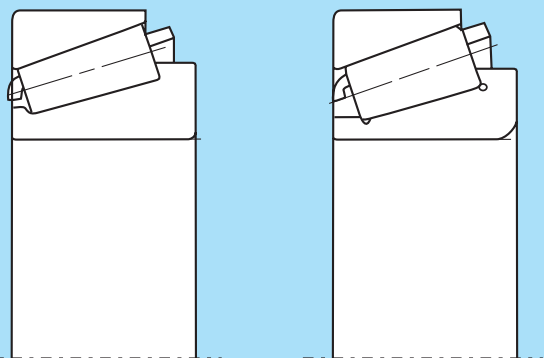
Fig. 18. Cross-section views of tapered roller bearings.

Fig. 19. Frictional torque comparison of tapered roller bearings and ball bearings

We achieved further reductions in rolling friction (Tr) in the second-generation product by optimizing the bearing interior design. In conventional products, life and rigidity will deteriorate if internal specifications are based solely on reducing frictional torque. Our second-generation design is based on a two-bearing combination that has improved internal specifications without sacrificing bearing life and rigidity. The low frictional torque design (Fig. 18) of NSK's second-generation tapered roller bearing reduces frictional torque by 20 % compared with that of first-generation products (Fig. 17).

3.3.3 Replacing tapered roller bearings with ball bearings

Replacing tapered roller bearings with ball bearings has made it possible to further reduce frictional torque. Simply replacing the bearings would normally result in a significant deterioration of life, durability, and rigidity. However, we successfully prevented such problems using NSK's original bearing analysis program (BRAIN[2]), original material, and proprietary technologies. Fig. 19 illustrates the positive results of our ball bearing design.

3.3.4 Long-life material and heat-treatment technology

Transmission lubricants are invariably contaminated with wear debris. Most types of bearing flaking is surface originated flaking that starts from the edge of an indentation as a result of contaminants that damage the surface of a race or rolling element in the load zone. Fig. 20 illustrates the development of flaking. First, a debris particle dents the bearing surface creating an indentation. Stress concentration sites develop along the edges of the indentation. Repetitive stress at those sites forms cracks that propagate until surface material is liberated from the surface of a raceway or rolling element in the load zone.

Wear debris in the lubricant of an AT is generally less than that of a manual transmission. Regardless, test results and fatigue analyses[3] of AT bearings reveal that

Fig. 20.   Process of surface originated flaking

Wear debris forms indentation

Stress concentration sites develop under subsequent contact

Cracks develop from stress concentration sites

Cracks propagate and flaking occurs

Enlarged photo of inner ring raceway surface	Fatigue index
0.5 mm	

Fig. 21.   Fatigue analysis of bearing endurance test for an AT

Test conditions
  P/C–0.43 oil bath lubrication
  N=4 000 rpm
  Wear debris ⎡ Hardness : 870 HV
              ⎢ Dimension: 14 mm to 147 μm
              ⎣ Amount   : 150 ppm

Fig. 22.   Life test results of bearings operated under contaminated lubricant conditions

Photo 4.   Microstructure of carbonitrided SAC steel
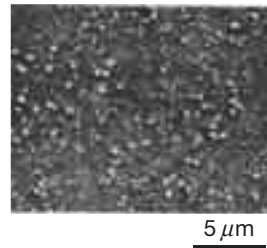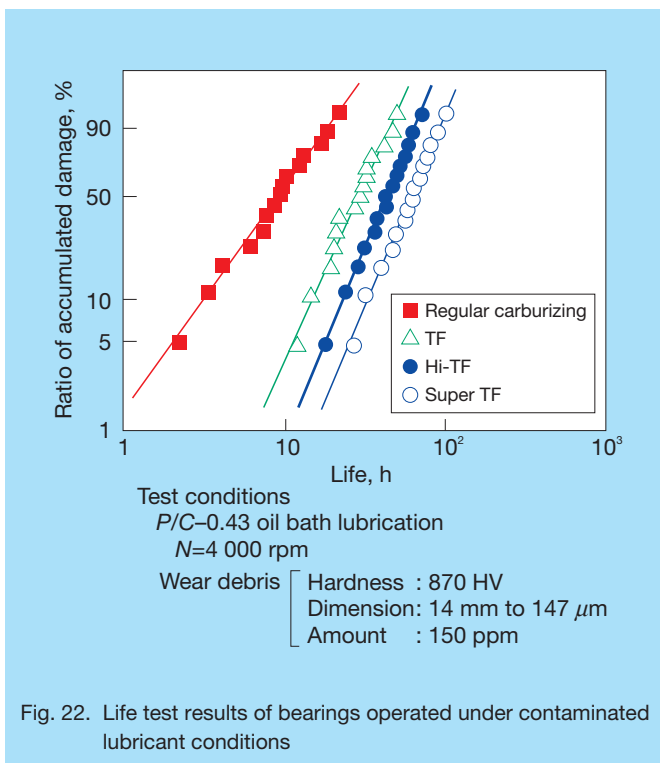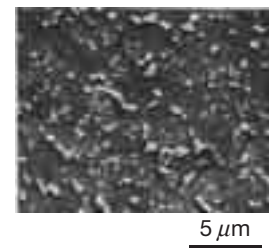

Photo 5.   Microstructure of carburized conventional steel

surface fatigue still poses a formidable threat to the raceway surface of the bearings. Fig. 21 shows fatigue analysis results of an AT bearing after endurance testing. In order to alleviate stress concentration sites along the edge of the indentation, increasing the amount of retained austenite of bearing material has proven effective. Austenite itself, however, has a soft structure that reduces the hardness of the bearing material. To ensure sufficient hardness that is required of the bearing material, NSK developed a technology[4] that promotes the uniform distribution of fine carbide and carbonitride particles in the bearing material that is more evenly dispersed than normal carburized products (Photo 5). This technology was applied to a new original steel, SAC (Photo 4), and combined with a new heat treatment method. The final result is NSK's original TF series bearings, which adopt this technology for excellent long life compared to bearing steel and carburized material (Fig. 22). Many automatic transmissions now use TF series bearings.

This long life technology is indispensable to improving fuel economy. Furthermore, this technology enables bearing size reductions, in addition to various advantages including enhanced durability, low frictional torque design, and an expanded range of applications by replacing tapered roller bearings with ball bearings.

4. Conclusion

This article has introduced highly efficient AT bearings for six-speed AT and CVT applications where demand for efficiency is rapidly growing. By applying our tribology technologies, material and heat treatment technologies, and high-precision processing technologies, we will continue to dedicate ourselves to developing products that respond to stricter demands in the market.

References
1) Toyota Motor Corporation, "Electronics Manual No. 7A02510," Camry ACV3# (2003)
2) H. Aramaki, "Rolling Bearing Analysis Program Package 'BRAIN'," NSK Technical Journal No. 663 (1997) 1-7.
3) K. Furumura, S. Shirota, and A. Fujii, "Fatigue Analysis of Rolling Bearings (Part 3)," NSK Technical Journal 646 (1986) 18-25.
4) Y. Murakami "Long Life Bearing Technology by Carbo-Nitriding," NSK Technical Journal 673 (2002) 3-6.

Tatsuya Ootsubo

Satoshi Kadokawa

Efficiency Analysis of Half-Toroidal CVT Considering Deformation of Pivot Shaft

Masayuki Ochiai
Corporate Research & Development Center

ABSTRACT

This article describes efficiency analysis of a half-toroidal continuous variable transmission (CVT) that takes into consideration deformation of the pivot shaft. Recent advancements made in automotive transmissions require the development of a high-performance half-toroidal CVT that is compact, highly efficient, and provides high-torque capability. In order to develop such a high-performance CVT, CVT efficiency must be predicted accurately. In CVTs, a large load is applied to a traction contact point to obtain traction force, which may cause deformation and displacement of some CVT components. Until now, conventional analysis failed to consider the deformation of CVT components. NSK has developed a new calculation method for predicting half-toroidal CVT efficiency with greater precision.

1. Introduction

Recent advancements in automotive transmission systems have created demand for enhanced performance of half-toroidal continuously variable transmissions (CVT). CVTs for newer vehicles will need to have greater efficiency, higher torque capacity, while further reducing overall size. Accurately predicting CVT efficiency is important for manufacturing such a high-performance CVT.

Fig. 1 shows a schematic view of the front-side power rollers in a double cavity CVT. Power is transmitted from the engine to the loading cam, input disk, power rollers and output disks[1]. Transmission of power from the input disks through the power rollers to the output disks is accomplished by means of traction force at the traction contact points where high pressure is a crucial requirement. However, the large amount of traction force and contact force being applied to the parts that compose the CVT (input / output disks, power rollers, trunnions, etc.) can result in deformation. Although deformation was not originally taken into account when calculating CVT efficiency[2], it will have to be more accurately predicted to further enhance efficiency. Gaining a quantitative understanding of the degree to which deformation affects CVT efficiency is important to reduce size and raise torque

: Traction contact point

Loading cam

Output disk

Inner ring of power roller

Power roller bearing

Input disk

Trunnion
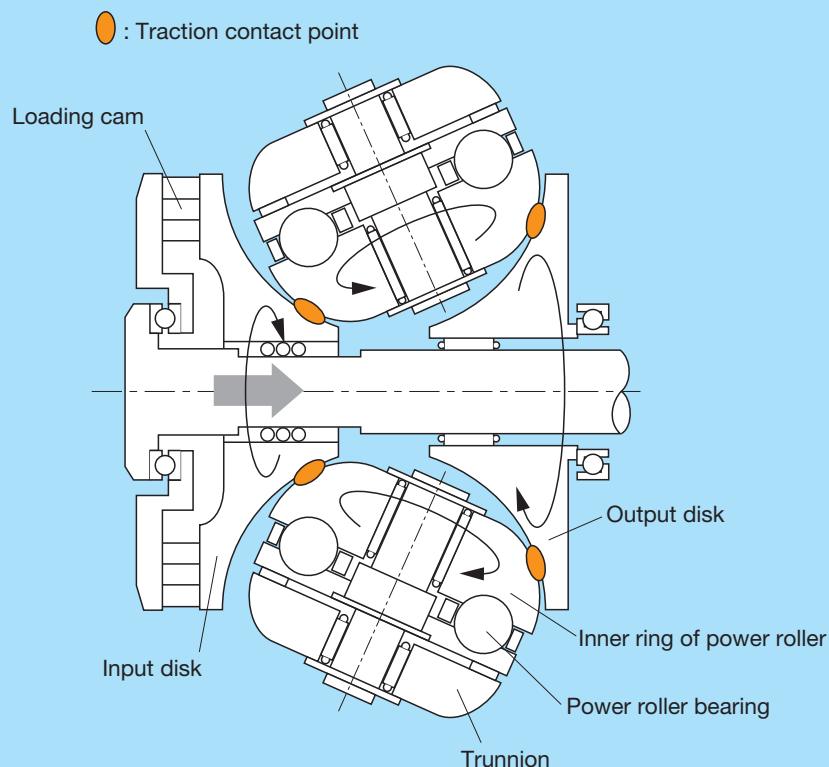
Fig. 1 Schematic view of a half-toroidal CVT

capability.

Under these circumstances, establishment of a more accurate method of calculating CVT efficiency that takes the effect of deformation into account was called for [3) 4)]. This article provides a description of an efficiency calculation method that takes the deformation of the pivot shaft and power rollers into account.

2. Comparison of Integrated and Separated Types of Pivot Shafts

Frictional loss needs to be included when calculating CVT efficiency. Since frictional loss of the power rollers is the dominant loss in double-cavity CVTs compared with other bearings, the amount of such loss must be estimated accurately [5)]. Fig. 2 shows two support structures of power rollers. The separate-type pivot shaft shown in Fig. 2 (a) is the conventional structure. Here, the pivot shaft and power roller outer rings are separate to allow for machining. Because the pivot shaft and outer rings of the power rollers are mounted with a clearance fit, the pivot shaft becomes slightly inclined when traction force (radial load) is applied to the inner rings of the power rollers, and the raceways of the inner and outer rings become misaligned in the radial direction as shown in Fig. 2 (a). After overcoming some machining challenges, we successfully developed an integrated type pivot shaft and power roller as shown in Fig. 2 (b). This power roller integrates the pivot shaft and outer ring, and since it has fewer parts than the separate type, it offers the advantage of lower machining costs. Fig. 3 shows the results of an experiment comparing misalignment of the inner ring of the power rollers and trunnion when a radial load is applied for both types of pivot shafts.

(a) Separate-type pivot shaft (conventional)

(b) Integrated-type pivot shaft (improved)

Fig. 2 Separate type and integrated type of pivot shaft

Fig. 3 Amount of inner ring displacement for both types of pivot shaft under F_r=2 000N
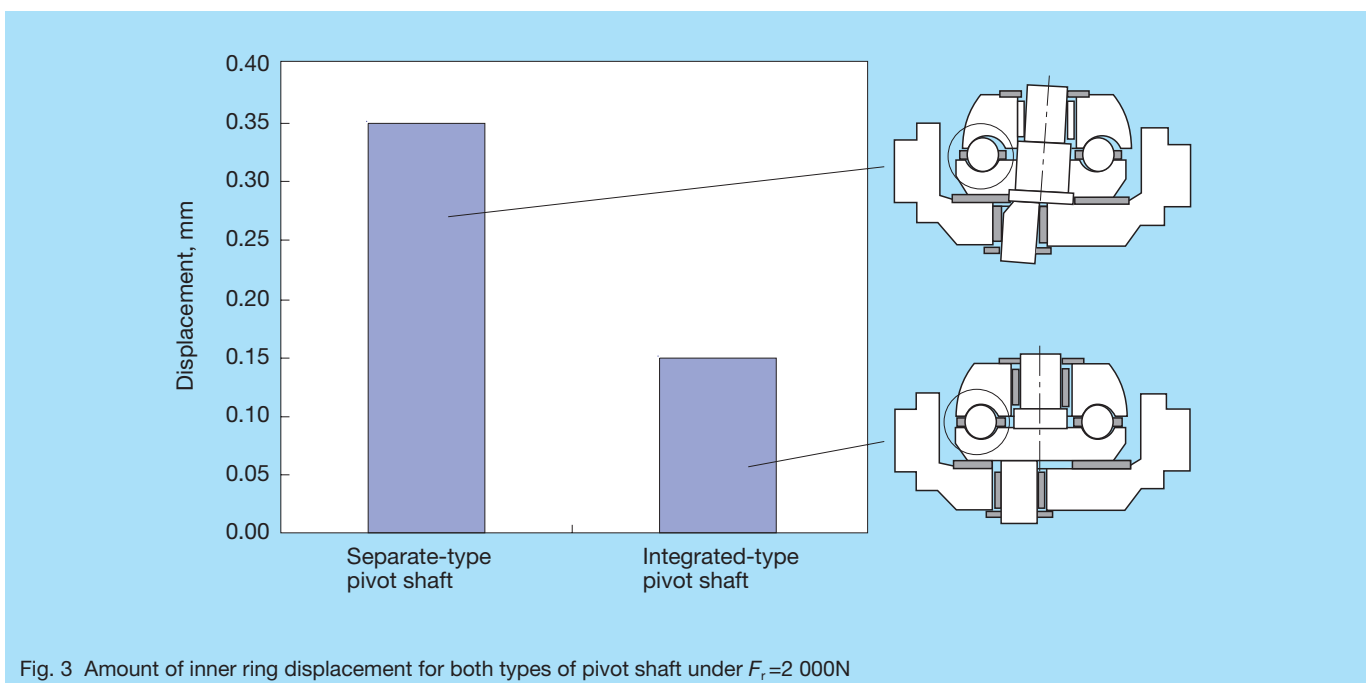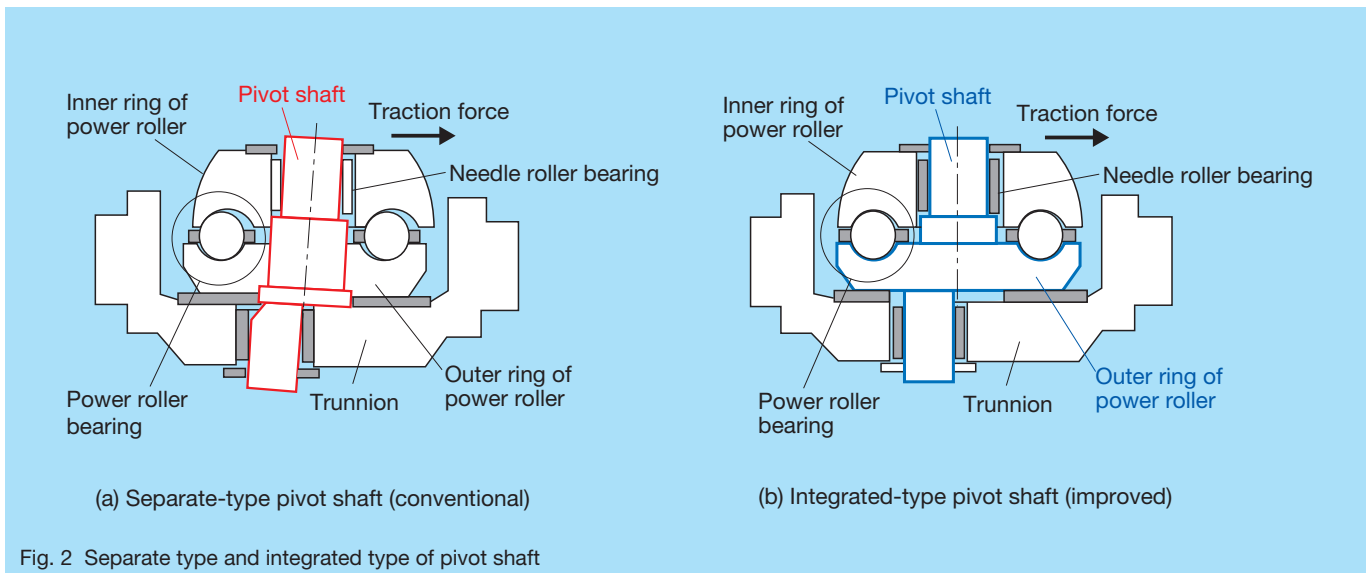
Radial rigidity of separate-type pivot shaft and power roller suffers due to the low rigidity that exsists where two parts connect. It does, however, show a drastic improvement for the integrated type pivot shaft and power roller. Because misalignment of the inner and outer rings increases when there is insufficient radial rigidity, behavior of the rolling elements inside the bearing is affected, which has a negative impact on CVT efficiency.

3. Performance Calculation of the Power Rollers Considering Deformation of the Pivot Shaft

3.1 Calculation model

As was previously stated, there is a difference in radial rigidity between the integrated and separated types of pivot shaft and power rollers. However, past calculating methods ignored rigidity of the pivot shaft, thus making it impossible to include differences in radial rigidity in efficiency calculations. NSK has therefore come up with a new method that enables these differences to be calculated.

Fig. 4 shows the calculation model used for analysis. The pivot shaft is modeled as a one-dimensional beam, where the power roller bearings (thrust ball bearings) and needle roller bearings support radial loads. Furthermore, the bearings perform the functions of a nonlinear spring having a gap mutually coupled in the axial and radial directions, and in the rotating direction. By using this model, elastic deformation of the pivot shaft can be taken into account for calculating the amount of load shared by each bearing. NSK's bearing analysis program, BRAIN [6], was used for performing calculations and to determine various bearing characteristics such as surface pressure distribution and load on the rolling

elements of the bearing, and frictional loss that occurs between rolling elements and the raceways in addition to the contact surface area of the cage.

3.2 Calculated results of bearing load sharing

Table 1 shows the CVT specifications used for calculation. The number of power roller revolutions and the amount of load applied to the power rollers are calculated using the specifications given in the table according to operating conditions.

Fig. 5 shows the calculation of input torque and radial load applied to the power roller bearings and needle roller bearings when speed ratio i = 1.0. Calculation results show that radial load on the needle roller bearings is greater than load on the power roller bearings for both the integrated and separated types of pivot shafts. Radial load on the power roller bearings and needle roller bearings increases with input torque, but the proportion of load sharing is approximately the same for both the integrated and separated types of pivot shafts regardless of input torque.

Fig. 6 shows the calculated radial load-sharing of the power roller bearings and needle roller bearings for three speed ratios when input torque T_{in} = 350 N·m. While the load-sharing ratio for the power roller bearings differs somewhat according to the speed ratio, it is about 20 percent for the separate-type pivot shaft as shown in Fig. 6 (a) and about 10 percent for the integrated-type pivot shaft shown in Fig. 6 (b). As illustrated in Fig. 3, the low rigidity of the separate-type pivot shaft causes a large amount of displacement of the inner ring of the power roller, resulting in a larger percentage of the radial load being supported by the power roller bearings.
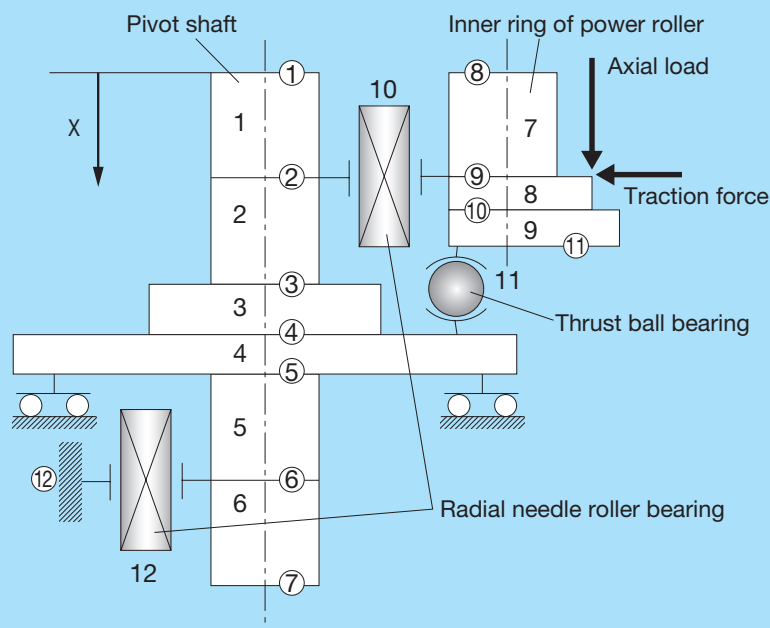

Fig. 4 Calculation model of power roller

Table 1 CVT specifications

Cavity diameter	132 mm
Disk radius	40 mm
Half contact angle	62.5 °
Speed change ratio	0.5 – 1.9
Max. torque	350 N·m
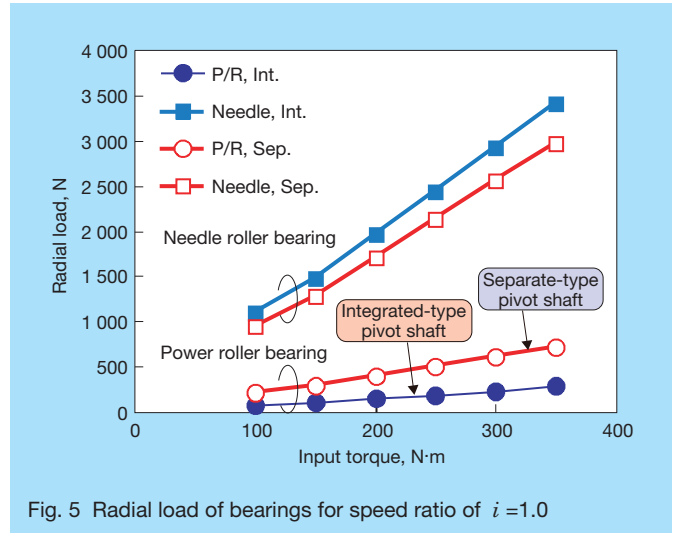
Fig. 5 Radial load of bearings for speed ratio of i =1.0

(a) Separate-type pivot shaft

(b) Integrated-type pivot shaft
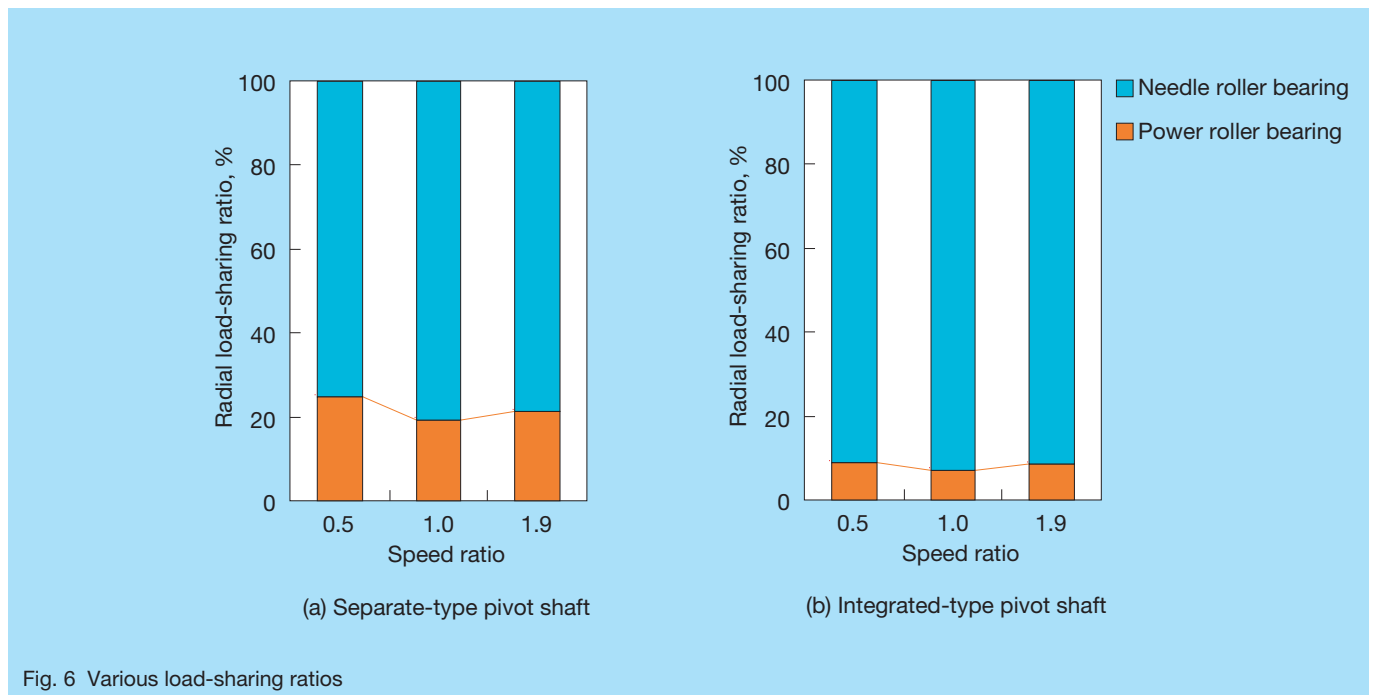
Fig. 6 Various load-sharing ratios

3.3 Frictional loss of power roller bearings

Fig. 7 shows calculated heat generation (frictional loss) of the power roller bearings for both of the integrated and separated types of pivot shafts. As the figure shows, more heat is generated in the separate-type pivot shaft than in the integrated-type pivot shaft. The figure does not show much difference in the amount of heat generated other than for the cages used in both types of pivot shafts, but more frictional loss is primarily generated at the cage/ball contact points in the separate-type pivot shaft.

As was previously mentioned, radial load is greater for the separate-type pivot shaft than the integrated type, but because axial load is predominant, no difference in heat generation on the contact surface of the balls and raceway is observed. Fig. 8 illustrates misalignment between the power roller inner and outer rings. When traction force is

applied to the power rollers, the inner and outer rings become misaligned, resulting in a contact angle as shown in the figure. Because the distance between the point of contact of the power roller inner ring race surface and the rotating axis is asymmetrical on the left and right sides (r_1 < r_2), rolling element 1 rotates slower than under ordinary circumstances where there is no contact angle, whereas rolling element 2 rotates faster. This difference in running speeds results in position of rolling elements being advanced or delayed.

Fig. 9 shows the excursion of the rolling elements calculated from variations in the contact angle. Variations in the amount of excursion among rolling elements is larger for the separate-type pivot shaft. If variation in amount of excursion is greater than the clearance between the cage pocket and the balls, significant contact force is applied to the
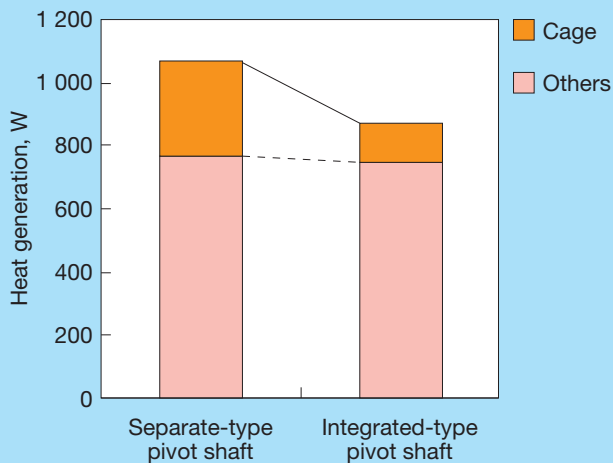
Fig. 7 Heat generation of power roller bearings when
i= 1.9, n_{in}= 2 000rpm, T_{in} =350N·m
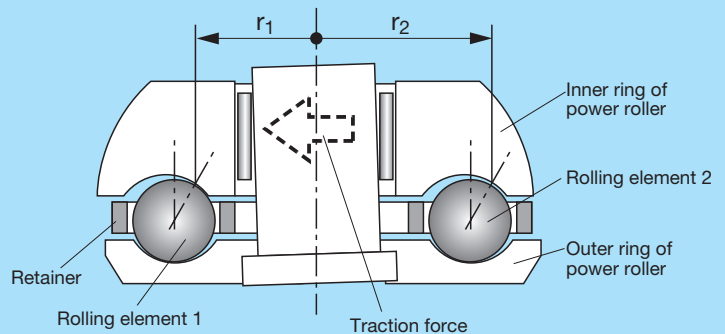
Fig. 8 Misalignment between the power roller inner
and outer rings
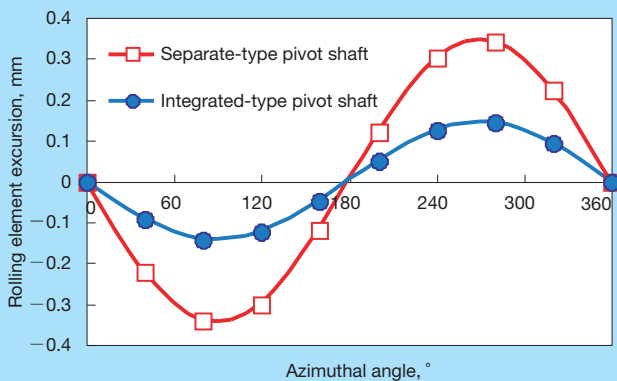
Fig. 9 Ball excursion when i =1.9, n_{in} =2 000rpm, T_{in} =350N·m
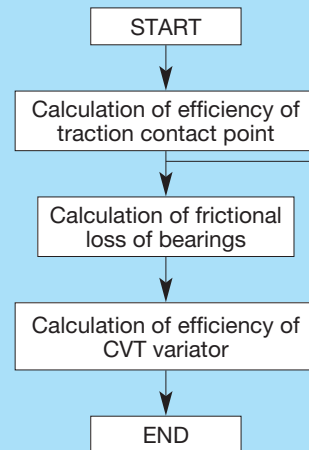
Fig. 10 Flow diagram for calculating half-toroidal CVT efficiency

cage. Frictional force produced between the cage and rolling elements increases along with the contact force, causing the amount of heat generated by the power rollers to rise. The amount of heat generated by the cage of the separate type is consequently greater than that of the integrated type.

4. CVT Variator Efficiency Considering Deformation of the Pivot Shaft

4.1 Calculation method of variator efficiency

Fig. 10 shows the procedure for calculating CVT efficiency. The value of variator efficiency is calculated from the results of traction contact point efficiency and frictional loss of the bearings. CVT power transmission efficiency is expressed as the product of speed transmission efficiency and torque transmission efficiency as shown in equation (1).

$$\eta_p = \eta_T \; \eta_S \quad\quad\quad (1)$$

Here:

$$\eta_T = \eta_{T1} \; \eta_{T2} - 4 \; \eta_{T2} \; e_1 \; T_{brg} / T_1 \quad\quad (2)$$

$$\eta_S = (1 - Cr_1) \; (1 - Cr_2) \quad\quad (3)$$

η_T : Torque transmission efficiency
η_S : Speed transmission efficiency
e_1 : Input side speed ratio (r_1/r_2)
Cr : Creep
T_1 : Input torque
T_{brg} : Power roller bearing torque

Subscript 1 : Value for input side traction contact point
2 : Value for output side traction contact point

4.2 Comparison of experimental results

Fig. 11 shows the relationship between CVT variator efficiency and input torque for input shaft speed n_{in} = 2 000 rpm based on calculated results and experimental results. This figure shows variator efficiency at three ranges of speed ratios, such as reduction speed (i = 1.9), intermediate speed (i = 1.0), and increasing speed (i = 0.5).

The figure also shows a two-percent improvement of variator efficiency for the integrated-type pivot shaft over that of the separate type for all speed ratios.

The calculation used in the past was unable to predict differences in variator efficiency. The calculation method that takes into account distortion of the pivot shaft described in this paper is effective for expressing
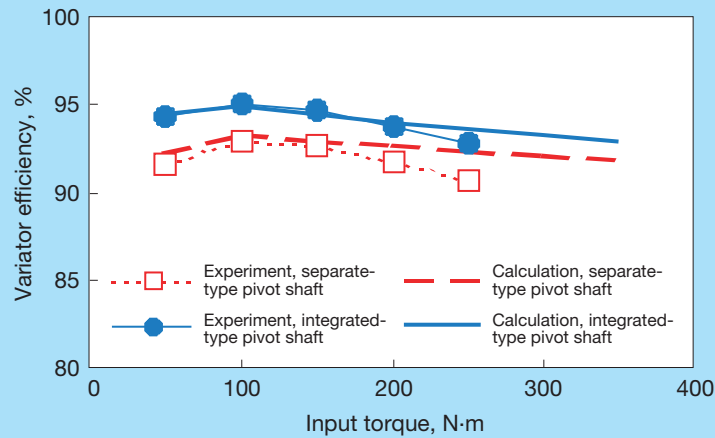
(a) i = 1.9
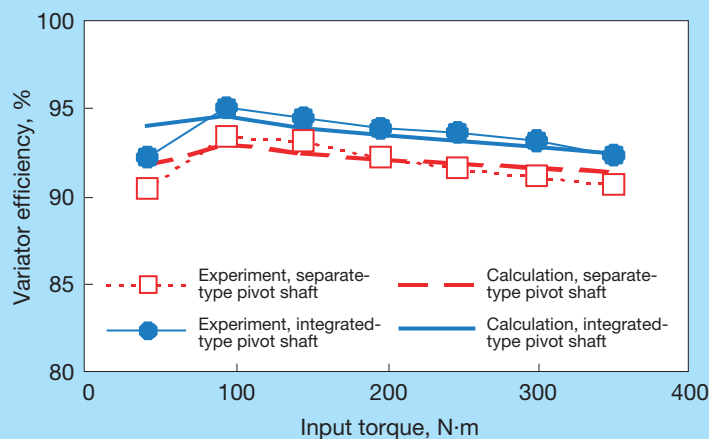
(b) i = 1.0
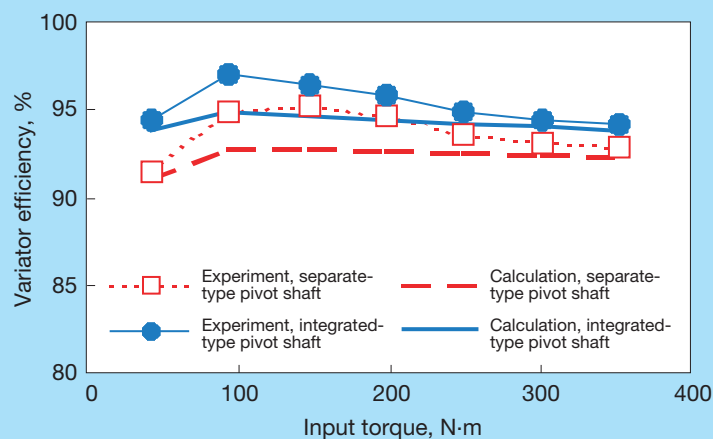
(c) i = 0.5

Fig. 11 Efficiencies of CVT variator with input torque at n_{in}=2 000rpm

differences in efficiency for the integrated and separated types of pivot shafts. Calculations using the speed ratio $i = 1.9$ concur with the results of actual tests at low torque. However as torque increases, the calculated results gradually exceed the results of actual tests. This is due to the increase of contact force as torque increases, resulting in a large deformation of the disk and trunnion. Efficiency can be calculated more accurately by taking this deformation into account. Conversely, at low torque of speed ratio $i = 0.5$, calculations tend to be lower than the results of actual tests. We intend to conduct further studies in regards to this matter.

5. Conclusion

This paper describes a method of calculating CVT efficiency that takes into account the deformation of the pivot shaft that supports the power rollers. The paper shows that the difference in efficiency for integrated and separated types of pivot shafts can be calculated by taking deformation of the pivot shaft into account. The author will continue to develop a CVT of better performance using these methods of analysis described here.

References:
1) Hisashi Machida, Yasuo Murakami, "Development of Traction Drive Continuously Variable Transmission (CVT) POWERTOROS Unit, No.1," NSK Technical Journal, 669 (2000), 9-20
2) Hirohisa Tanaka, Research of Toroidal Continuously Variable Transmission (CVT) (No.1 Speed Transmission Efficiency and Torque Transmission Efficiency), Transactions of the Japan Society of Mechanical Engineers, 53-491 C (1987) 1500-1506
3) Masayuki Ochiai, Aya Kikuchi, Takashi Nogi, "On the Advanced efficiency analysis for Half Toroidal CVT (No.1)," Proceedings of Society of Automotive Engineers of Japan Inc., No.21-03 (2003), 1-4
4) Masayuki Ochiai, Kinji Yukawa, "On the Advanced Efficiency Analysis for Half Toroidal CVT (No.2), Proceedings of Society of Automotive Engineers of Japan Inc., No.65-03 (2003), 9-12
5) Hirohisa Tanaka, "Toroidal CVT," (2000) 64, Corona Publishing Co., Ltd.
6) Shinichi Natsumeda, "Computer Simulation Technique for Predicting Performance of Rolling Bearings" NSK Technical Journal, 673 (2002) 31-35

Masayuki Ochiai

HUBK Series of Hub Unit Bearings for Minivehicles

NSK has developed a third generation hub unit for minivehicles called the HUBK series in conjunction with growing modularization and platform integration of automobile production. The HUBK series focuses on the growing market of minivehicles in Japan. Features of the HUBK series include a design that is lightweight, provides basic functionality, meets the performance requirements of minivehicles, and offers excellent cost performance. This article will discuss the construction and features of NSK's HUBK series is greater detail.

1. Construction

Conventional hub units have two single row ball bearings mated to a spindle. An adjusting nut, which is a one-piece nut that locks on the spindle threads, seats the bearings into place and prevents them from coming loose (Fig. 1).

The HUBK series is different in that it uses double-row angular contact ball bearings mated to the spindle and has an outer ring with flanges (Photo 1).

Several hub bolts are press-fitted and evenly spaced around the circumference of the flange for mounting the wheels with hub nuts. The flange of the outer ring has bores where components of the suspension system are mounted with bolts. The inner ring and hub spindle are forged together using a swaging process to secure the inner ring to the hub and to provide appropriate preload for the bearings. Furthermore, the sensor rotor, which is mounted on the outer circumference of the inner ring, works with the anti-lock brake system (ABS) sensor, which is press-fitted onto the outer ring for detecting wheel speed (Fig. 2).

2. Features

2.1 Weight reduction

We conducted strength and stiffness analyses of the hub spindles and outer rings. Based on analysis results, the thickness and shape of the outer ring was optimized while relieving some stress concentrations. Analysis results also contributed to achieving an optimal design where portions of the outer flange were eliminated for weight reductions

Fig. 1 Conventional hub bearing for minivehicles

- Single row ball bearing
- Single row ball bearing
- Wheel bearing adjusting nut
- Spindle
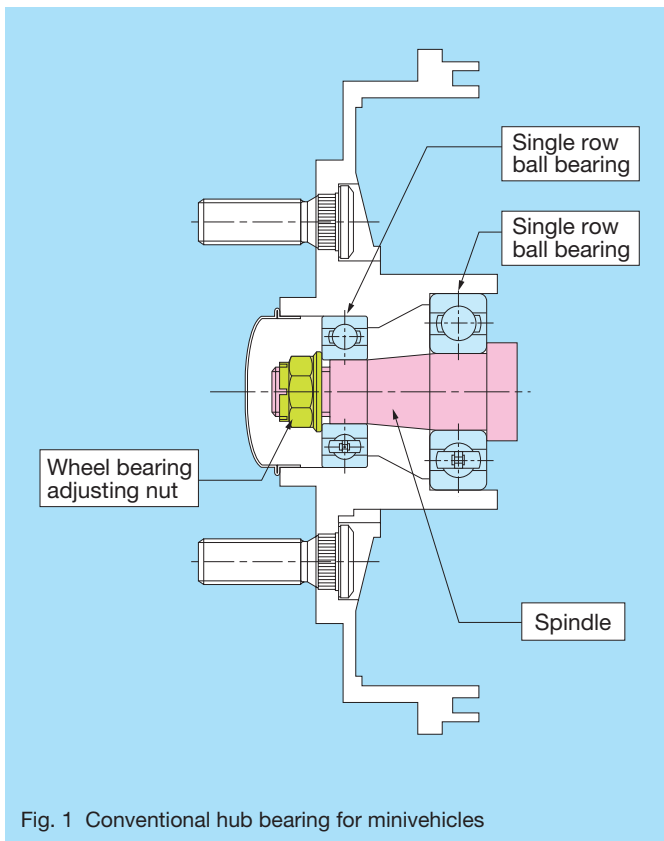
Photo 1 NSK's HUBK Series
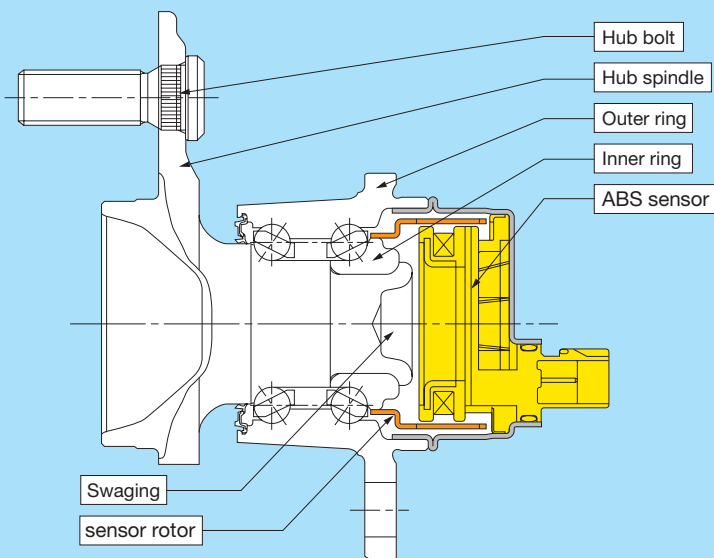
Fig. 2 HUBK series for minivehicles
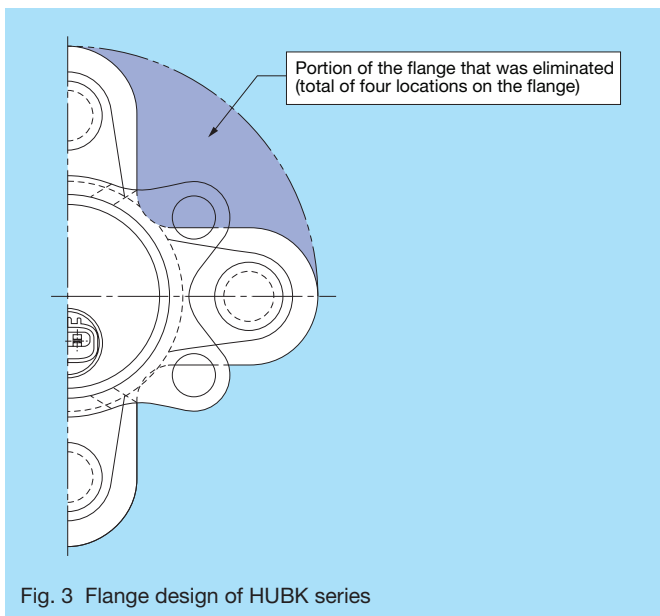
Fig. 3 Flange design of HUBK series

while maintaining sufficient strength and stiffness of the hub unit (Fig. 3). Swaging of the inner ring with the hub spindle eliminates the need for adjusting nuts and cap screws for significant weight and size reductions while maintaining high reliability.

2.2 Cost reductions

Cost performance of the HUBK series was enhanced by a thorough review process that aimed to optimize parts specifications.

1) Reviewed permissible dimension gaps of each part or component
2) Eliminated unnecessary material using an optimal design

3) Reduced the number of parts using the swaging process

2.3 Reliability improvement of ABS sensor

Trends in market demand show that antilock brake systems (ABS) are becoming standard equipment on most new vehicles. In order to control ABS properly and effectively, ABS sensors need to be able to detect and monitor wheel speed accurately. The HUBK series ensures the reliability of ABS sensors with a sensor rotor that is mated inside the hub unit to protect it from road debris, including gravel and dust.

2.4 Easier mounting

The HUBK series helps to streamline the automotive assembly line process by eliminating the need to mount single row ball bearings onto the spindle, tighten adjusting nuts, integrating the ABS sensors, and eliminates the need to install the sensor rotor. The HUBK series is made for easy mounting on the assembly line, thus helping to boost cost efficiency of the automotive manufacturing process.

3. Applications

The HUBK series is designed for non-driven wheels of minivehicles.

4. Conclusion

We will continue our efforts towards further developments that are focused on meeting customer needs for lightweight and low-cost products that provide basic functionality and quality performance.

Column-Type Electric Power Steering

Growing environmental concerns associated with automobiles are increasing the demand for environmentally friendly products that offer energy-saving benefits and reduce CO_2 emissions.

Electric power steering (EPS), which requires less energy consumption in comparison to traditional hydraulic power steering systems, has received considerable attention for its contributions towards fuel efficiency.

In addition to offering environmentally sound benefits, NSK has recently commercialized a new type of compact, high-performance, column-type EPS (Photo 1).

1. System Overview

Fig. 1 shows the construction of the new column-type EPS system.

This EPS system consists of a torque sensor that detects the amount of force applied to the steering wheel by the driver, an electric control unit (ECU) that processes signals from the sensor, a motor that generates torque based on ECU output, and reduction gears that decelerate motor rotation.
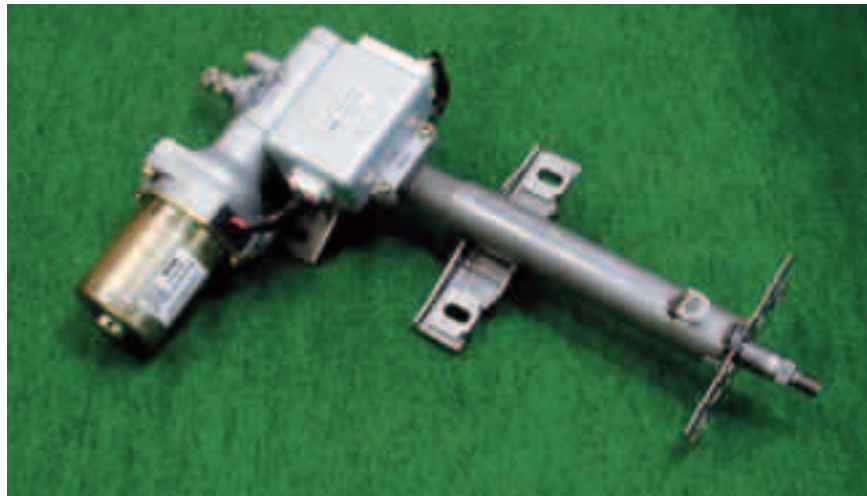
Photo 1 Column type EPS
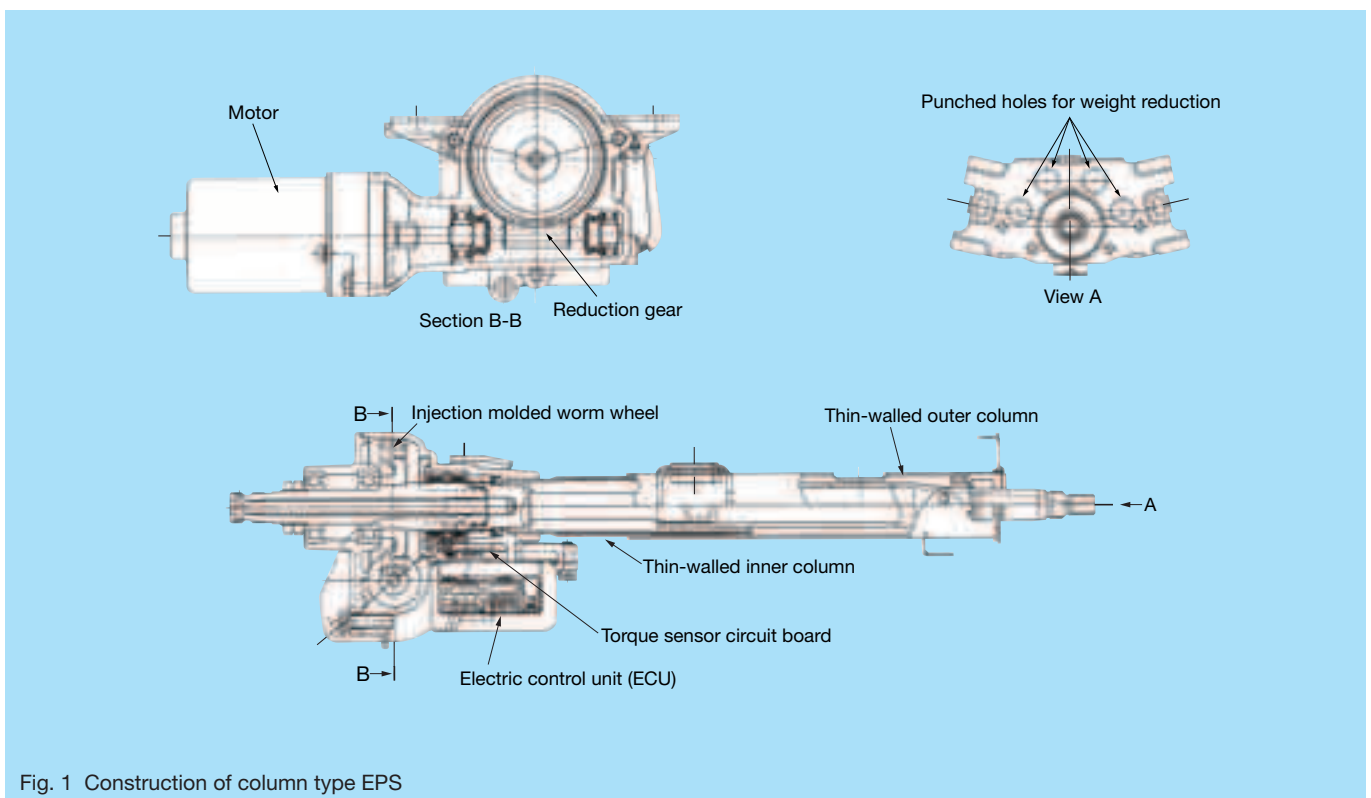
Fig. 1 Construction of column type EPS

2. EPS Advantages

a. Low cost
- Reduction gears
  Injection molding of the worm wheel helps to reduce manufacturing costs.
- ECU
  Installing the ECU under the torque sensor reduced the number of component parts where the ECU heat sink also serves as a sensor cover.
  Size and costs have been reduced by using an ECU circuit board comprising of three components: a base, a hybrid integrated circuit (HIC), and a power module. Further cost reductions have been achieved by using standard parts across different EPS systems used in different vehicle platforms.
- Torque sensor board
  A time-tested, non-contact torque sensor has been adopted in the new EPS design.
  Cost effectiveness of the application specific integrated circuit (ASIC) implemented on the board was maintained by complete customization (Photo 2).
- Motor
  Standardizing the compact brush motor for improving volume efficiency contributed to reducing costs.

b. Lightweight
  Weight was reduced by using thin-walled brackets and column tubing, while maintaining the same level of stiffness of the steering support when mounted. Further weight reductions were achieved by drilling holes in the switch bracket.

c. High performance

- Next-generation electronic control unit (ECU)
  In addition to smooth steering control enabled by the traditional NSSH control, feedback control for self aligning torque (SAT) was implemented to estimate the suspension jounce and rebound from tires for improved return to center positioning, good turning response, and on-center feel without an angle sensor.
- Motor
  Noise reductions have been achieved by optimizing brush and commutator contact, and by eliminating the floating structure of the brush holder assembly.

3. Specifications

Table 1 shows the EPS system specifications

4. Summary

This compact, cost-effective, high-performance, column-type electric power steering is designed for minivehicles.

Based on the advantages discussed in this article, we are committed to further promoting the use of EPS systems in a greater variety of applications while working toward standardization.

Circuit board with a current ASIC
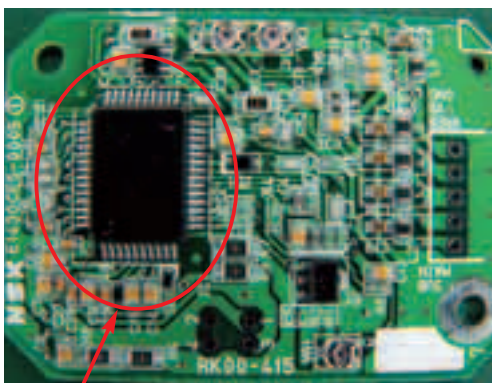
Circuit board with the new compact ASIC

Current ASIC
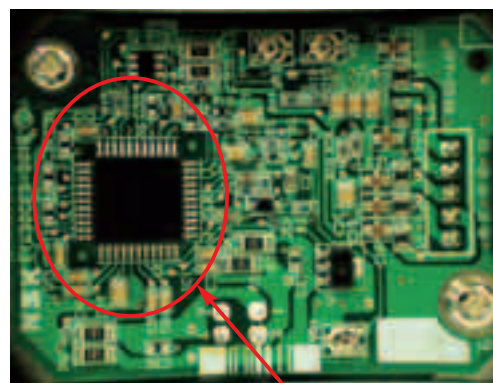
New compact ASIC

Photo 2 Torque sensor circuit board

Table 1 EPS system specification

Items		Details
Assembly	Assist torque	21.6 N·m
Reduction gear	Type	Worm and worm wheel
		(Wheel gear : Injection molding) Two-thread
	Reduction ratio	16.5 : 1
Motor	Type	DC brushless motor
	Rated current	30 A
	Rated speed	1 360 rpm
	Rated torque	1.54 N·m
Torque sensor	Type	Non-contact self-inductance
	Power supply voltage	DC9.5 V
Controller	Rated voltage	DC12 V
	Control range of motor current	0 – 30 A
	Communication functions	Off-board diagnostic tool
	Self-diagnosis &fail-safe functions	Initial check, Monitor EPS system (Upon detecting any failure, stores failure data in the ECU)
	Control items	1) Phase compensation controller
		2) Robust stabilizing compensation controller
		3) Friction compensation controller
		4) Inertia compensation controller
		5) Yaw damping controller
		6) Feedback controller for SAT

NSK LCube Series of Highly Durable Tappet Rollers

With the growing awareness of environmental concerns and stricter regulations that enforce energy conservation, many engines have pivot rocker arms that use valve lifters (tappets) with needle roller bearings (tappet rollers). The outer ring rolls over the cam lobe instead of sliding on it to reduce friction and improve fuel economy.

From 1984, NSK became the first company in Japan to mass-produce tappet rollers for rocker arms. Specifications for various tappet rollers had to be selected based on the materials used for different cams. Cam action, contact area, and other specific characteristics varied for each cam, resulting in poor formation of an oil film between the outer ring and the cam. Thus, damage to the cam surface sometimes occurred. To further ensure protection from occasional damage to the cams due to cam specifications and operating conditions, NSK developed the NSK LCube series of highly durable tappet rollers that feature a special processed roller surface (Photos 1 and 2).

The LCube series helps prevent damage to the surface areas of the cam lobe and tappet roller. The rollers undergo special surface finish processes, and are compatible with any cam regardless of the cam material.

1. Features

- Low friction: Loss of dynamic torque has been reduced by 60% (Fig. 1) by switching from sliding bearings to needle roller bearings for the tappet (valve lifter).
- Lean lubrication resistance: Lubrication oil reservoirs are formed by a process that randomly positions microscopically small dimples that act as oil reservoirs on the outer surface of the outer ring, which work to prevent cam surface failure under poor lubricating conditions (Fig. 2). Also, the smooth surface area helps reduce surface pressure.
- Long life: Durability is improved by reducing stress concentrations across a wide, uniform, flat area for a very fine surface finish, having a "grainless" appearance. The LCube series ensure robust compatibility with cams made of hardened to highly hardened material.

The name "LCube" reflects the three Ls of low friction, lean lubrication resistance, and long life.

Photo 1 NSK LCube series highly durable tappet rollers
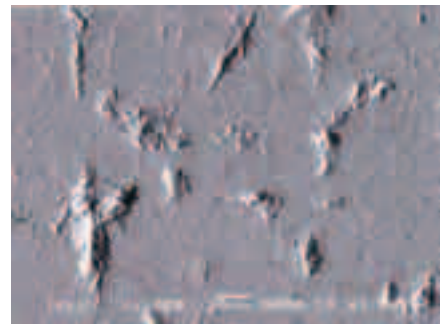
Photo 2 SEM image showing outer surface of tappet roller
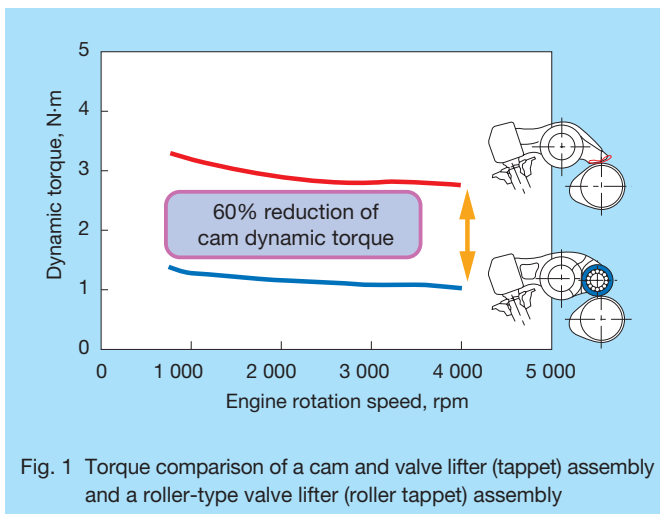
Fig. 1 Torque comparison of a cam and valve lifter (tappet) assembly and a roller-type valve lifter (roller tappet) assembly
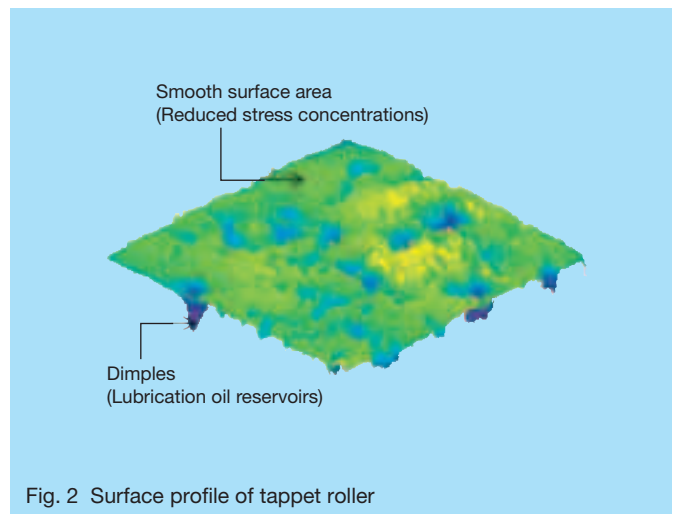
Fig. 2 Surface profile of tappet roller

2. Long life under insufficient lubricating conditions

Poor lubricating conditions in a cam follower and valve lifter system results in a thin oil film between the cam lobe and tappet roller. Bench test results of conventional tappet rollers under lean lubrication conditions showed damage to the cam after less than 500 hours of testing. The NSK LCube series showed excellent durability with no damage to both hardened and highly hardened cams even after more than 1 000 hours of testing (Fig. 3).

3. Applications

- Tappets for automotive engines
- Automotive fuel injection pumps
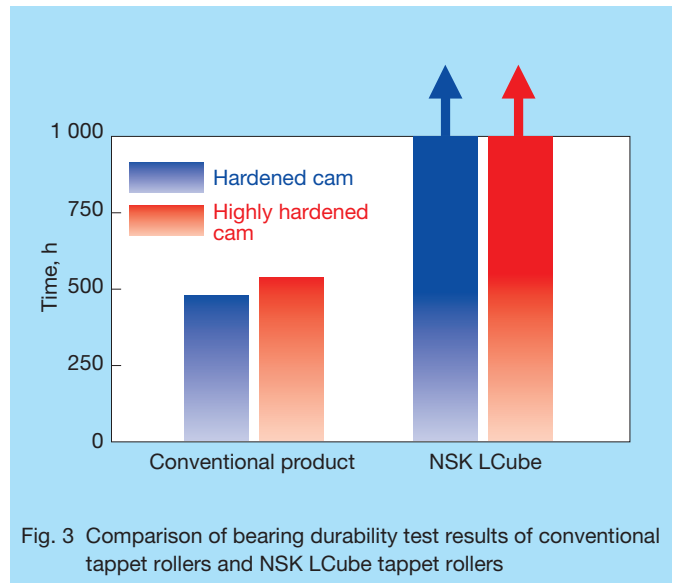
Fig. 3 Comparison of bearing durability test results of conventional tappet rollers and NSK LCube tappet rollers

Long-Life Double-Row Angular Contact Ball Bearings

Automakers have been focusing on reducing the weight and size of automotive transmission for improving efficiency in order to achieve development of vehicles with better fuel economy and lower exhaust emissions. The efficiency of automatic transmissions (AT) has improved by adding additional overdrive gear ratios and by reducing frictional loss. With engines becoming more compact in size while having more power and rotating speed, the parts and components of an AT are under increasing pressure to ensure durability. This article will introduce NSK's long-life double-row angular contact ball bearings (Photo 1) that have been developed for support-gear applications in order to meet the needs of automakers.

1. Construction and Specifications

Fig. 1 illustrates a cross-section view of a long-life double-row angular contact ball bearing with an integrated snap ring groove in the outer ring to axially position the bearing in the gear case. Preloading is secured when the inner rings are brought into face-to-face contact with each other by tightening a locknut.

This long-life double-row angular contact ball bearing allows adequate initial axial clearance to be specified based on the forces of a shaft by tightening the locknuts and interference between the shaft and the inner ring and housing and the outer ring. The required preload can be secured by tightening nuts with regulated clamp torque. Lubrication grooves are formed intermittently in the radial direction on the contact faces of the two inner rings, and are then mated together to form lubrication holes. Lubrication oil is supplied from the center of the shaft into the bearing interior. Bearing specifications are provided in Table 1.

2. Features

2.1 Superior durability

Bearing material was developed using either NSK's proprietary TF technology or a special heat treatment process for bearing steel that ensures bearing durability without changing bearing size or space requirements.

A plastic cage has been adopted in these high-load bearings for use with the design of larger than normal balls. The cage provides lightweight and low-friction features, which contribute to bearing durability under high-speed operating conditions. NSK's proprietary polyamide cage offers excellent high-temperature resistance as shown in Fig. 2.

Fig. 1 Cross section view of a long-life double-row angular contact ball bearing
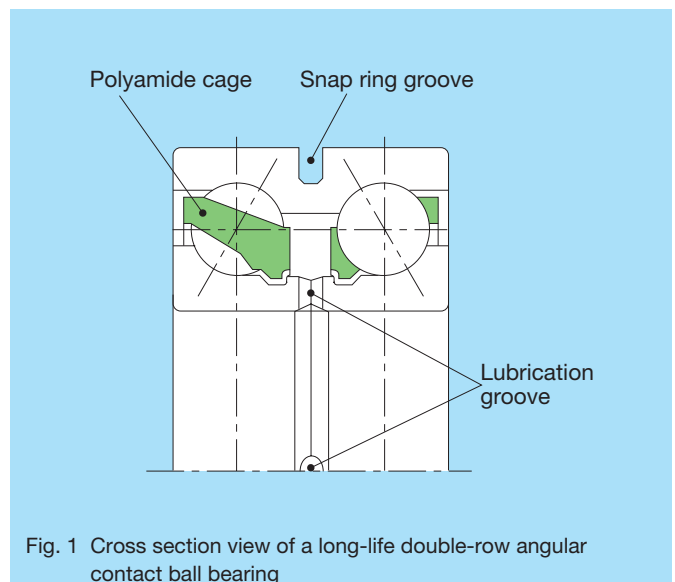
Photo 1 Long-life double-row angular contact ball bearings
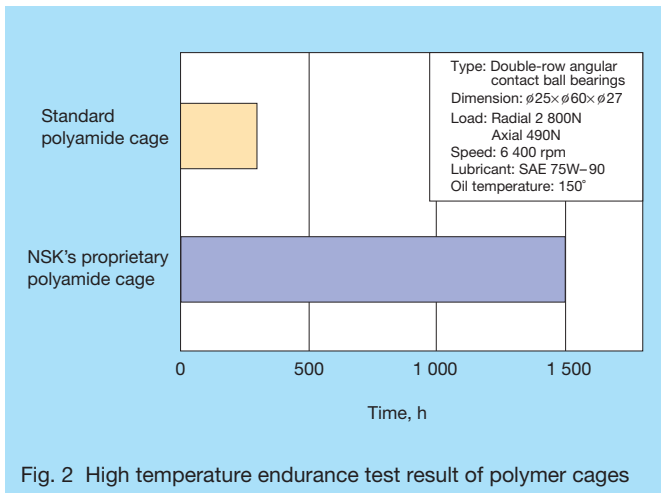
Fig. 2 High temperature endurance test result of polymer cages
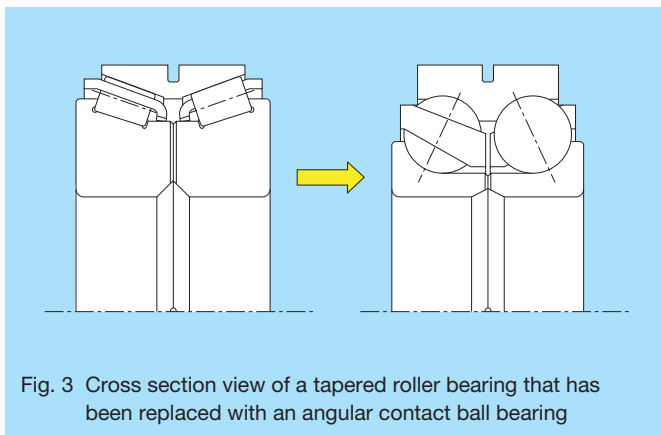
Fig. 3 Cross section view of a tapered roller bearing that has been replaced with an angular contact ball bearing

Table 1 Specifications of mass-produced angular contact ball bearings for ATs

Dimensions (mm)	Bore diameter : ∅27–∅56
	Outside diameter : ∅63–∅91
	Width : 28–36
Configuration	Outer ring with snap ring groove
	Flanged outer ring
	Outer ring with a lubrication groove
	Outer ring with spline

2.2 Low frictional torque

Frictional torque of ball bearings is generally lower than that of tapered roller bearings. If a comparison is made of ball bearings and tapered roller bearings of equal size, load capacity of ball bearings is lower and life is shorter than that of tapered roller bearings. However, NSK has extended the range of ball bearing applications by a proprietary heat treatment technology and optimum interior design to meet the load requirements of our customers, which has consequently contributed to the increased efficiency of ATs. For comparison, Fig. 3 illustrates a cross-section view of a tapered roller bearing that has been replaced by an angular contact ball bearing.

3. Summary

NSK's long-life double-row angular contact ball bearings are mass-produced for use in ATs of compact and subcompact vehicles. We will continue to develop state-of-the-art bearings in response to demands of sufficient durability, size reduction, and low frictional torque.

Long-Life Double-Row Tapered Roller Bearings

In recent years, automatic transmissions (ATs) have had to meet increasingly strict requirements for higher capacity, increased rigidity, greater compactness, and lower frictional torque. In response to these requirements, NSK has developed a new series of long-life double-row tapered roller bearings for automotive transmission parts that require high-rigidity and high load capacity within a small envelope design, such as with the planetary gears of a front-wheel drive train mated to a high-output front engine.

1. Construction and Specifications

There are two types of outer ring configurations for double-row tapered roller bearings for ATs based on the method of mounting in the transmission. Photo 1 and Fig. 1 show a pair long-life double-row tapered roller bearings each with a snap ring groove in the outer ring.

Photo 2 and Fig. 2 show a pair of bearings where each one has an outer ring snap groove in addition to an outer mounting flange and splines, which integrate with the inner races of a one-way clutch. There are two types of this double-row tapered roller bearing where the inner ring is split into halves. The first type has two rings that are mounted face-to-face with each other (Fig. 1). The second type uses a spacer between the two ring faces (Fig. 2).

The bearing illustrated in Fig. 1 uses locknut forces applied to the two inner rings for preloading the bearing. This design allows for initial adequate axial clearance to be specified based on the axial force centering on the shaft by tightening the locknuts and by the interference of a shaft-inner ring and case-outer ring. Thus, the required preload can be set by tightening nuts with a regulated clamp torque. Radial grooves formed after mating the faces of the inner ring halves feed oil directly into the bearings from the center of the shaft.

Photo 1   Long-life double-row tapered roller bearings

Fig. 1   Example of mounted long-life double-row tapered roller bearing

Photo 2   Double-row tapered roller bearings with outer mounting flange
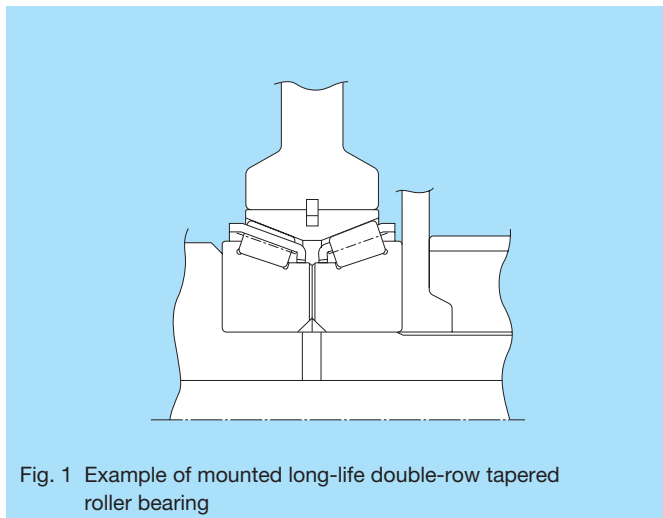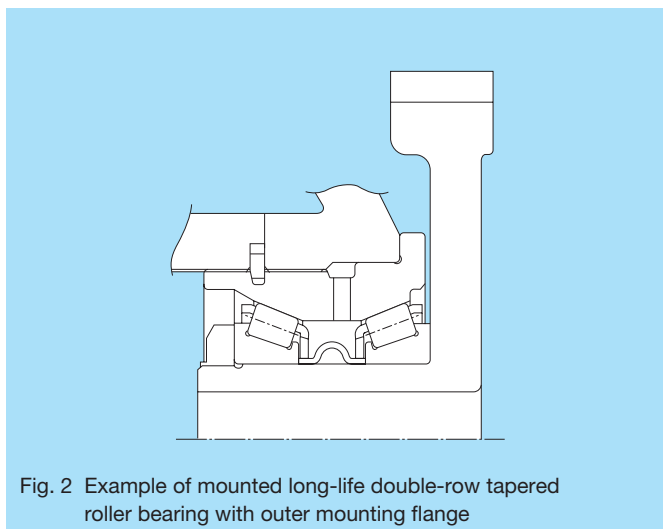
Fig. 2   Example of mounted long-life double-row tapered roller bearing with outer mounting flange

Conventional design   Low-friction design
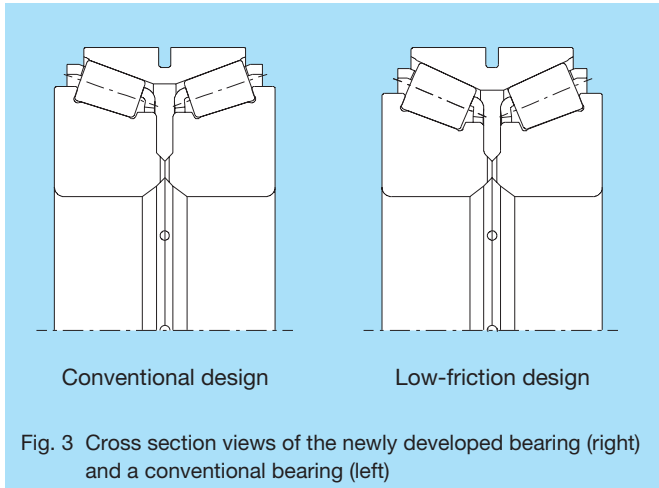
Fig. 3 Cross section views of the newly developed bearing (right)
        and a conventional bearing (left)
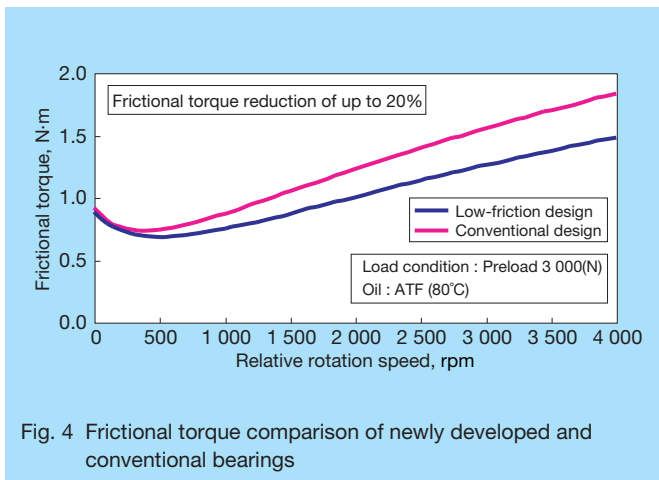
Fig. 4 Frictional torque comparison of newly developed and
        conventional bearings

2. Features

2.1 High capacity and high rigidity

In a comparison with ball bearings, these tapered roller bearings show higher load capacity and longer rolling fatigue life. Therefore, when higher load capacity is required in a limited space, tapered roller bearings are commonly adopted. Furthermore, the high rigidity of these new bearings helps to reduce displacement of gear meshing, which further reduces gear noise.

2.2 Low friction

We have achieved reduction of frictional torque using NSK's proprietary long-life material, heat treatment technology, and have achieved an optimum bearing interior design using NSK's Bearing Analysis Software Package (BRAIN). Fig. 3 and 4 show a comparison of conventional bearings and our new product.

3. Summary

NSK's long-life double-row tapered roller bearings have been mass-produced for ATs used in front-wheel drive trains mated to high-output front engines. As requirements for greater size reductions and lower torque become increasingly strict, we will strive to develop sophisticated products to meet the needs of our customers.

Notes

Notes

Worldwide Sales Offices and Manufacturing Plants

NSK LTD.-HEADQUARTERS, TOKYO, JAPAN   www.nsk.com
Nissei Bldg., 1-6-3, OHSAKI SHINAGAWA-KU, TOKYO 141-8560, JAPAN
ASIA BUSINESS STRATEGIC DIVISION-HEADQUARTERS
P: 03-3779-7145   F: 03-3779-7433   C: 81
INDUSTRIAL MACHINERY BEARINGS DIVISION-HEADQUARTERS
P: 03-3779-7227   F: 03-3779-7644   C: 81
AUTOMOTIVE DIVISION-HEADQUARTERS
P: 03-3779-7917   F: 03-3779-7917   C: 81
NEEDLE ROLLER BEARINGS STRATEGIC DIVISION-HEADQUARTERS
P: 03-5487-2563   F: 03-3779-7017   C: 81
PRECISION MACHINERY & PARTS DIVISION-HEADQUARTERS
P: 03-3779-7219   F: 03-3779-7644   C: 81

Africa
South Africa:
NSK SOUTH AFRICA (PTY) LTD.
JOHANNESBURG   25 Galaxy Avenue, Linbro Business Park, Sandton, Gauteng,
P.O. Box 1157, Kelvin, 2054 South Africa
P: 011-458-3600   F: 011-458-3608   C: 27

Asia and Oceania
Australia:
NSK AUSTRALIA PTY. LTD.   www.nskaustralia.com.au
MELBOURNE   11 Dalmore Drive, Scoresby, Victoria 3179, Australia
P: 03 9764-8302   F: 03 9764-8304   C: 61
SYDNEY   Unit 1, Riverside Centre, 24-28 River Road West, Parramatta, N.S.W. 2150, Australia
P: 02-9893-8322   F: 02-9893-8406   C: 61
BRISBANE   91 Wellington Road, East Brisbane, Queensland 4169, Australia
P: 07-3393-1388   F: 07-3393-1236   C: 61
ADELAIDE   64 Greenhill Road, Wayville, South Australia 5034, Australia
P: 08-8373-4811   F: 08-8373-1053   C: 61
PERTH   Unit 4, 36 Port Kembla Drive, Bibra Lake, Western Australia 6163, Australia
P: 089-434-1311   F: 089-434-1318   C: 61

China:
NSK HONG KONG LTD.
HONG KONG   Room 512, Wing On Plaza, Tsim Sha Tsui East, Kowloon, Hong Kong
P: 2739-9933   F: 2739-9323   C: 852
KUNSHAN NSK CO., LTD.
KUNSHAN PLANT   258 South Huang Pu Jiang Rd Kunshan E&T Development Zone Jiang Su 215335, China
P: 0512-5771-5555   F: 0512-5771-5689   C: 86
GUIZHOU HS NSK BEARINGS CO., LTD.
ANSHUN PLANT   Dongjiao, Anshun, Guizhou 561000, China
P: 0853-3521505   F: 0853-3522722   C: 86
NSK STEERING SYSTEMS DONGGUAN CO., LTD.
DONGGUAN PLANT   High-tech Park, Shilong Road, Guanlong Section, Dongguan, Guanlong, 523119, China
P: 0769-242-7230   F: 0769-242-7837   C: 86
ZHANGJIAGANG NSK PRECISION MACHINERY CO., LTD.
JIANGSU PLANT   Zhenxing Rd., Guotai North Rd., Zhangjiagang Economic Development Zone.,
Zhangjiagang City Jiangsu 215600, China
P: 0512-5867-6496   F: 0512-5818-0970   C: 86
TIMKEN-NSK BEARINGS (SUZHOU) CO., LTD.
JIANGSU PLANT   Taishan Road 22 Suzhou New District, Jiangsu 215129, China
P: 0512-6665-5666   F: 0512-6665-9108   C: 86
NSK CHINA TECHNOLOGY CENTER
JIANGSU   258 South Huang Pujing Road, Kunshan Economic & Technical Development Zone, Jiangsu 215335, China
P: 0512-5771-5654   F: 0512-5771-0748   C: 86
NSK (SHANGHAI) TRADING CO., LTD.
SHANGHAI   10th Fl. Building No. A, Shanghai Far East International Plaza, Bldg. A 319 Xian Xia Road, Shanghai 200051, China
P: 021-6235-0198   F: 021-6235-1033   C: 86
NSK REPRESENTATIVE OFFICES   www.nsk.com.cn
BEIJING   Room 1001, Beijing Fortune Bldg., 5 Dong san Huan Bei Lu, Chao Yang District, Beijing 100004, China
P: 010-6590-8161   F: 010-6590-8166   C: 86
SHANGHAI   10th Fl. Building No. A, Shanghai Far East International Plaza, 319 Xian Xia Road, Shanghai 200051, China
P: 021-6235-0198   F: 021-6235-1033   C: 86
GUANGZHOU   Room 2701-02, Guangzhou International Electronics Tower 403,
Huan Shi Rd East, Guangzhou 510095, China
P: 020-8732-0583   F: 020-8732-0574   C: 86
ANSHUN   Dongjiao, Anshun, Guizhou 561000, China
P: 0853-3522522   F: 0853-3522522   C: 86
CHENGDU   Room1901, Green Land Hotel, No.99 Zhonglieci Xi Street, Chengdu, 610016, China
P: 028-8661-4200   F: 028-8661-4343   C: 86
NSK (CHINA) INVESTMENT CO., LTD
SHANGHAI   10th Fl. Building No. A, Shanghai Far East International Plaza, 319 Xian Xia Road, Shanghai 200051, China
P: 021-6235-0198   F: 021-6235-1033   C: 86

India:
RANE NSK STEERING SYSTEMS LTD.
CHENNAI PLANT   14, Rajagopalan Salai, Vallancherry Guduvancherry, Pin-603 202, India
P: 04114-266002   F: 04114-266001   C: 91
NSK LTD. INDIA BRANCH OFFICE
CHENNAI   2A, First Street, Cenotaph Road, Chennai, 600 018, India
P: 044-2433-4732, 044-2434-3036, 3067   F: 044-2433-4733   C: 91

Indonesia:
PT. NSK BEARINGS MANUFACTURING INDONESIA
JAKARTA PLANT   Blok M-4, Kawasan Berikat, MM2100, Industrial Town, Cikarang Barat,
Bekasi 17520, Jawa Barat, Indonesia
P: 021-898-0155   F: 021-898-0156, 021-898-0183   C: 62
PT. NSK INDONESIA
JAKARTA   Summitmas II 6th Fl., Jl. Jend. Sudirman Kav. 61-62, Jakarta 12190 Indonesia
P: 021-252-3458   F: 021-252-3223   C: 62

Korea:
NSK KOREA CO., LTD.   www.kr.nsk.com
SEOUL   9F (West Wing) Posco Center 892, Deachi 4 Dong Kangnam-Ku, Seoul, Korea
P: 02-3287-0300   F: 02-3287-0345, 0445   C: 82
CHANGWON   60, Seongsan-Dong, Changwon, Kyungsangnam-Do, Korea
PLANT   P: 055-287-6001   F: 055-285-9982   C: 82

Malaysia:
NSK BEARINGS (MALAYSIA) SDN. BHD.
KUALA LUMPUR   1001, Level 10, Uptown.2, 2 Jalan SS21/37, Damansara Uptown,
47400 Petaling Jaya, Selangor Darul Ehsan, Malaysia
P: 03-7722-3373   F: 03-7728-5543, 7728-7450   C: 60
PRAI   10, Lengkok Kikik 1, Taman Inderawasih, 13600 Prai, Penang, Malaysia
P: 04-3991763   F: 04-3991830   C: 60
JOHOR BAHRU   Ground Floor, No. 27, Jalan Bakawali 50, Taman Johor Jaya,
81100 Johor Bahru, Johor, Malaysia
P: 07-3546290   F: 07-3546291   C: 60
KOTA KINABALU   Lot 10, Lrg. Kurma 4, Likas Ind. Centre, 5½ Miles, Jalan Tuaran,
88450 Inanam Sabah, Malaysia
P: 088-421260   F: 088-421261   C: 60
NSK MICRO PRECISION (M) SDN. BHD.
MALAYSIA PLANT   No.43 Jalan Taming Dua,Taman Taming Jaya, 43300 Balakong, Selangor Darul Ehsan, Malaysia
P: 03-8961-6288   F: 03-8961-6488   C: 60

New Zealand:
NSK NEW ZEALAND LTD.   www.nsk-rhp.co.nz
AUCKLAND   3 Te Apunga Place Mt. Wellington, Auckland, New Zealand
P: 09-276-4992   F: 09-276-4082   C: 64

Philippines:
NSK REPRESENTATIVE OFFICE
MANILA   Unit 910 Philippine AXA Life Centre, 1286 Seno Gil Puyat Avenue,
Makati City 1200, Metro Manila, Philippines
P: 02-759-6246   F: 02-759-6249   C: 63

Singapore:
NSK INTERNATIONAL (SINGAPORE) PTE LTD.
SINGAPORE   2 Toh Guan Road East #02-02 Singapore 608837
P: 6273-0357   F: 6275-8937   C: 65
NSK SINGAPORE (PTE) LTD.
SINGAPORE   2 Toh Guan Road East #02-03 Singapore 608837
P: 6278-1711   F: 6273-0253   T: RS24058   C: 65

Taiwan:
TAIWAN NSK PRECISION CO., LTD.
TAIPEI   9th Fl., 34, Chung Shan N. Rd., Sec. 3, Taipei, Taiwan R.O.C.
P: 02-2591-0656   F: 02-2597-3101   C: 886
TAICHUNG   107-6, SEC. 3, Wenxin Rd., Taichung, Taiwan R.O.C.
P: 04-2311-7978   F: 04-2311-2627   C: 886
TAINAN   No.48, Lane 62, Fusing Rd., Sinshin Township, Tainan County 744, Taiwan, R.O.C.
P: 06-589-2703   F: 06-589-2719   C: 886

Thailand:
NSK BEARINGS (THAILAND) CO., LTD.
BANGKOK   25th Fl. RS Tower, 121/76-77 Rachadaphisek Road, Dindaeng, Bangkok 10320, Thailand
P: 02-6412-150~58   F: 02-6412-161   C: 66
NSK BEARINGS MANUFACTURING (THAILAND) CO., LTD.
CHONBURI PLANT   700/430 Moo 7, Amata Nakorn Industrial Estate T. Donhualor,
A. Muangchonburi, Chonburi 20000 Thailand
P: 038-454010~454016   F: 038-454017, 454020   C: 66
SIAM NSK STEERING SYSTEMS CO., LTD.
CHACHOENGSAO   90 Moo 9, Wellgrow Industrial Estate, Km. 36 Bangna-Trad Road, Bangwao,
PLANT   Bangpakong, Chachoengsao 24180, Thailand
P: 038-522-343~350   F: 038-522-351   C: 66
NSK ASIA PACIFIC TECHNOLOGY CENTRE (THAILAND) CO., LTD.
CHONBURI   700/430 Moo 7, Amata Nakorn Industrial Estate T. Donhualor,
A.. Muangchonburi, Chonburi 20000 Thailand
P: 038-454631-454633, 454634   C: 66

Europe
NSK EUROPE LTD. (EUROPEAN HEADQUARTERS)   www.eu.nsk.com
MAIDENHEAD, UK   Belmont Place, Belmont Road, Maidenhead, Berkshire SL6 6TB U.K.
P: 01628-509800   F: 01628-509808   C: 44

France:
NSK FRANCE SAS
PARIS   Quartier de l'Europe, 2 Rue Georges Guynemer, 78283 Guyancourt Cedex, France
P: 01-30-57-39-39   F: 01-30-57-00-01   C: 33

Germany:
NSK DEUTSCHLAND GMBH
DÜSSELDORF   Harkortstrasse 15, 40880 Ratingen, Germany
P: 02102-481-0   F: 02102-481-2290   C: 49
STUTTGART   Sielminger Str. 65, 70771 Leinfelden-Echterdingen, Germany
P: 0711-79082-0   F: 0711-79082-289   C: 49
LEIPZIG   Zschortauer Str. 76, 04129 Leipzig, Germany
P: 0341-5631241   F: 0341-5631243   C: 49
NSK PRECISION EUROPE GMBH
DÜSSELDORF   Harkortstrasse 15, 40880 Ratingen, Germany
P: 02102-481-0   F: 02102-481-2290   C: 49
NSK STEERING SYSTEMS EUROPE LTD.
STUTTGART   Sielminger Strasse 65 D-70771 Leinfelden-Echterdingen, Germany
P: 0771-79082-277   F: 0771-79082-289   C: 49
NEUWEG FERTIGUNG GMBH
CORPORATE   Ehinger Strasse 5, D-89597 Munderkingen, Germany
OFFICE/PLANT   P: 07393-540   F: 07393-5414   C: 49

Italy:
NSK ITALIA S.p.A.
MILANO   Via Garibaldi, 215, I-20024 Garbagnate Milanese (MI), Italy
P: 02-99-5-19-1   F: 02-990-25-778, 02-990-28-373   C: 39
INDUSTRIA CUSCINETTI S.p.A.
TORINO PLANT   Via Giotto 4, 10080, S. Benigno C. se, Torino, Italy
P: 0119824811   F: 0119880284   C: 39

Netherlands:
NSK EUROPEAN DISTRIBUTION CENTRE B.V.
De Kroonstraat 38, 5048 AP Tilburg, Nederland
P: 013-4647647   F: 013-4647648   C: 31

Poland:
NSK EUROPE LTD. WARSAW LIAISON OFFICE
WARSAW LIAISON   Przedstawicielstwo w Warszawie, ul. Migdalowa 4 lok. 73, 02-796 Warsaw, Poland
OFFICE   P: 022-645-1525, 1526   F: 022-645-1529   C: 48
NSK ISKRA S.A.
CORPORATE   Ul. Jagiellonska 109, 25-734 Kielce, Poland
OFFICE/PLANT   P: 041-366-5001   F: 041-366-5008   C: 48
NSK EUROPEAN TECHNOLOGY CENTER, POLAND OFFICE
UL. Jagiellonska 109, 25-734 Kielce, Poland
P: 041-366-5812   F: 041-366-5206   C: 48

Spain:
NSK SPAIN S.A.
BARCELONA   Calle de la Hidráulica, 5, P.I. "La Ferrería" 08110 Montcada i Reixac (Barcelona), Spain
P: 093-575-4041   F: 093-575-0520   C: 34

Turkey:
NSK BEARINGS MIDDLE EAST TRADING CO., LTD.
ISTANBUL   Fevzi Cakmak Caddesi, No.11/4, Maltepe 34844, Istanbul, Turkey
P: 0216-442-7106   F: 0216-305-5505   C: 90

United Kingdom:
NSK BEARINGS EUROPE LTD.
PETERLEE   3 Brindley Road, South West Industrial Estate, Peterlee, Co. Durham, SR8 2JD U.K.
PLANT   P: 0191-586-6111   F: 0191-586-3482   C: 44
PETERLEE (FORGE)   Davy Drive, North West Industrial Estate, Peterlee, Co. Durham, SR8 2PW U.K.
PLANT   P: 0191-518-0777   F: 0191-518-0303   C: 44
NEWARK   Northern Road, Newark, Nottinghamshire, NG24 2JF U.K.
PLANT   P: 01636-605123   F: 01636-643072   C: 44
NSK EUROPEAN TECHNOLOGY CENTRE
NEWARK, UK   Northern Road, Newark, Notts, NG24 2JF U.K.
P: 01636-605123   F: 01636-643241   C: 44
NSK UK LTD.
NEWARK   Northern Road, Newark, Nottinghamshire, NG24 2JF U.K.
P: 01636-605123   F: 01636-643050   C: 44
NSK STEERING SYSTEMS EUROPE LTD.
CORPORATE   Silverstone Drive, Rowley's Green, Coventry, Warwickshire CV6 6PA U.K.
OFFICE   P: 024-76-588588   F: 024-76-588599   C: 44
PETERLEE   6/7 Doxford Drive, South West Industrial Estate, Peterlee, Co. Durham, SR8 2RL U.K.
PLANT   P: 0191-518-6400   F: 0191-518-6440   C: 44

North and South America
NSK AMERICAS, INC. (AMERICAN HEADQUARTERS)
ANN ARBOR   4200 Goss Road, Ann Arbor, Michigan 48105-2703, U.S.A.
P: 734-913-7500   F: 734-913-7511   C: 1

Argentina:
NSK ARGENTINA SRL
BUENOS AIRES   Garcia del Rio 2477 PISO 7º OF. ¨ A¨ C1429DEA-Buenos Aires-Argentina
P: 11-4704-5100   F: 11-4704-0033   C: 54

Brazil:
NSK BRASIL LTDA.   www.br.nsk.com
SÃO PAULO   Rua Treze de Maio, 1633-14° Andar-Bela Vista São Paulo-SP, Brazil 01327-905
P: 011-3269-4723   F: 011-3269-4720   C: 55
SUZANO PLANT   Av. Vereador João Batista Fitipaldi, 66-Vila Maluf Suzano-SP, Brazil 08685-000
P: 011-4741-4900   F: 011-4748-2355   C: 55
BELO HORIZONTE   Rua Ceará, 1431-4° andar-sala 405-Funcionários Belo Horizonte-MG, Brazil 30150-311
P: 031-3274-2477   F: 031-3273-4408   C: 55
JOINVILLE   Rua Blumenau, 178-sala 910-Centro Joinville-SC, Brazil 89204-250
P: 047-422-5445/433-3627   F: 047-422-2817   C: 55
PORTO ALEGRE   Av. Cristovão Colombo, 1694-sala 202-Floresta Porto Alegre-RS, Brazil 90560 001
P: 051-3222-1324/3346-7851   F: 051-3222-2599   C: 55
RECIFE   Av. Conselheiro Aguiar, 2738-6° andar-conj. 604-Boa Viagem Recife-PE, Brazil 51020-020
P: 081-3326-3781   F: 081-3326-5047   C: 55

Canada:
NSK CANADA INC.   www.ca.nsk.com
HEAD OFFICE   5585 McAdam Road, Mississauga, Ontario, Canada L4Z 1N4
P: 905-890-0740   F: 905-890-0488   C: 1
MONTREAL   2150-32E Avenue, Lachine, Quebec, Canada H8T 3H7
P: 514-633-1220   F: 514-633-8164   C: 1
TORONTO   5585 McAdam Road, Mississauga, Ontario, Canada L4Z 1N4
P: 905-890-0561   F: 905-890-1938   C: 1
VANCOUVER   3353 Wayburne Drive, Burnaby, British Columbia, Canada V5G 4L4
P: 604-294-1151   F: 604-294-1407   C: 1

Mexico:
NSK RODAMIENTOS MEXICANA, S.A. DE C.V.   www.mx.nsk.com
MEXICO CITY   Minas Palacio No.42-6, Col. San Antonio Zomeyucan, Naucalpan de Juarez, C.P. 53750, Estado de Mexico, Mexico
P: 55-5301-2741, 55-5301-3115, 55-5301-4762   F: 55-5301-2244, 55-5301-2865   C: 52

United States of America:
NSK CORPORATION   www.nsk-corp.com
[CORPORATE OFFICE]
ANN ARBOR   4200 Goss Road, Ann Arbor, Michigan 48105-2703, U.S.A.
P: 734-913-7500   F: 734-913-7511   C: 1
[NSK AMERICAN TECHNOLOGY CENTER]
ANN ARBOR   4200 Goss Road, Ann Arbor, Michigan 48105-2703, U.S.A.
P: 734-913-7500   F: 734-913-7852   C: 1
[BRANCHES and DISTRIBUTION CENTERS]
CERRITOS   13921 Bettencourt Street, Cerritos, California 90703, U.S.A.
P: 562-926-2975   F: 562-926-3553   C: 1
PLAINFIELD   1581 S. Perry Road, Plainfield, Indiana 46168, U.S.A.
P: 317-837-8879   F: 317-837-7207   C: 1
FRANKLIN   3400 Bearing Drive, Franklin, Indiana 46131-9660, U.S.A.
P: 317-738-5000   F: 317-738-4310   C: 1
[PLANTS]
ANN ARBOR   5400 South State Road, Ann Arbor, Michigan 48108-9754, U.S.A.
P: 734-996-4400   F: 734-996-4707   C: 1
CLARINDA   1100 North First Street, Clarinda, Iowa 51632-1983, U.S.A.
P: 712-542-5121   F: 712-542-4905   C: 1
FRANKLIN   3400 Bearing Drive, Franklin, Indiana 46131-9660, U.S.A.
P: 317-738-5000   F: 317-738-4310   C: 1
LIBERTY   1112 East Kitchel Road, Liberty, Indiana 47353-8985, U.S.A.
P: 765-458-5000   F: 765-458-7832   C: 1
NSK PRECISION AMERICA, INC.   www.npa.nsk.com
CHICAGO   2171 Executive Drive, Suite 100 Addison, Illinois 60101-5600, U.S.A.
P: 630-620-8500   F: 630-620-8555   C: 1
SAN JOSE   780 Montague Expressway, Suite 508, San Jose, California 95131, U.S.A.
P: 408-944-9400   F: 408-944-9405   C: 1
[DISTRIBUTION CENTER]
FRANKLIN   3400 Bearing Drive, Franklin, Indiana 46131-9660, U.S.A.
P: 317-738-5000   F: 317-738-4310   C: 1
NSK STEERING SYSTEMS AMERICA, INC.   www.nastech.nsk.com
CORPORATE   110 Shields Drive, Bennington, Vermont 05201-8309, U.S.A.
OFFICE/PLANT   P: 802-442-5448   F: 802-442-2253   C: 1
ANN ARBOR   4200 Goss Road, Ann Arbor, Michigan 48105-2703, U.S.A.
P: 734-913-7500   F: 734-913-7102   C: 1
NSK LATIN AMERICA, INC.   www.latinamerica.nsk.com
MIAMI   2500 NW 107th Avenue, Suite 300, Miami, Florida 33172, U.S.A.
P: 305-477-0605   F: 305-477-0377   C: 1

P: Phone   F: Fax   T: Telex   C: Country Code   Printed in Japan

Motion & Control

No.17 May 2005

Published by NSK Ltd.